INVESTIGATION OF MOSA, A PROTEIN IMPLICATED IN RHIZOPINE BIOSYNTHESIS

A Thesis Submitted to the College of Graduate Studies and Research

in Partial Fulfillment of the Requirements for the

Degree of Doctor of Philosophy

In the Department of Chemistry

University of Saskatchewan, Saskatoon

by

Christopher Peter Phenix

Permission To Use

In presenting this thesis in partial fulfillment of the requirements for a postgraduate degree from the University of Saskatchewan, I agree that the libraries of this University may make it freely available for inspection. I further agree that permission for copying of this thesis in any manner, in whole or in part, for scholarly purposes may be granted by the professors who supervised my thesis work, or in their absence, by the Head of the Department of Chemistry or the Dean of Arts and Science. It is understood that any copying or publication or use of this thesis or parts thereof for financial gain shall not be allowed without my written permission. It is also understood that due recognition shall be given to me and to the University of Saskatchewan in any scholarly use which may be made of any materials in my thesis.

Requests for permission to copy or make other use of material in this thesis in whole or in part should be addressed to:

Head of the Department of Chemistry

University of Saskatchewan

Saskatoon, Saskatchewan, S7N 5E5

Abstract

MosA is a protein found in *Sinorhizobium meliloti* L5-30 and has been suggested to be responsible for the biosynthesis of the rhizopine 3-*O*-methyl-*scyllo*-inosamine (3-MSI) from *scyllo*-inosamine (SI). However, we have shown MosA is a dihydrodipicolinate synthase (DHDPS) catalyzing the condensation of pyruvate with aspartate-β-semialdehyde (ASA). Since the DHDPS reaction occurs through a Schiff base aldol-type mechanism it was proposed that MosA could be an *O*-methyltransferase utilizing 2-oxo-butyrate (2-OB) as a novel methyl donor. This interesting yet unlikely possibility would explain MosA's role in the biosynthesis of 3-MSI without ignoring its similarity to DHDPS. Alternatively, MosA may have two catalytic domains one of which possesses a novel binding motif for S-Adenosyl methionine (SAM) to account for methyltransfer activity. *In vitro* demonstration of MosA's methyltransferase activity is required to resolve this apparent contradiction.

This dissertation describes the chemical synthesis of the rhizopines, investigation into whether MosA has a direct role in rhizopine biosynthesis and the thermodynamic characterization of compounds interacting with MosA as observed by isothermal titration calorimetry.

Initial investigation into MosA's methyltransferase activity began with 2-OB's interaction with the enzyme. Inhibition experiments determined 2-OB is a competitive inhibitor with respect to pyruvate of the DHDPS reaction of MosA. Furthermore, protein mass spectrometry of MosA in the presence of 2-OB and sodium borohydride indicated that a Schiff base enzyme intermediate was indeed being formed providing evidence that the proposed mechanism may exist. However, neither of the rhizopines had any effect on the DHDPS activity and HPLC assays determined that no 3-MSI was being produced by MosA in the presence of SI and 2-OB. Furthermore, HPLC assays failed to detect methyl transfer activity by MosA utilizing the SAM as a methyl donor.

Isothermal titration calorimetry provided thermodynamic characterization of the pyruvate and 2-OB Schiff base intermediates formed with MosA. In addition, ITC provided insight into the nature and thermodynamics of (*S*)-lysine's inhibition of MosA. ITC failed to detect any interactions between the rhizopines or SAM with MosA. These

results indicate that MosA is only a DHDPS and does not catalyze the formation of 3-MSI from SI as hypothesized in the literature.

Acknowledgements

I would first like to thank my supervisor Dr. David R. J. Palmer. As a new professor he had the very difficult job developing a research program, producing classes, making up committees and supervising graduate students. Despite all of this, he always found time to sit and discuss science, give advice, support, encourage and chat with all of his graduate students. I appreciate the large degree of freedom and independence that was giving to me over the years which has given me confidence to learn new techniques and tackle problems without hesitation. It was great to be able to freely discuss issues from enzymology to football with my supervisor.

Over the years, many people have found themselves in the Palmer lab. The vast majority of the time we were able to have fun while simultaneously carry out experiments. People such as Richard, Tony, Grant, Jennifer, Zhou, Ma, Yunhua, Andrea, Fang, Honyan, Melanie, Karen, Junior, Milan and Andrei all helped to create a fun and productive environment to work in. We had a lot of fun together and helped each other out when we could. In addition, the friendly and approachable people at the SSSC such as Jason, Keith, Gabriele and Ken were always extremely helpful in operating and troubleshooting the instruments vital to my research.

I would also like to thank the members of my committee; Dr. Louis Delbaere, Dr. Marek Majewski, Dr. Ron Verrall and Dr. Matt Paige. I appreciate the time, effort and occasional tough love they put into developing me as a young chemist. In addition the Department of Chemistry, Dr. Palmer, NSERC and the Indigenous Peoples Health Research Centre deserve thanks for the financial support I was provided over my time of study.

I owe my dear wife Rachelle great thanks for her tremendous love, support, understanding, and encouragement throughout the good and the bad times. Without her, life was more difficult. Additionally, my cousin Tom, who has been there for me since my first day of university, has provided me with advice, encouragement and a great friendship for over a decade. I would also like to thank my parents Bev and Lorraine, my sister Angie (and Rod) for their love, encouragement and support. Furthermore, thanks to Roland, Lorraine, Mike, Lisa, Bob, Catherine, Luke, Noah and

Braydon for their support, encouragement and often alteration of their plans to include me in family events. Finally, I would like to acknowledge my friends Dale, Rhett, Ignace, Marla, Eyvind, Burton and many others too numerous to mention for the great nights at Winston's, BBQ's and the many parties we had.

Dedication

This thesis is dedicated to my wonderful wife Rachelle and all of the family and friends listed in the acknowledgments. All of you have influenced my life far more than I verbally communicate and therefore, this thesis is dedicated to you.

Table of Contents

List of Tables

List of Schemes

List of Figures

List of abbreviations

A	alanine
ACN	acetonitrile
ASA	aspartate-β-semialdehyde
ATP	adenosine 5'-triphosphate
ΔC_p	change in heat capacity at constant pressure
CSC	Calorimetery Sciences Corporation
DHDPS	dihydrodipicolinate synthase
DNA	deoxyribonucleic acid
E	glutamate
E. coli	*Escherichia coli*
FMOC-Cl	9-fluorenylmethylchloroformate
FMOC-OH	9-fluorenylmethylcarbonic acid
FMOC-SI	9-fluorenylmethylcarbamate of *scyllo*-inosamine
FMOC-3-MSI	9-fluorenylmethylcarbamate of 3-*O*-methyl-*scyllo*-inosamine
ΔG	change in Gibbs free energy
G	glycine
H	histidine
ΔH	change in enthalpy
HPLC	high performance liquid chromatography
HPLC-MS	high performance liquid chromatography mass spectrometry
HBPHA	*trans*-*O*-hydroxybenzylidenepyruvate hydratase-aldolase
HTPA	4-hydroxytetrahydrodipicolinic acid
ITC	isothermal titration calorimetry
IPTG	isopropyl-β-thiogalactopyranose
K	lysine
K_a	association constant
K_d	dissociation constant
kDa	kilodaltons
kb	kilobases
3-MSI	3-*O*-methyl-*scyllo*-inosamine
Mb	megabases
$NaBH_4$	sodium borohydride
NAL	N-acetylneuraminic acid lyase
n	stoichiometery in ITC
N	asparagine
pSym	symbiotic plasmid
2-OB	2-oxobutyrate
OPA	O-phthaldehyde
ORF	open reading frame
PITC	phenylisothiocyanate
R	arginine
R. meliloti	*Rhizobium meliloti*
S	serine

ΔS	change in entropy
SAM	S-adenosylmethionine
SAH	S-adenosylhomocysteine
SI	*scyllo*-inosamine
Sm-220-3	*Sinorhizobium meliloti* 220-3
Sm-1021	*Sinorhizobium meliloti* 1021
Sm-L5-30	*Sinorhizobium meliloti* L5-30
T	threonine
TBAB	tetrabutylammonium bromide
TEA	triethylamine
TRIS	Tris(hydroxymethyl)aminomethane
TIM	triosephosphate isomerase
$T\Delta S$	entropy change at a given temperature
Y	tyrosin

1 Introduction

1.1 Sinorhizobia form symbiotic relationships with leguminous plants

Sinorhizobia are beneficial soil bacteria that form symbiotic relationships with leguminous plants such as beans, peas and lentils. Through a complex process, the bacteria induce the plants to grow root nodules where the bacteria then reside using plant nutrients while fixing nitrogen for the plants. Once in the root nodules, the sinorhizobia then differentiate into bacteroids where the genes used for nitrogen fixation are expressed and nitrogen fixation begins.[1] The conversion of atmospheric nitrogen to amino compounds that have biological roles in plants is very important agriculturally. In fact commercial products such as Rhiz-Up™ which are sinorhizobium inoculants are now available for leguminous crops.

The interaction between plants and sinorhizobia is described as symbiotic meaning that both the plant and the bacterium benefit from establishing this relationship.[2] In fact, plants that are able to form symbiotic relationships with sinorhizobia are actually given a competitive advantage over other species which cannot.[3] The plants benefit by obtaining nitrogen-containing compounds that were produced by sinorhizobia through nitrogen fixation. Nitrogen fixation is the process where atmospheric nitrogen gas (N_2) is incorporated into compounds that are

biologically important. Interestingly, the bacteria that produce the nitrogen-containing compounds are unable to utilize them, illustrating the importance of this relationship. Bacteria are believed to benefit by utilizing plant nutrients in the nodules and the soil immediately surrounding the roots of the plant known as the rhizosphere, although this process is less well understood.[4]

Competition in the soil between endogenous species of bacteria is an important issue in soil biology. Consequently, any type of nutritional advantage gained by a species is going to help in its propagation. One of the most highly studied plant-microbe interaction is the parasitic relationship formed between agrobacteria and plants. Agrobacteria are closely related to sinorhizobia and induce plants to grow tumors creating a diseased state known as crown gall disease. Within the tumors, bacterial DNA from large megaplasmids is transported into the plant's genome. Here the plants' cellular machinery expresses the genes of bacterial origin, resulting in proteins that essentially hijack plant metabolism, producing compounds beneficial to the microbe. One of the main goals of the redirected metabolism is the production of a class of compounds known as opines.[5]

1.2 Rhizopines are analogous to opines from agrobacteria

Opines are strain-specific compounds produced by the crown galls induced by agrobacteria. They are used as selective growth substrates by members of the inducing strain. Structurally, opines fall into two broad classes: sugar phosphodiesters and

imines. The imine class (two of which are shown in Figure 1), which is the most populous, refers to the biosynthetic intermediates in which an imine is formed between a primary amine and an aldehyde or ketone.[6] Enzymatically catalyzed reductions or rearrangements produce the final opine structure. The most common examples of opines are derivatives of primary metabolites such as pyruvate, 2-oxoglutarate or sugars conjugated to amino acids (see Figure 1). Over the years more than twenty opines have been discovered from many different strains of agrobacteria.[7] In an attempt to explore the generality of the opine phenomenon in other species, sinorhizobia were chosen to be screened for "opine like" compounds.

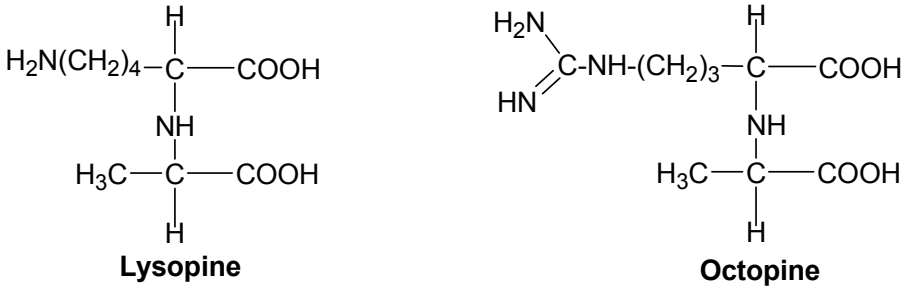

Figure 1. **Chemical structures of two opines obtained from the crown galls induced by the parasitic *Agrobacterium tumafaciens***

The decision to test sinorhizobia for "opine-like" compounds was made for several reasons. Sinorhizobia and agrobacteria are closely related species both belonging to the family *Rhizobiacae*. In addition, the pathogenic and symbiotic states of *Agrobacterium* and sinorhizobia are surprisingly quite similar. One induces the growth of tumors while the other induces the growth of root nodules. Finally the genes mainly responsible for the plant-microbe interactions are found on large megaplasmids.[1] Taking the similarities into account, the idea that sinorhizobia may have "opine like" compounds is not unreasonable.

Interestingly, two closely related "opine like" compounds were discovered in the root nodules of a legume infected by *Sinorhizobium meliloti* L5-30 (Sm L5-30). These compounds were identified as *scyllo*-inosamine (**SI**) and 3-*O*-methyl-*scyllo*-inosamine (**3-MSI**) (see Figure 2).[1] Although not structurally related to the opines, the newly found "opine-like" compounds were given the name "rhizopines" as they are found in the root nodules located in the rhizosphere and share some biological functions with opines.

***scyllo*-inosamine (SI)** **3-*O*-methyl-*scyllo*-inosamine (3-MSI)**

Figure 2. The chemical structure of the two rhizopines found in the root nodules of a legume induced by *Sinorhizobium meliloti* L5-30

1.2.1 Characteristics of rhizopines

Rhizopines, as with opines, are strain-specific compounds. However, unlike opines, only 11% of *R. meliloti* and 12% of *R. leguminosarum* bv. Viciae could both synthesize and catabolize rhizopines.[8] In addition, all strains that were able to produce

rhizopines were able to catabolize them suggesting co-evolution of the genes responsible for rhizopine metabolism.

The function of rhizopines is poorly understood. However, it is known that those species of sinorhizobia that are able to catabolize rhizopines are given a competitive advantage in nodulation over those which cannot.[5] This could be explained by the rhizopines being selective growth substrates; however, competition studies did not support this role.[9] Rather, rhizopines somehow give catabolizing strains the ability to populate nodules at an enhanced rate over those that cannot. To this date, the mechanism and biological function of rhizopines is unclear.

1.2.2 The genes implicated in rhizopine biosynthesis

Sinorhizobia contain much of the genetic information necessary for nitrogen fixation and nodulation on two extremely large plasmids estimated to be in excess of 1.6 Mb.[10] The genes responsible for rhizopine catabolism (*moc*) and synthesis (*mos*) were found closely linked on the pSym megaplasmid suggesting that these metabolic genes evolved as a functional unit important in symbiosis.[1] Further support for involvement of rhizopines in symbiosis came from the finding that they are regulated by the symbiotic nitrogen fixation regulatory gene *nif*A.[11] This ensures that the *mos* and *moc* genes are controlled in an identical transcriptional manner to those genes involved in symbiosis.

A 4.5 kb fragment of DNA believed to house the genes responsible for rhizopine synthesis was isolated and sequenced.[12] The DNA sequencing revealed four open

reading frames named *mos*A, *mos*B, *mos*C and ORF1. Sequence analysis of ORF1 suggested that it encodes a small peptide, however, no ORF1-derived protein was ever detected using Western blot analysis of nodule extracts.[12] Antibody analysis detected gene products corresponding to *mos*A, *mos*B and *mos*C. Information regarding possible functions of the proteins MosA, MosB and MosC was obtained by deducing the amino acid sequences and scanning a data base of known proteins.

MosA has high sequence similarity (~45% identity) to dihydrodipicolinate synthase (DHDPS) from *E. coli*, an enzyme in the (*S*)-lysine biosynthetic pathway. MosB, on the other hand, has sequence similarities to proteins such as DegT, EryC1, DnrJ, StrS ranging from 37 – 41%. All these proteins are members of the aminotransferase family. Perhaps the most interesting is MosB's similarity to StsC (38% amino acid identity and 56% similarity) an inosose-aminotransferase.[13] MosC showed no sequence similarities to any known sequences in the protein data bank. However, MosC is a very hydrophobic protein with 12 different membrane-spanning regions typical of membrane-bound carbohydrate transport proteins.[12]

The metabolic function of these proteins was initially investigated by comparison of the *mos* genes found in *Sinorhizobium meliloti* 220-3 (Sm 220-3).[14] This strain, when compared to Sm L5-30, shared significant homology within the mos locus with the exception that it lacked *mos*A. Analysis of the rhizopines present in Sm 220-3, which lacks the *mos*A gene, revealed that only **SI** was produced. Since Sm 220-3 only produces **SI** and the only major genetic difference in the mos locus was the absence of *mos*A, it was suggested that *mos*A may be responsible for the biosynthesis of **3-MSI** from **SI**.[14] To support this hypothesis, researchers constructed a plasmid containing a

truncated *mos*A gene from Sm L5-30. This would result in the expression of a nonfunctioning MosA protein while keeping intact the rest of the genes important for rhizopine synthesis. This plasmid was then used to introduce the *mos* genes into *Sinorhizobium meliloti* 1021 (Sm 1021), a strain that does not produce rhizopines. Upon inoculation of this transformed strain into root nodules, rhizopine analysis revealed that only **SI** was being produced.[15] These experiments provided further support that MosA may be an *O*-methyltransferase.

The suggestion that MosA is an *O*-methyltransferase caught the attention of several researchers primarily due to high sequence similarity of MosA to DHDPS from *E. coli*.[16,17] DHDPS is a type I aldolase that catalyzes the condensation of pyruvate with aspartate-β-semialdehyde (ASA) as shown in Figure 3. In fact, MosA is more closely related to DHDPS from *E. coli* than some DHDPS's are to each other.[18] MosA is a tentative member of the *N*-acetylneuraminate lyase (NAL) sub-family of aldolases. Each member of the NAL sub-family catalyzes a type I aldolase or aldolase-like reaction of a 2-oxo-acid with a carbonyl-containing compound.

The sequence of MosA suggests that it belongs to the NAL sub-family of enzymes. Enzymes belonging to this subfamily all possess the $(\beta/\alpha)_8$ barrel folds and catalyze aldol chemistry via a protonated Schiff base intermediate.[16] In the NAL sub-family all members form the Schiff base between a 2-oxo acid substrate and an active site lysine as shown in Figure 3. In addition to DHDPS and NAL, other members of this family include: *trans*-*ortho*-hydroxybenzylidenepyruvate-hydratase aldolase and D-4-deoxy-5-oxoglucarate dehydratase-decarboxylase. Since all of the above proteins catalyze Schiff base dependent aldol chemistry, the suggestion that MosA is a

methyltransferase is interesting. It is possible that MosA may be a methyltransferase despite its similarity to DHDPS or alternatively, as a review article on the NAL sub-family suggests, the assigned function of MosA as a methyltransferase may simply be incorrect.[16]

Sequence alignments of MosA, DHDPS and NAL illustrated in Figure 4 show that MosA is 45% identical to DHDPS from *E. coli* and should be a tentative member of the NAL sub-family. All of the residues identified in the active site and structurally important residues of DHDPS are present in the MosA sequence. In a review article by Babbitt and Gerlt[17] discussing enzyme evolution, MosA was brought up as a potential enzyme that confounds the accepted paradigm of enzyme evolution. It was suggested that MosA may rely on a mechanism analogous to the DHDPS reaction that would result in the transfer of a methyl group. This would explain MosA's role in rhizopine biosynthesis without ignoring its similarity to DHDPS. The proposed reaction illustrated in Figure 5 begins with the formation of a Schiff base between 2-oxobutyrate (2-OB) and MosA. Subsequent nucleophilic attack by the C-3 hydroxyl group of **SI** would produce pyruvate and **3-MSI**.

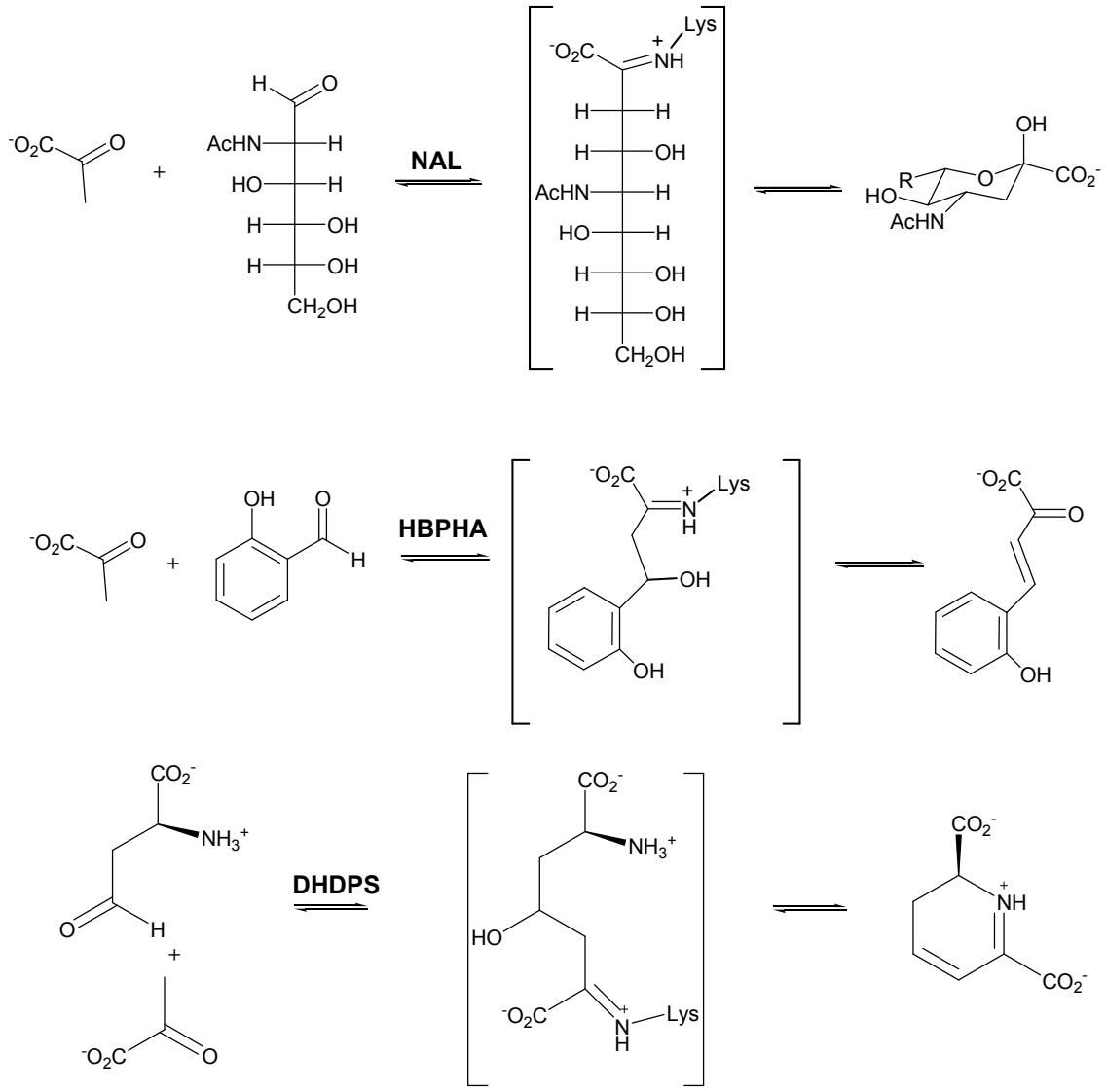

Figure 3. The reactions catalyzed by some members of the NAL sub-family
(NAL = N-acetylneuramic acid lyase, HBPHA = trans-*o*-hydroxybenzylidenepyruvate hydratase-aldolase and DHDPS = dihydrodipicolinate synthase). The enzyme-substrate Schiff base intermediate is highlighted in each case.

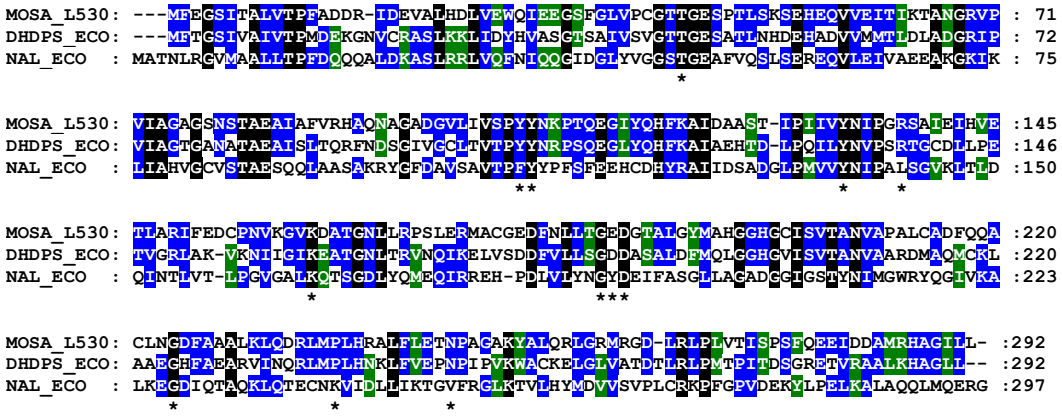

Figure 4. Sequence alignment of MosA from Sm L5-30, DHDPS from *E. coli* and NAL from *E. coli*. The alignment was created by Dr. David Palmer using ClustalW 1.82 and visualized with Genedoc 2.6. Residues highlighted in black are identical in all three sequences, residues highlighted in blue are identical in two of the sequences and residues highlighted in green are similar in at least two of the sequences. Those residues marked with an asterisk have been identified by X-ray crystallography or mutational analysis as being important in the active site or of structural significance.

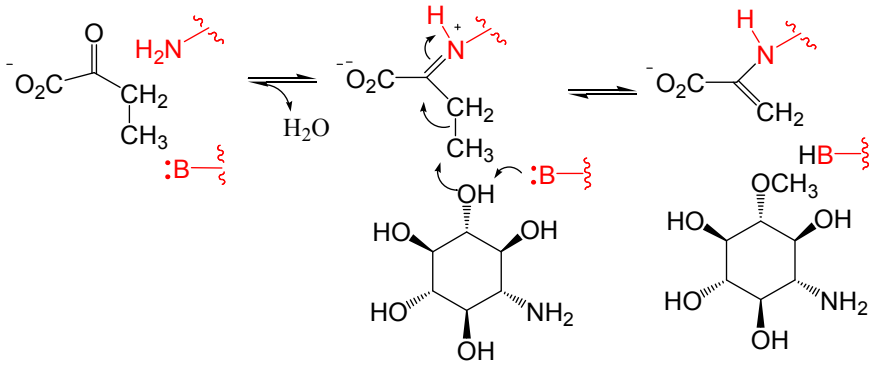

Figure 5. The proposed novel methyltransferase reaction using 2-OB as a methyl donor catalyzed by MosA in the production of 3-MSI from SI in rhizopine biosynthesis.[17]

1.3 Dihydrodipicolinate synthase (DHDPS) from E. coli

1.3.1 What is known about DHDPS from *E. coli*

Dihydrodipicolinate synthase (EC 4.2.1.52) catalyzes the condensation of pyruvate with aspartate-β-semialdehyde (ASA) to produce 4-hydroxy-tetrahydro-dipicolinic acid (HTPA) as shown in Figure 6. This enzyme catalyzes a reaction in the (*S*)-lysine biosynthetic pathway in bacteria shown in Scheme 1. In plants, DHDPS is the enzyme responsible for the first reaction in the metabolic pathway in the biosynthesis of (*S*)-lysine. This enzyme has garnered significant interest in the scientific community because of its potential as a target for antimicrobial and herbicidal compounds.[19] DHDPS also received attention from agricultural scientists interested in producing lysine-rich crops examining the use of engineered DHDPS enzymes.[20] The end product of the metabolic pathway, (*S*)-lysine, is an allosteric feedback inhibitor of DHDPS from plants and certain bacteria. DHDPS isozymes have been classified based on their sensitivity to (*S*)-lysine inhibition. Typically DHDPS from plants such as *Zea mays*[21]and *Psium sativum*[22]are strongly inhibited by (*S*)-lysine with IC_{50} values around 0.01 – 0.05 mM. Those DHDPS enzymes from gram-negative bacteria such as *E. coli*,[23] *Methanobacterium thermoautotrophicum*[24] and *Bacillus sphaericus*[25] are weakly inhibited with IC_{50} values 0.1 – 0.5 mM. Interestingly, DHDPS enzymes from gram-positive bacteria such as *Bacillus cereus*,[26] *Corynebacterium glutamicum*[27] and *Bacillus lactofermentum*[28]displayed low sensitivity with IC_{50} values around 10 mM .[29]

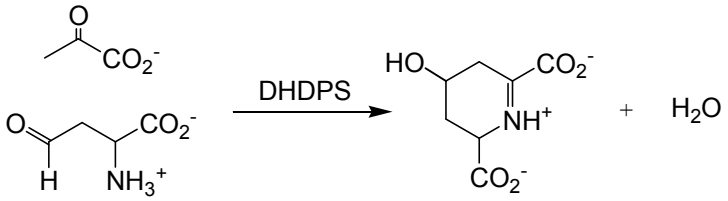

Figure 6. The reaction catalyzed by DHDPS from *E. coli*.

DHDPS from *E. coli* is the most thoroughly studied of the DHDPS isozymes. Initial experimentation on DHDPS from *E. coli* determined that the denatured enzyme possessed a molar mass of about 31 kDa.[30] DHDPS was later revealed to be a homotetrameric protein that relied on an active site lysine (K161) to form a Schiff base with pyruvate during the reaction mechanism.[31] A covalent intermediate between the pyruvate and DHDPS was later confirmed by mass spectrometry.[32] The mechanism has been studied by NMR using ^{13}C labeled pyruvate[33] and has been proposed to follow ping-pong kinetic mechanism.[34] After the formation of a Schiff base with pyruvate and release of water, deprotonation creates a nucleophilic α-carbon atom. The hydrate form of ASA binds to the active site and is dehydrated by the enzyme. Subsequent nucleophilic attack by the enamine on the carbonyl of ASA forms the new carbon-carbon bond. Cyclization and transamination releases the product HTPA into solution.[33] The currently accepted mechanism is depicted in Scheme 2.

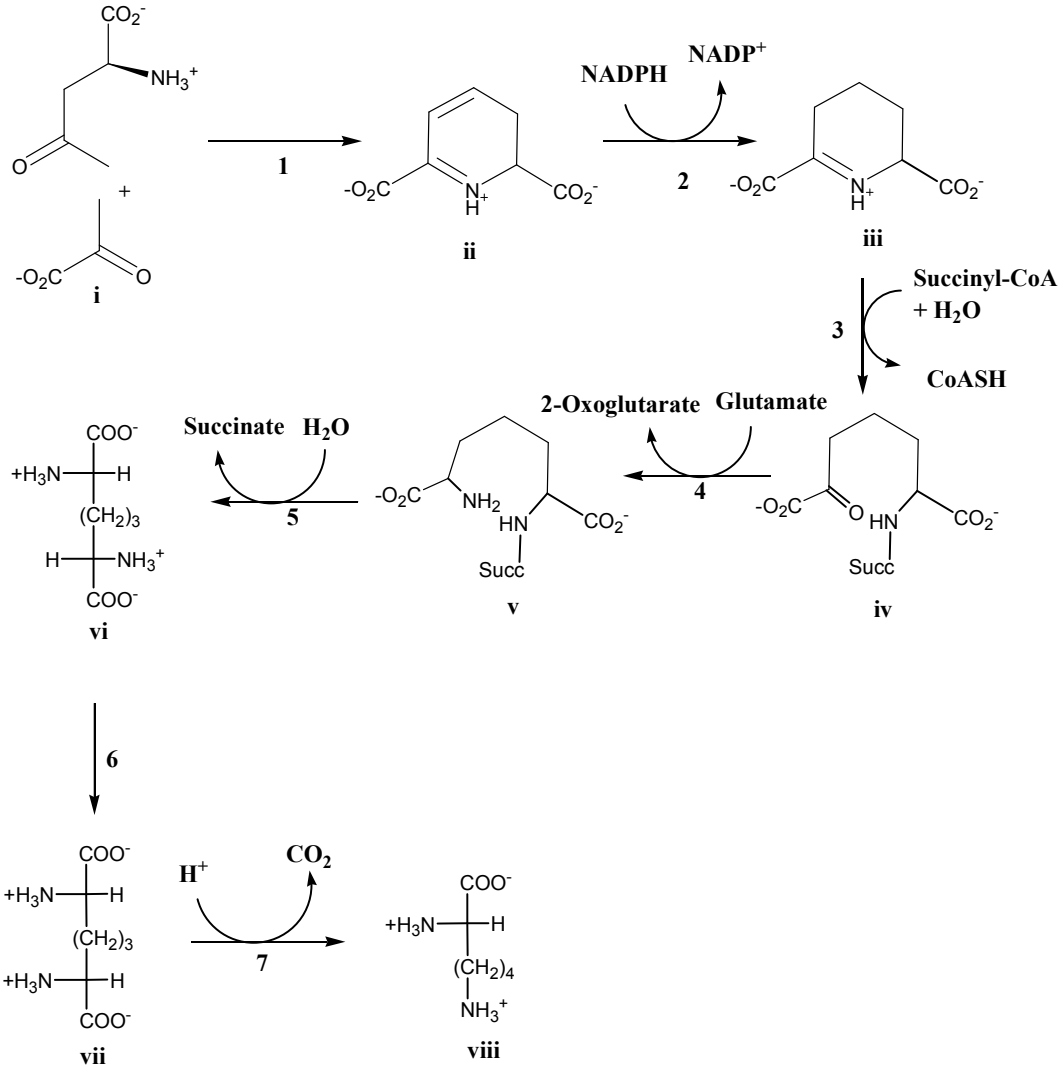

Scheme 1. The biosynthetic pathway of (*S*)-lysine in bacteria adapted from reference 35.
Names of metabolites in pathway are: i) pyruvate and ASA ii) 2,3 dihydrodipicolinate iii) 2,3,4,5-tetrahydrodipicolinate iv) *N*-succinyl-2-amino-6-keto-L-pimelate v) *N*-succinyl-L,L-α,ε-diaminopimelate vi) L,L-α,ε-diaminopimelate vii) *meso*-α,ε-diaminopimelate vii) L-lysine The enzymes catalyzing each step are: 1) dihydrodipicolinate synthase 2) dihydrodipicolinate reductase 3) N-succinyl-2-amino-6-keto-L-pimelate synthase 4) succinyl-diaminopimelate aminotransferase 5) succinyl-diaminopimelate desuccinylase 6) diaminopimelate epimerase 7) diaminopimelate decarboxylase.

Crystal structures of DHDPS have identified many residues involved in the aldol mechanism. These include K161 which has been observed covalently linked to the pyruvate.[31] A catalytic triad of Y133, T44 and Y107 is believed to provide a proton relay system to and from the solvent. Upon mutation of any of the residues in the triad, DHDPS activity was significantly reduced.[36] R238, which sits at the entrance of the active site, is proposed to bind ASA as well as to stabilize the catalytic triad.[37] All of the above residues are strictly conserved in all DHDPS enzymes, including MosA.

In addition to active site residues, tertiary and quaternary structural information is available from solved crystal structures. Bacterial DHDPS is a homotetramer, which is best characterized as a dimer of dimers as shown in Figure 7. Each dimer is comprised of a set of strongly associated monomers which, through the weak association of another dimer, form the tetramer observed.[38] Each monomer possesses the well known $(\beta/\alpha)_8$ ("TIM") barrel structure and at the C-terminal position of the barrel is the active site.[31]

The TIM barrel is made up of 8 β strands and 8 α helixes which alternate forming the easily recognizable barrel structure shown in Figure 8. This type of $(\beta/\alpha)_8$ folds are widespread throughout nature. In fact, it is the most common fold found in the protein data bank and is a structural feature of at least 15 distinct enzyme families.[39]

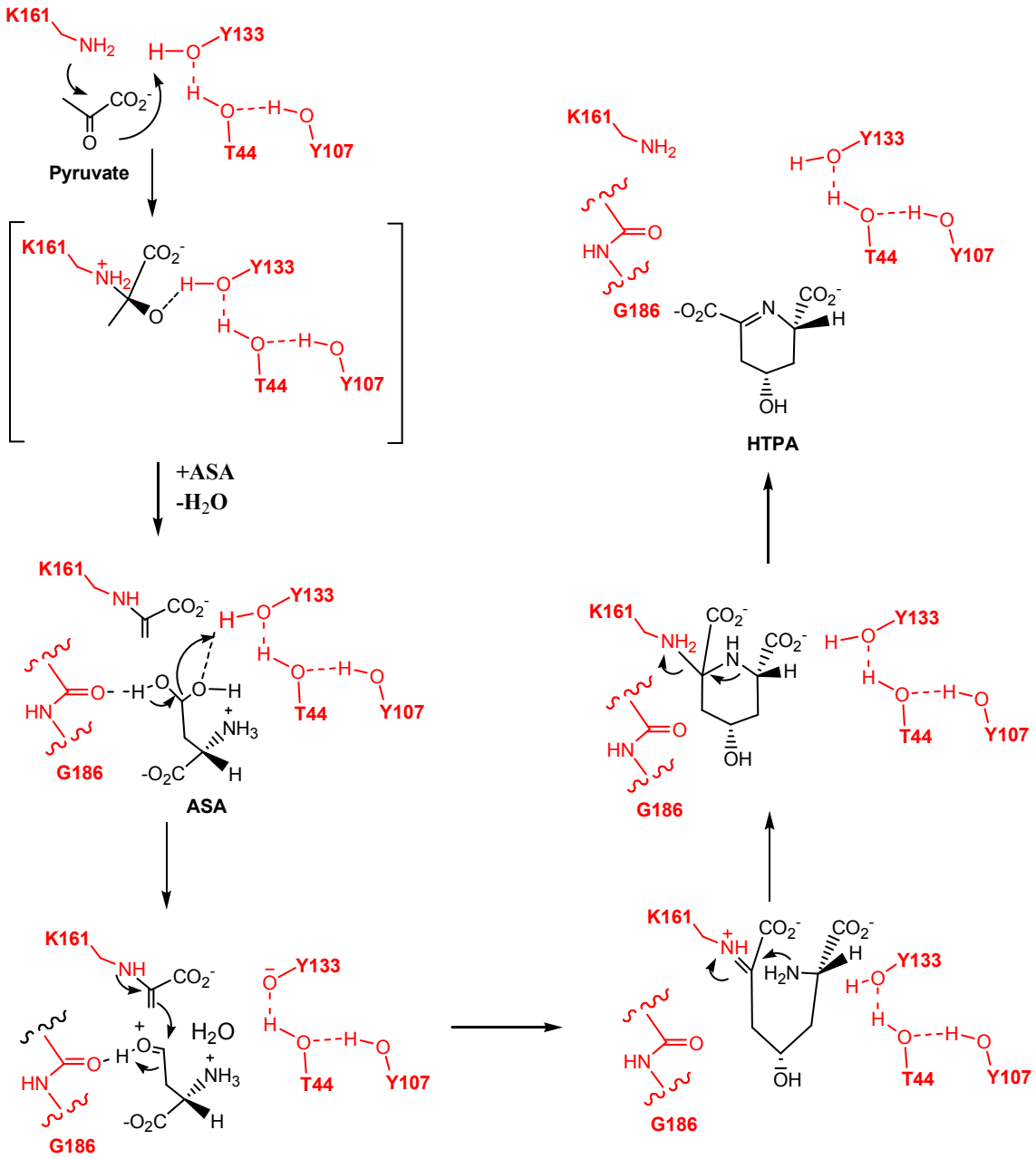

Scheme 2. The currently accepted mechanism of DHDPS from *E. coli*. Scheme adapted from Dobson et al.[40] Active site residues are red.

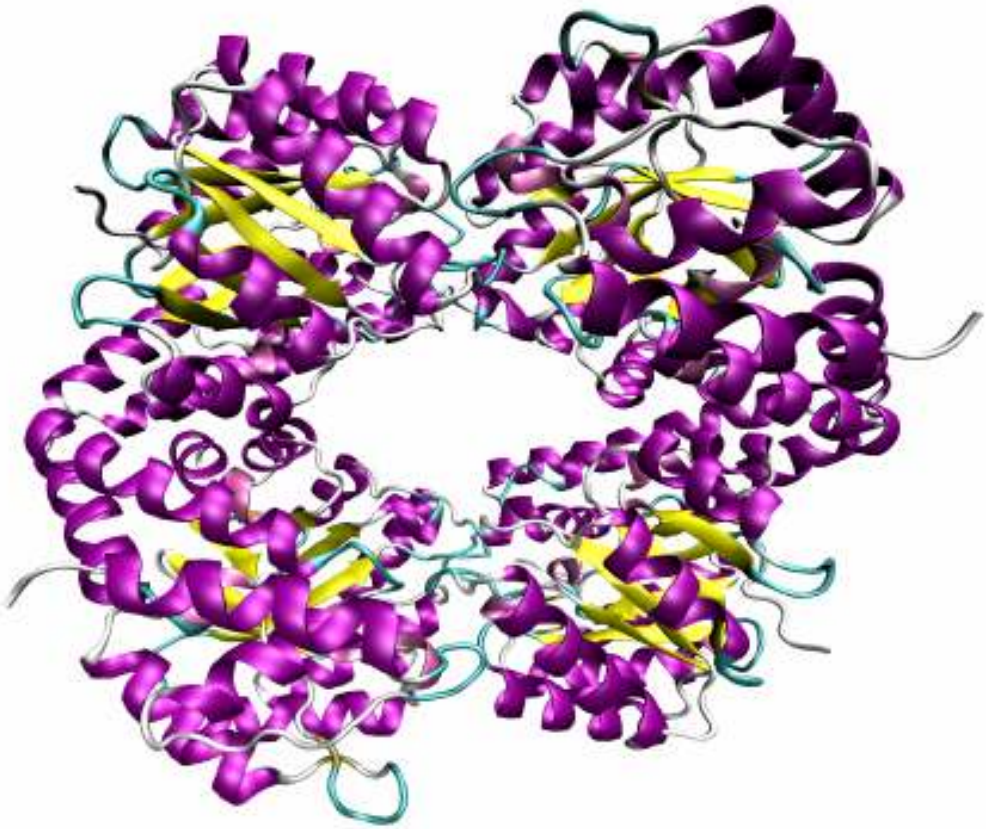

Figure 7. The quaternary structure of DHDPS from *E. coli* displaying the dimer of dimers. Each dimer is made up of strong contacting monomers which come together forming the overall tetramer. Figure produced using VMD[41] and POV-Ray software.[42]

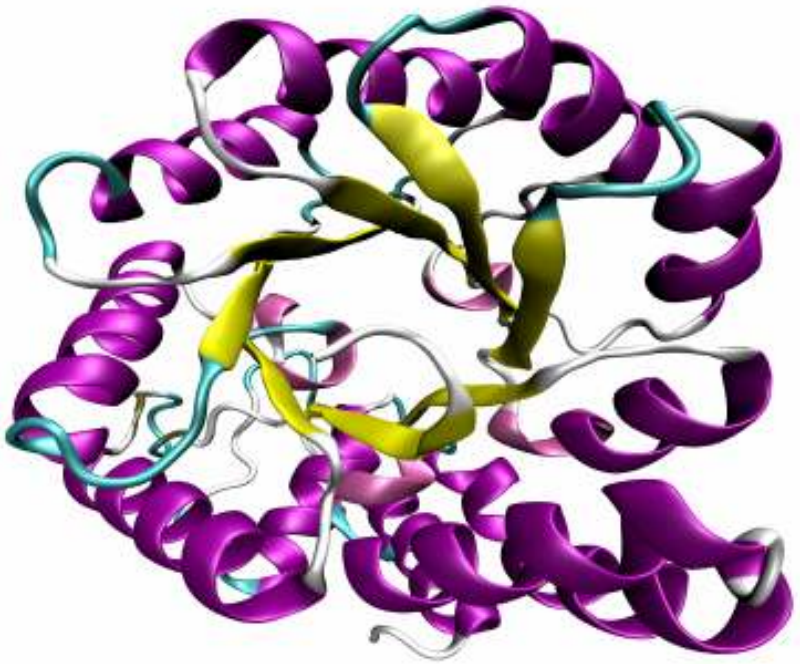

Figure 8. The monomer structure of DHDPS from E. coli. Structure displays the commonly observed $(\beta/\alpha)_8$ TIM barrel. Figure produced by VMD[41] and POV-Ray software.[42]

In DHDPS from *E. coli*, kinetic and structural studies determined that (*S*)-lysine is an allosteric, cooperative inhibitor.[31,33] Allosteric inhibition refers to an inhibitor that binds at a site different from the active site of the enzyme. The crystal structure of DHDPS from *E. coli* determined that the (*S*)-lysine binding site is located at the dimer interface with each (*S*)-lysine bound to a neighboring monomer. A water-filled channel is found between the active site and the (*S*)-lysine binding site. The cooperativity observed is not surprising due to the fact that the first (*S*)-lysine makes up part of the binding site of the second (*S*)-lysine.[33] Another interesting point regarding bound (*S*)-lysine is that the side chain of the inhibitors are in a conformationally strained bow shape shown in Figure 9.

Many enzyme-inhibitor contacts are observed between (*S*)-lysine and the binding site. The α-carboxylate of (*S*)-lysine contacts Y106 and N80 (of monomer B). The α-amino group contacts A49, E84 and N80 while the ε-amino has contacts with H56, S48 and Y133 *via* a water molecule. Upon the binding of (*S*)-lysine Y106 moves

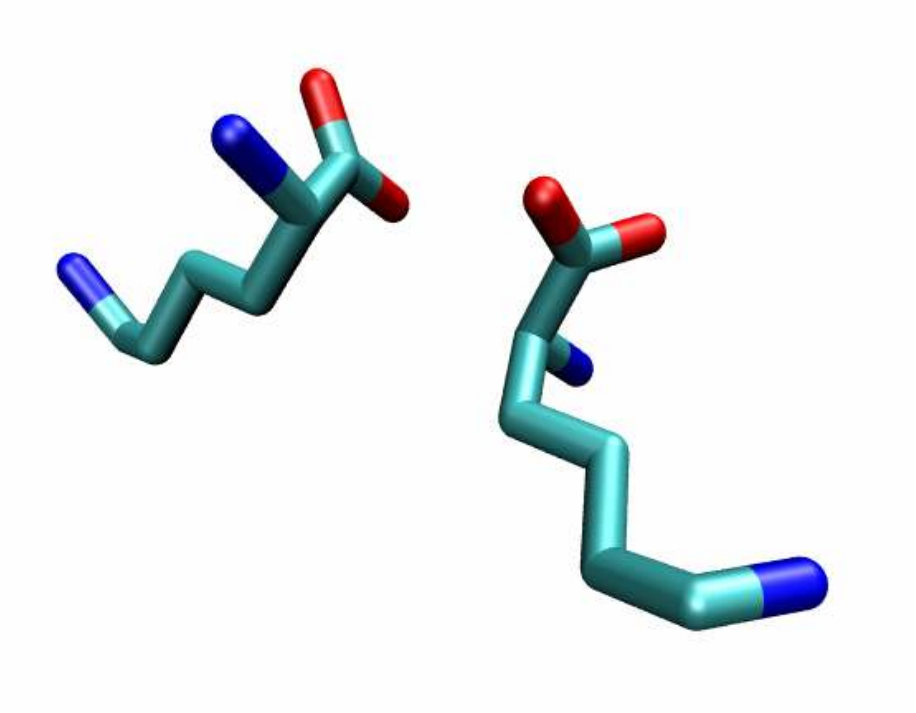

Figure 9. The conformationally strained bow shape of the (*S*)-lysines bound at the dimer-dimer interface. Figure created using VMD[41] and POV-Ray software.[42]

towards the α-carboxyl group of the inhibitor, altering the aromatic stack between Y106 and Y133. Y106 is a catalytically important residue which sits directly above the active site and is part of a hydrogen-bonded proton relay system with Y133 and T43.[36] Another catalytically important residue, R238, displayed increased B values suggesting increased movement of that residue in the (*S*)-lysine-bound structure.[37] It is very likely that the same contacts are made between MosA and (*S*)-lysine as all of the residues mentioned are conserved. No major tertiary and quaternary changes were observed by overlaying DHDPS structure with and without (*S*)-lysine. However, DHDPS from

Nicotiana sylvestris which shares 29% identity with MosA but possesses a different quaternary structure from *E. coli*, displayed significant movement in a helix portion of protein upon binding of (*S*)-lysine.[43]

1.3.1 MosA is a DHDPS

The gene for MosA was kindly supplied to our lab from Dr. Peter J. Murphy. MosA was subsequently cloned, expressed and purified as an N-terminal hexahistidine fusion protein allowing easy purification. Upon sequencing of the mosA gene, it was discovered that the originally reported sequence was missing a single deoxyguanosine base. This resulted in a frame shift which introduced a stop codon making MosA 41 amino acids shorter than originally described.[18] The extra 41 amino acids that resulted from the sequencing error were originally hypothesized to form a domain that could allow catalytic methyltransferase activity.

ASA was chemically synthesized[44] and MosA examined for DHDPS activity. The resulting assays clearly supported that MosA is indeed an efficient DHDPS with a k_{cat} value of 7.3 s^{-1}. The enzyme possessed similar Michaelis constants to DHDPS from *E. coli* with a $K_{M(Pyr)}$ of 0.6 mM and $K_{M(ASA)}$ of 0.21 mM.[13] In addition, bi-substrate kinetic analysis was performed and the initial velocity patterns indicated that the condensation of pyruvate and ASA followed the ping-pong mechanism.[13]

The k_{cat} value of 7.3 s^{-1} determined for MosA is lower than the value of 188 s^{-1} determined by Karsten[34] studying DHDPS from *E. coli*, but is still too fast to be considered as a side reaction. Furthermore, MosA is not identical to *E. coli* DHDPS,

meaning there may be some slight differences in MosA affecting turnover rate of the enzyme. Another important difference is the effects that the enzymatic assay may have on the kinetic parameters obtained. The imidazole assay,[32] which monitors the spontaneous formation of dipicolinic acid at 270 nm, has been suggested to be inferior to the dihydrodipicolinate reductase coupled assay.[45] However, this assay was sufficient in demonstrating the catalytic efficiency of MosA as a DHDPS. In fact, examining earlier reports that used the imidazole assay to determine the kinetic parameters of DHDPS from *E. coli*, the k_{cat} observed is much more consistent with that determined for MosA.[13]

DHDPS from plants and gram-negative bacteria is partially inhibited by (*S*)-lysine, the end product of the metabolic pathway. If MosA were a DHPDS belonging to the same or a similar pathway, it is possible that feedback inhibition would occur. Experiments monitoring MosA's DHDPS activity in the presence of (*S*)-lysine showed that at 5 mM concentrations a maximum inhibition of 94% was achieved.[18] Additionally, the binding of (*S*)-lysine to MosA displayed cooperativity consistent with other DHDPS enzymes.[18]

Other experiments performed to further characterize MosA as a DHDPS were imine trapping experiments and complementation analysis. Upon incubation of MosA with pyruvate and $NaBH_4$, mass spectrometry detected a major peak consistent with the mass of a reduced imine covalently attached to MosA. Furthermore, *in vivo* complementation analysis demonstrated that the presence of MosA allowed a DHDPS$^-$ mutant of *E. coli* (AT997) the ability to grow in medium not enriched with *meso*-diaminopimelate. In a control experiment, the same mutant of *E. coli* transformed with

the expression plasmid minus MosA showed no growth in media without diaminopimelate.[18] These results clearly indicate that MosA enables the cells to maintain a functional pathway to produce (*S*)-lysine.

The evidence discussed above clearly shows that MosA is a DHPDS with characteristics consistent with DHDPS from *E. coli*. Furthermore, a sequencing error led to the suggestion that an additional 41 amino acid domain may enable MosA to possess activity different from DHDPS. These findings cast serious doubt on MosA's role as a methyltransferase in rhizopine biosynthesis. However, more experimentation is required to thoroughly investigate this possibility.

1.3.2 The potential of 2-oxobutyrate as a novel methyl donor substrate for MosA

Throughout nature, methyl donors are extremely important cofactors for the maintenance of normal metabolic pathways. Only a few methyl donors have been identified as cofactors for enzymatically catalyzed methyltransfer reactions. The vast majority of enzymatic methyl transfers to oxygen rely on the ubiquitous methyl donor *S*-adenosyl-methionine (SAM). SAM is such an important molecule that it has been suggested to be second only to adenosine 5'-triphosphate (ATP) in the variety of biochemical reactions in which it is a cofactor.[46]

In addition to SAM, other less commonly utilized methyl donors are known. For example, tetrahydrofolates are used as sources of one-carbon units typically found in biosynthetic pathways of DNA, phospholipids, proteins, and neurotransmitters.[35] Of the six C-1 donating folates, only N^5-methyl-tetrahydrofolate donates a methyl group

while the others donate either a methylene or a formyl group.[47] Other less common examples of methyl carriers are methylcobalamin, a methyl derivative of vitamin B-12 that is best known for its role in synthesis of methionine from homocysteine; and betaine (trimethylglycine), a mitochondrial methylating agent involved in replication and detoxification of phenolic xenobiotics.[48]

In 1998, Babbitt and Gerlt suggested a novel methyltransferase reaction (see Figure 5) that could explain MosA's role in rhizopine biosynthesis without ignoring its similarity to DHDPS.[17] In a reaction analogous to DHDPS, 2-OB forms a Schiff base with an active site lysine providing an electron sink for nucleophilic attack by **SI** on the terminal methyl of the imine. This would result in the release of **3-MSI** and pyruvate into solution. No known methyltransferase reactions similar to this have ever been observed. Furthermore, 2-OB, a molecule typically found in amino acid metabolism, has never been determined to be a methyl donor in a biochemical reaction.

The finding that MosA has DHDPS activity seriously calls into question its implication in rhizopine biosynthesis. However, many examples of proteins with dual functions have been discovered in nature. These "moonlighting" proteins often have different functions which are typically not enzymatic. These functions often depend on their cellular location (both intracellular and extracellular), oligomerization state, and the physiological concentration of specific ligands.[49] In addition to these multifunctional proteins, there are several examples of enzymes that are catalytically promiscuous which utilize a wide range of substrates at the same active site.[50] A classic example of a promiscuous enzyme that maintains broad substrate specificity is cytochrome P450. This enzyme serves to detoxify a wide range of compounds in the

liver, therefore promiscuity is a functional advantage. On the other hand, an example more relevant to MosA comes from an "N-acylamino acid racemase" whose main biochemical role was later determined to be a *o*-succinylbenzoate synthase.[51]

In the case of MosA, it is not difficult to imagine that 2-OB could easily replace pyruvate as described in the first half of the novel methyl reaction. However, the binding and subsequent reaction of SI with the methyl group of the Schiff base is where some skepticism about MosA begins. Nevertheless, *in vitro* investigation is required as there is microbiological experimental evidence that suggests MosA may have a function in rhizopine biosynthesis separate from its DHDPS activity.

1.4 Inositol chemistry

1.4.1 Regioselective alkylations of the orthoformate of *myo*-inositol

Over the past fifteen years, research into the biological roles of inositol-based compounds has led to a greater understanding into such processes as cellular signaling, calcium release as well as the importance of inositol derivatives in anchoring of proteins to membranes.[52] The need for chemical preparations of these compounds, especially inositol phosphates, has stimulated the interest of organic chemists resulting in a wide array of synthetic methods to selectively functionalize the inositol structure.[53]

Of the eight possible diastereomers of cyclitols shown in Figure 10. only *myo*-, *neo*-, *chiro*-, and *scyllo*-inositol have been found in nature while the others *allo*-, *muco*-, *epi*- and *cis*-inositol, have not.[54] By far, the most prevalent isomer in nature is *myo*-inositol and its phosphate derivatives. Consequently, much of the synthetic work done with inositols begins with selective protection of *myo*-inositol.

One of the most popular protecting groups of *myo*-inositol is the 1,3,5-orthoester **1**. Formation of this compound, illustrated in Figure 11, requires flipping of the cyclohexanol ring such that all of the hydroxyl groups are in the axial orientation except the hydroxyl at the C-2 position. Subsequent reaction with triethyl orthoformate produces the well known adamantane-like structure. This compound is easily obtained on a large scale without the need for column chromatography.[55] The orthoformate **1** has one pair of chemically equivalent C-4 and C-6 axial hydroxyl groups and a chemically distinct C-2 hydroxyl group. The difference in reactivity between these groups allows the regioselective protection of **1** with very good yields.

The chemical reactivity of the C-4 and C-6 hydroxyl groups results from the formation of a hydrogen bond, increasing the acidity of these groups compared to the hydroxyl at the C-2 position (see Figure 12).[56] Consequently, the use of bases that can deprotonate the more acidic C-4/6 hydroxyl groups result in the corresponding anion available for subsequent addition of an electrophile at these positions. Furthermore, the use of metal hydrides as bases results in the formation of a metal chelate stabilizing the anion at the C-4/6 position.[57] The regioselectivity observed is typically independent of the electrophilic reagent but rather depends on the base employed in the reaction.[58]

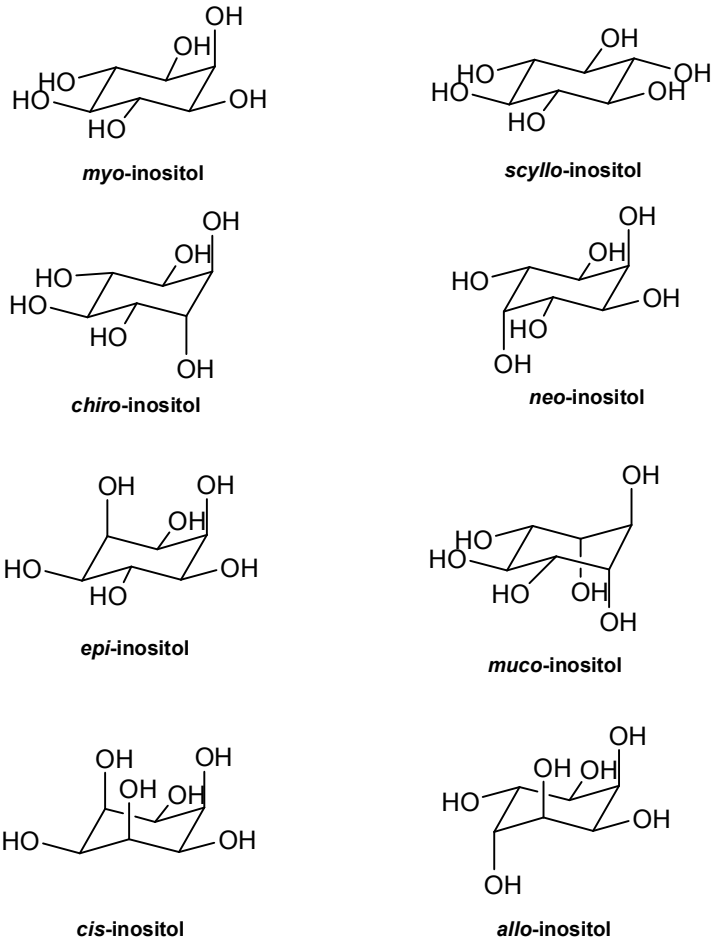

Figure 10. All possible diastereomers of inositol. The top four, *myo*-, *scyllo*-, *chiro*- and *neo*- are naturally occurring while the bottom four *epi*-, *muco*-, *cis*-, and *allo*-inositol are unnatural synthetic products.

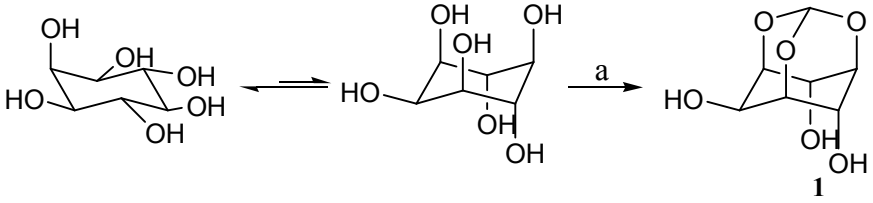

Figure 11. Formation of the orthoester of *myo*-inositol (a) toluenesulfphonic acid, triethylorthoformate, DMF, 120 ºC

In addition to selective protection at the C-4/C-6 positions, reactions that allow selective reaction at C-2 position are well known. These reactions include acylation,[59] sulfonylation[60] and silylation[61] which all offer potential orthogonal protection at the C-2 versus the C-4/C-6 positions. Regioselectivity at this position is typically accomplished with the use of weak bases that serve as nucleophilic catalysts during the reaction. Consequently, the regioselectivity relies on the relative nucleophilicity and steric hindrance of the hydroxyl groups of the orthoformate. Since hydrogen bonding between the C-4 and C-6 hydroxyl groups increases the acidity of these groups, this also reduces their basicity and nucleophilicity. In addition, increased steric hindrance of the C-4/C-6 position also contributes to the observed regioselectivity. This is especially pronounced when the electrophilic species is an ionic intermediate formed between the nucleophilic catalyst and the electrophile. This would result in selectivity by the intermediate reacting at the less hindered C-2 position.[62]

Figure 12. Rationalization of the regioselectivity demonstrated by the orthoformate of *myo*-inositol: **a** illustrates the intermolecular hydrogen bond accounting for the lower pKa at the C-4 and C-6 hydroxyl groups: **b** illustrates the chelate formed upon reaction of the orthoformate with a metal hydride

In addition to commonly used protecting groups, sulfonyl protecting groups have also been used for regioselective protection of the orthoformate.[60,63] The

regioselectivity can be controlled depending on the conditions used. One distinct advantage of the sulfonates such as tosyl and mesyl is that they do not suffer from intramolecular migrations as do the acyl derivatives, increasing their synthetic use as protecting groups.[62] A major disadvantage when using these protecting groups which are also good leaving groups is the displacement reactions that often accompany their removal. Fortunately, the removal of these groups with Mg or Na in methanol does not result in significant displacement on the adamantane like structure of **1**.

1.4.2 Aminocyclitols

Aminocyclitols were first brought to the attention of synthetic chemists by studying the chemical structure of the well known antibiotic streptomycin.[64] Since then, an entire family of amino-cyclitol antibiotics has been discovered increasing interest in the synthesis of these inosamine natural products. Structure-activity relationship studies conclude that the inosamine moiety of these antibiotics is essential for biological activity.[65] Figure 13 shows the structure of several aminocyclitols which are important parts of various antibiotics. In addition to antibiotics, aminocyclitol derivatives have also been studied as potent glycosidase[66] and glucosylceramide hydrolase inhibitors.[67] Despite the use of aminocyclitols for various biological studies, very little work has been done synthesizing *myo*-inosamine and *scyllo*-inosamine (SI) derivatives.

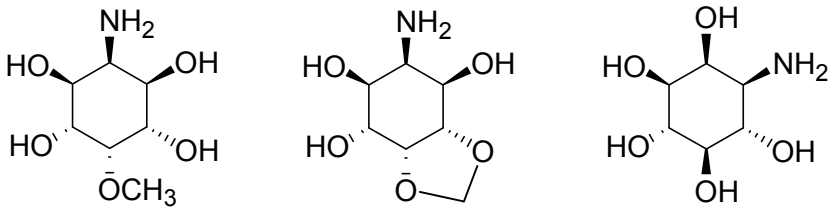

methoxyhygromycin **hygromycin A** **minosaminomycin**

Figure 13. The inosamine part of several antibiotics

The first reported synthesis of *myo*- and *scyllo*-inosamines relied on the reduction of the phenylhydrazones and oximes of inosose with Raney nickel.[68] The formation of phenylhydrazones and oximes begin with inosose, a compound easily obtained by microbial oxidation of *myo*-inositol with *Gluconobacter oxydans*.[69] However, the reductions of the phenylhydrazones and oximes showed very little stereoselectivity resulting in a mixture of both *scyllo*- and *myo*-inosamine. This required several rounds of crystallization to obtain the pure inosamine diastereomers.

The stereoselectivity of the reduction was later improved upon by Anderson and Lardy.[70] This was accomplished by switching the hydrogenation catalyst to platinum oxide and the solvent to acetic acid, resulting in almost exclusively the *myo*-inosamine isomer. **SI**, on the other hand, was obtained in about 70% stereoselectivity using sodium amalgam as the reducing agent. Despite the better selectivity, acetylation and several rounds of crystallization were still required to obtain pure compounds.

In the 1960's various inosamines were synthesized via the mesylation and S_N2 azidolysis of inositol derivatives. Despite an increased control of stereoselectivity, mixtures were still unavoidable due to acyl protecting groups participating in the azidolysis.[71] On the other hand, the participation of the acyl groups allowed the synthesis of several *chiro*-, *allo*- and *neo*- methyl inosamines with the retention of the

configuration of the reactant in the product.[72] In the synthesis of 2-deoxy derivatives of inosamine, protecting group participation was avoided by use of benzyl ethers.[73,74]

More recently, **SI** derivatives were synthesized *via* epoxide ring-opening reactions of suitably protected conduritol-B epoxides[67,75] and 1,2-diacetylconduritol E.[76] The method of the conduritol-B epoxides worked well for synthesis of **SI**, however, the conduritol-B epoxide is commercially unavailable and requires synthesis[77] increasing the overall route to 11 steps. More recently, **3-MSI** was synthesized by the reductive amination of 4-O-benzyl-6-O-methyl-2-oxo-1,3,5-*O*-methylidyne-*myo*-inositol.[78] This represents the only synthesis of inosamine via the orthoformate **1**.

1.5 Isothermal titration calorimetry (ITC)

Isothermal titration calorimetry is an increasingly important tool in biophysical chemistry. Much of its popularity is due to the ability to characterize the thermodynamics of a binding event in a single experiment. The simultaneous determination of the binding affinity (K_a), enthalpy (ΔH) and stoichiometry (n) subsequently allows the calculation of Gibbs free energy (ΔG) and entropy (ΔS) of the association. Furthermore, experiments done at different temperatures can determine heat capacity changes which also offer physical insight into the forces driving the association. In addition, the technique offers rapid thermodynamic analysis of a biomolecular system without the need to chemically modify or immobilize the species studied.

ITC directly measures the heat released or absorbed by the stepwise titration of one reactant into a sample cell containing the other. In a Calorimetry Sciences Corporation (CSC) calorimeter shown in Figure 14, removable sample and reference cells are maintained at a constant temperature in an adiabatic shield. The environment of the calorimeter is cooled by a water bath such that both cells require constant thermal energy to maintain experimental temperature. In addition to this, the cells are also maintained such that the temperature difference between the two is zero.

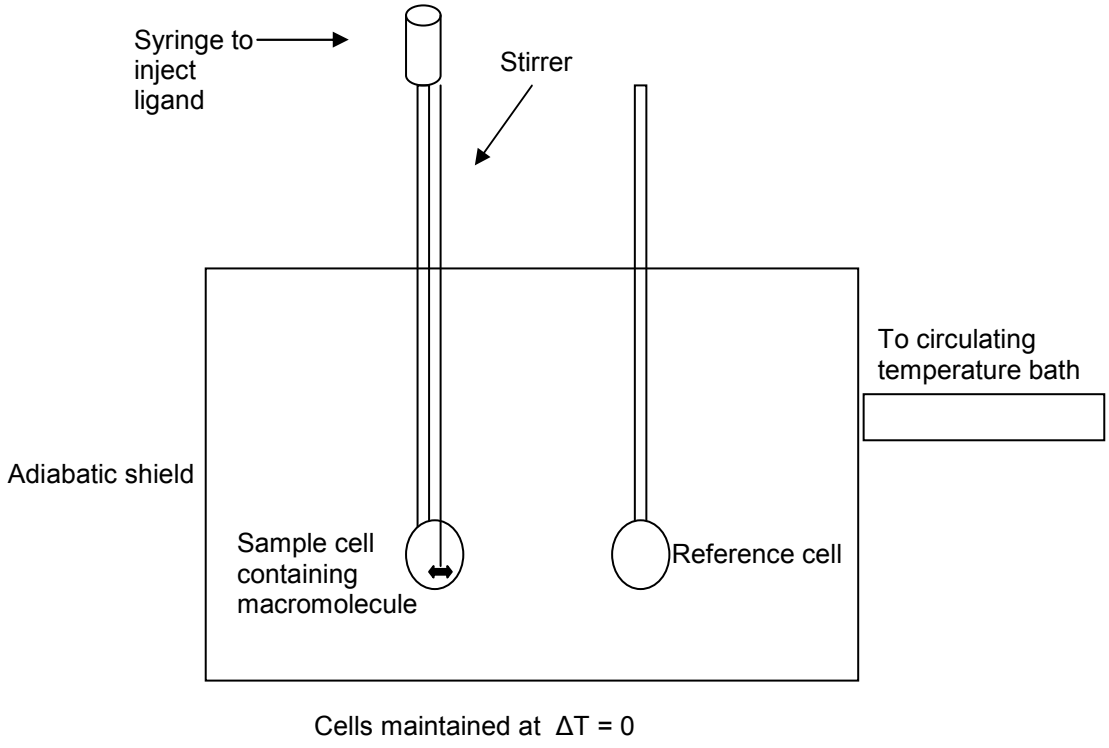

Figure 14. The basic design of a Calorimetry Sciences Corporation 4200 Calorimeter

The sample cell is filled with the enzyme solution and stirred at about 300 rpm to ensure quick mixing. The reference cell is usually filled with the same buffer used for sample cell. It is also important to minimize dilution heats by dissolving ligands

used for the titrations into buffer left over from dialysis of the protein. Upon injection of the ligand into the sample cell containing the macromolecule, thermal energy will be released or absorbed proportional to the amount of binding that takes place and the enthalpy of association. This would cause a change in the temperature of the sample cell which is relayed back to the power supply.

If the enthalpy of association is endothermic the sample cell would then require more thermal energy to maintain the temperature of the reference cell. If the association was exothermic, the reverse would occur. Thus, the raw data obtained is power (μJ/s) versus time for each injection. Integration of the power versus time data results in the heat released or absorbed during each injection. Over the course of the experiment the system becomes saturated with ligand leading to relatively small, uniform heats. These small uniform peaks correspond to the heats of dilution upon injection of the ligand which are subtracted from the experimental heats of each injection prior to data analysis. The heat changes are then normalized with respect to the moles of ligand injected and plotted against injection number or molar ratio of components. This results in the typical binding isotherm that accompanies ITC data in the literature from which curve fitting is performed.

Estimations of ΔH, K_a, and n are made by fitting the heat released or absorbed to changes in the total concentration of ligand. The calorimeter includes Bindworks software[79] which,by using nonlinear least-squares analysis, allows the fitting of the data to any of the three different binding models built into the software. This provides the estimations for association constant and the binding enthalpy making calorimetry unique.

ITC is an extremely valuable technique for those interested in thermodynamically characterizing molecular associations. ITC has contributed to a greater understanding of binding affinity especially in protein-protein[80] and protein-small molecule interactions.[81] Due to its versatility in studying various systems of low and high affinity, ITC is expected to play a vital role in rational drug design and protein-protein interactions.[82] Furthermore, since ITC is uniquely able to quantify enthalpic and entropic contributions, it is a useful bridge between computational and experimental techniques.[83]

1.6 Objectives of research

MosA is a protein originally suggested to be an *O*-methyltransferase in the conversion of the rhizopines **SI** to **3-MSI**.[14] To account for the sequence similarities between MosA and DHDPS from *E. coli* and the evidence that suggests the protein is an *O*-methyltransferase, Babbitt and Gerlt discussed the potential of a methyltransferase reaction using 2-OB as a methyl donor following a mechanism analogous to DHDPS.[17] However, it was later shown in our lab that MosA was an efficient DHDPS with kinetic constants similar to DHDPS from *E. coli*.[18] Consequently, this research will primarily focus on determining if MosA has any methyltransferase activity in producing **3-MSI** from **SI** using 2-OB or SAM as a methyl donor.

To begin with, the rhizopines were not commercially available and consequently required the development of convenient synthetic routes. Once the rhizopines were obtained, research focused on finding evidence that MosA may be an *O*-

methyltransferase. This was achieved by relying on methods typical of enzymology such as kinetic analysis, HPLC-MS, HPLC enzyme assays and ITC.

In addition to the rhizopine investigation, ITC will be used to study the binding thermodynamics of pyruvate, 2-OB and (*S*)-lysine to MosA. These experiments will lead to a greater understanding of the binding affinity that MosA has for its substrates and inhibitors. Furthermore, extraction of the thermodynamic parameters will provide insight into how (*S*)-lysine exerts its influence on MosA's DHDPS activity and the nature of its inhibition.

2 Experimental

2.1 Chemical synthesis

General

Experiments that required anhydrous conditions were performed under an inert atmosphere of either dry argon or nitrogen gas. Glassware was dried overnight in an oven set at 120 °C and assembled under a stream of inert gas. All reagents were obtained from commercial suppliers and unless indicated otherwise used without further purification. Dichloromethane was freshly distilled from calcium hydride. Thin layer chromatography (TLC) was performed on precoated silica gel plates (Merck Kieselgel $60F_{254}$, 0.25 mm thickness) and visualized with phosphomolybdic acid reagent, iodine vapours, ninhydrin (1.5 % w/v solution in *tert*-butanol) or ultraviolet light at 254 nm. Flash chromatography was performed using Merck silica gel 60 (230 – 400 mesh). NMR spectra were obtained using a Bruker 500 MHz spectrometer dissolving samples in the appropriate deuterated solvents ($CDCl_3$, CD_3OD and D_2O). Chemical shift was reported in ppm downfield from tetramethylsilane. Infrared spectra was obtained on a Bioread FTS-40 Fourier transform interferometer using a diffuse reflectance cell (DRIFT). Only those peaks

diagnostically important were reported in ν (cm^{-1}). Mass spectrometery was performed on a API Qstar XL pulsar hybrid lc/ms/ms. Melting points were measured on a Gallencamp melting point apparatus and were not corrected. NMR, mass spectrometry and elemental analysis facilities are a part of the Saskatchewan Structural Sciences Centre.

2.1.1 *Scyllo*-inosamine via reductive amination

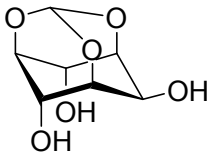

1,3,5-*O*-methylidyne-*myo*-inositol (1).[55]

This compound was made as described in the literature with an 85% yield.

^{1}H NMR (300 MHz, D_2O) δ_H 4.15 (3H, m), 4.24 (1H, m), 4.49 (2H,m), 5.51(1H, s)

^{13}C NMR (75 MHz, D_2O) δ 62.2, 69.4, 71.9, 76.4, 104.7

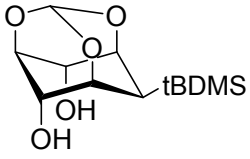

2-*O*-t-butyldimethylsilyl-1,3,5-*O*-methylidyne-*myo*-inositol (2).[61]

This compound was made as described in the literature with a 65% yield.

mp 176 – 178 °C (179 – 181 ºC)[84]

^{1}H NMR (300 MHz, $CDCl_3$) δ_H 0.16 (6H, s), 0.95 (9H, s), 3.27 (2H, d, J 7.7 Hz), 4.15-4.16 (2H, m), 4.25-4.28 (2H, m), 4.57-4.60 (2H, m), 5.51 (1H, d, J 1.2 Hz)

^{13}C NMR δ (75 MHz, $CDCl_3$) -4.4, 18.7, 60.8, 68.8, 69.0, 74.9, 102.6

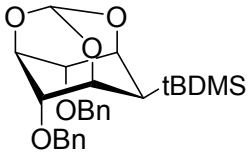

4,6-Di-*O*-benzyl-2-*O*-t-butyldimethylsilyl-1,3,5-*O*-methylidyne-*myo*-inositol (3).[84]

This compound was made as described in the literature with a 75% yield.

^{1}H NMR (300 MHz, $CDCl_3$) δ_H 0.14 (6H, s), 0.79 (9H, s), 4.17-4.18 (2H, m), 4.34-4.36 (2H, m), 4.42-4.43 (2H, m), 4.63 (4H**,** J_{AB} 11 Hz), 5.54 (1H, s), 7.29 (10 H, s)

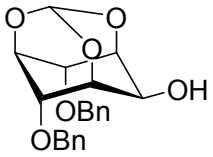

4,6-Di-*O*-benzyl-1,3,5-*O*-methylidyne-*myo*-inositol (4).[84]

This compound was made as described in the literature with a 72% yield.

^{1}H NMR (300 MHz, $CDCl_3$) δ_H 3.29 (1H, broad), 4.22 (3H, m), 4.38 (2H, m), 4.49 (1H, m), 4.62 (4H, J_{AB} 11 Hz), 5.51 (1H, d, 1.16 Hz) 7.29 (10H, m)

^{13}C NMR (75 MHz, $CDCl_3$) δ 61.6, 68.0, 71.9, 73.2, 74.0, 103.6, 127.9, 128.14, 128.7, 137.7

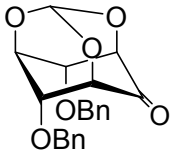

2-Oxo-4,6-di-*O*-benzyl-1,3,5-*O*-methylidyne-*myo*-inositol (5).[84]

This compound was made as described in the literature with a 85% yield

^{1}H NMR (300 MHz, $CDCl_3$) δ_H 4.42-4.51 (3H, m), 4.45-4.61 (7H, m), 5.66 (1H, s), 7.26-7.30 (5H, m)

^{13}C NMR (75 MHz, $CDCl_3$) δ 69.1, 71.8, 76.9, 78.1, 102.9, 128.0, 128.3, 128.7, 137.1, 199.4

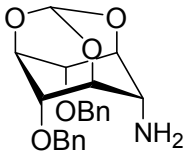

2-Deoxy-2-amino-4,6-di-*O*-benzyl-1,3,5-*O*-methylidyne-*scyllo*-inositol (6).[85]

Compound **5** (0.43 g, 1.2 mmol) was dissolved in a solution of NH_3 in MeOH (2 M, 11 mL, 22 mmol) and acetic acid (1.5 mL) was added and the reaction stirred at 0

°C for ten minutes. Sodium cyanoborohydride (0.19 g, 3.0 mmol) was added and the mixture was stirred for 3 days at room temperature. The reaction was quenched with aqueous HCl (20 mL, 10% w/v) and extracted with diethyl ether (20 mL). The aqueous phase was brought to a pH of 10 by the addition of KOH pellets and subsequently extracted with diethyl ether (3 × 20 mL). The organic layers were collected, dried ($MgSO_4$) and evaporated to yield amine **6** (0.18 g, 0.49 mmol, 43%) as a white solid that was used without further purification.

^{1}H NMR (500 MHz, $CDCl_3$) δ 2.34 (broad s, 2H, D_2O exchangeable), 3.36 (1H, m), 4.40 (4H, m), 4.61 (1H, m), 4.68 (4H, s), 5.56 (1H, s), 7.28 – 7.32 (10H, m)

^{13}C NMR (500 MHz) δ 50.88, 68.65, 71.81, 72.23, 73.99, 103.21, 128.13, 128.30, 128.95, 137.80

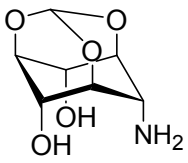

2-Deoxy-2-amino-1,3,5-*O*-methylidyne-*scyllo*-inositol.

In a 100 mL round bottom flask the inosamine **6** (0.11 g, 0.3 mmol) was dissolved in dichloromethane (1.5 mL) and diluted with methanol (9 mL) followed by the addition of palladium on activated charcoal (10 % w/w, 0.20 g). The flask was

fitted with a rubber septum and its contents were subjected to three rounds of evacuation with a water aspirator followed by flushing with hydrogen gas from a balloon fitted onto a stopcock. The mixture was stirred for 3 days, recharging the balloon with fresh hydrogen each day. The suspension was filtered through a bed of celite and the solvents removed to yield a white solid (0.055 g, 96% crude yield) that was used directly in the next step.

^{1}H NMR (500 MHz, D_2O) δ 4.17 (1H, m), 4.44 (1H, m), 4.47 (2H, m), 4.56 (2H, m), 5.64 (1H, s)

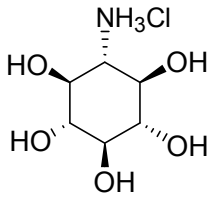

***Scyllo*-inosamine (SI).**

In a 50 mL round bottom flask the crude inosamine orthoformate (0.044 g, 0.23 mmol) was dissolved in water (8 mL). Dowex resin 50WX8-100 (H^+, 0.75 g) was added to the flask and the reaction stirred for 24 hours. The mixture was then poured into a 20 mL burette plugged with glass wool forming a column of Dowex. After the Dowex settled, the reaction water was allowed to elute and the column washed with another portion of water (10 mL). **SI** was eluted with HCl (20 mL, 0.5 M) and isolated as the HCl salt (0.04 g, 0.02 mmol, 87 % yield) upon removal of the solvent *in vacuo*.

^{1}H NMR (500 MHz, D_2O) δ 3.02 (1H, t, J = 10.6 Hz), 3.27 (1H, m), 3.34 (2H, t, J = 9.2), 3.46 (2H, t, J = 9.9 Hz)

^{13}C (500 MHz, D_2O) δ 56.25, 70.33, 73.57, 74.69

HRMS *m/z* cal'd for $C_7H_{15}NO_5$ ($M + H^+$) 180.0872, found 180.0873 (EI)

2.1.2 *Scyllo*-inosamine via isopropylidene of *myo*-inositol

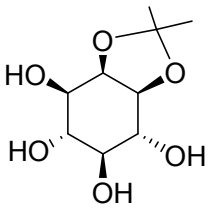

(±) 1,2-isopropylidene-*myo*-inositol (7)[86]

This compound was made as described in the literature with a 65% yield.

mp 174-176 ^{o}C (lit. mp 182-184 ^{o}C)

^{1}H NMR (500 MHz, D_2O) δ 1.25 (3H, s), 1.39 (3H, s), 3.11 (1H, t, J = 10 Hz), 3.40-3.51 (2H, m), 3.70 (1H, dd, J = 4.2Hz, 13.9Hz), 3.91 (1H, m), 4.34 (1H, t, J = 4.4 Hz)

^{13}C NMR (500 MHz) δ 25.52, 27.69, 69.79, 72.58, 72.96, 75.02, 76.45, 78.92, 110.79

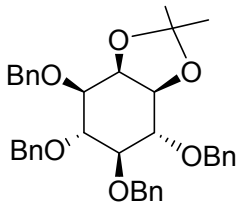

(±) 3,4,5,6-tetra-*O*-benzyl-1,2-isopropylidene-*myo*-inositol (8).[86]

This compound was made as described in the literature with an 82% yield.

^{1}H NMR (500 MHz, $CDCl_3$) δ 1.46 (3H, s), 1.57 (3H, s), 3.54 (1H, t, J = 8.9 Hz), 3.82 (1H, m), 3.92 (1H, m), 4.08 (1H, t, J = 8.5 Hz), 4.22 (1H, t, J = 6.2 Hz), 4.39 (1H, m), 4.86-5.03 (8H, m), 7.36-7.49 (20H, m)

^{13}C NMR (500 MHz) δ 26.27, 28.21, 73.77, 74.32, 75.04, 75.67, 75.72, 79.39, 79.60, 81.40, 82.70, 82.95, 110.28, 128.01, 128.07, 128.12, 128.30, 128.44, 128.48, 128.51, 128.74, 128.81, 128.86, 128.89, 138.74, 139.09, 139.13

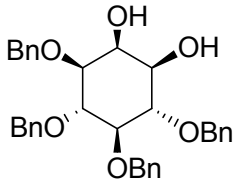

(±) 3,4,5,6-tetrabenzyl-*myo*-inositol (9).[87]

This compound was made as described in the literature with 81% yield

mp 125-126 ^{o}C (lit. 126–128 ^{o}C)

^{1}H NMR (500 MHz, $CDCl_3$) δ 2.51 (1H, broad s, D_2O exch), 2.55 (1H, broad s, D_2O exch), 3.51 (3H, m), 3.87 (1H, t, J = 9.5), 4.01 (1H, t, J = 9.5 Hz), 4.23 (1H, t, 2.6 Hz), 4.72 - 5.02 (8H, m), 7.32-7.51 (20H, m);

^{13}C NMR (500 MHz) δ 69.60, 72.17, 73.17, 76.05, 76.15, 76.38, 80.43, 81.74, 82.08, 83.65, 128.06, 128.25, 128.32, 128.39, 128.81, 128.84, 128.96, 129.01, 138.21, 138.92, 138.05

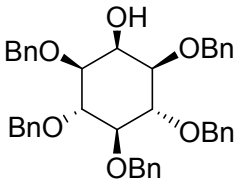

1,3,4,5,6-pentabenzyl-*myo*-inositol (10).

A solution of tetrabenzyl **9** (6.00 g, 10.6 mmol), tetrabutyl ammonium bromide (3.80 g, 11.8 mmol), dibutyltin oxide (2.90 g, 11.6 mmol) and benzyl bromide (2 mL, 16.8 mmol) in acetonitrile (230 mL) was refluxed for 24 hours. The solvents were removed *in vacuo* to yield a brownish red residue that was taken up in diethyl ether (150 mL) and washed with water (50 mL). The diethyl ether was evaporated to yield crude pentabenzyl **10** that was recrystallized with hot methanol to yield 5.01 g of pure product as long needles. Another 1.01 g (92 % total yield) was obtained upon slow evaporation of the methanol in the fume hood.

mp 124-125 ^{o}C (lit. mp 124-127 ^{o}C)[88]

^{1}H NMR (500 MHz, $CDCl_3$) δ 3.41 (2H, dd, J = 9.7 Hz, 2.7 Hz), 3.47 (1H, t, J = 9.4),4.01 (2H, J = 9.5), 4.28 (1H, t, J = 2.6 Hz), 4.75 (4H, s), 4.85-4.93 (6H, m), 7.28-7.37 (25H, m)

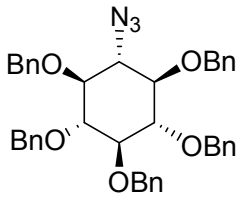

2-azido-1,3,4,5,6-tetrabenzyl-*scyllo*-inositol (11).[67]

The pentabenzyl inositol **10** (2.6 g, 4.0 mmol) was dissolved in anhydrous pyridine (25 mL). The solution was cooled to 0 ^oC when mesylchloride (1.5 mL, 20 mmol) was added dropwise while stirring. The reaction was allowed to gradually reach room temperature and was stirred for 16 hours. The solvents were removed *in vacuo* to yield a yellow residue that was taken up in CH_2Cl_2 (50 mL), washed with 1M HCl (3 × 50 mL), 1M $NaHCO_3$ (2 × 30 mL), brine (2 × 30 mL) and dried ($MgSO_4$). Without further purification the crude mesyl inositol was dissolved in dimethylformamide (22 mL) under argon. Sodium azide (1.25 g, 19.3 mmol) was added in one portion and the reaction kept at a temperature of 80 °C with continuous stirring for 20 hours. The mixture was allowed to cool and was then extracted between CH_2Cl_2 (100 mL) and water (100 mL). The organic layer was washed with $NaHCO_3$ (1M, 1 × 50 mL), water (1 × 50 mL), brine (1 × 50 mL), dried ($MgSO_4$)

and evaporated to yield a crude solid. Purification was achieved using flash chromatography (silica gel, 1:3 v/v ethyl acetate/hexane) yielding azide **11** (1.6 g, 2.5 mmol, 63 % yield).

mp 95-96 $^{\circ}$C

IR ν_{N3} 2109 cm^{-1}

^{1}H NMR (500 MHz, $CDCl_3$) δ 3.44 (2H, t, 9.3 Hz), 3.56-3.69 (4H, m)), 4.94-4.99 (10H, m), 7.33-7.46 (25H, m)

^{13}C NMR (500 MHz) δ 67.45, 76.41, 76.44, 76.48, 81.56, 83.03, 83.74, 128.20, 128.25, 128.32, 128.42, 128.70, 128.92, 128.96, 138.27, 138.72, 138.74

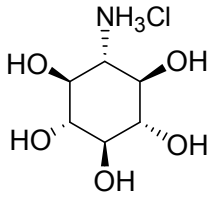

***Scyllo*-inosamine (SI).**

The azide **11** (0.07 g, 0.91 mmol) was dissolved in dichloromethane (1 mL) and diluted with methanol (10 mL). Di-*tert*-butyl dicarbonate (0.24 g, 1.1 mmol) and palladium on activated charcoal (10 % w/w, 0.14 g) were added. The flask was fitted with a rubber septum and it contents were subjected to three rounds of evacuation with a water aspirator followed by flushing with hydrogen gas from a balloon fitted onto a stopcock. The mixture was allowed to react for 2 days recharging the balloon with fresh hydrogen each day. After this time, the mixture

was filtered through a pad of celite, the solvents removed *in vacuo* to yield a white solid. The precipitate was dissolved in water (2 mL) and stirred with Dowex resin (50WX8-100, 0.3 g) for 16 hours. The mixture was then poured into a 20 mL burette plugged with glass wool forming a column of Dowex. After the Dowex settled into the column the reaction water was allowed to elute and the column washed with another portion of water (10 mL). The amine was eluted with HCl (15 mL, 0.1 M) and isolated as the HCL salt (0.17 g, 0.74 mmol, 81 % yield) upon removal of the solvent. Spectroscopic properties identical to **SI** as described above.

2.1.3 *Scyllo*-inosamine via tin chloride deprotection

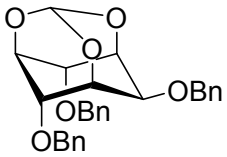

2,4,6-Tri-*O*-benzyl-1,3,5-*O*-methylidyne-*myo*-inositol (12).[57]

To a solution of **1** (1.0 g, 5.2 mmol) in dry DMF (40 mL) at room temperature and under argon, sodium hydride (1.25 g of 60 % dispersion in oil, 31.2 mmol) **(Caution: evolution of hydrogen gas!)** was added. The reaction mixture was stirred for ten minutes and then benzyl bromide (3.7 mL, 31 mmol) was added dropwise followed by continuous stirring for an additional 14 hours. The reaction was quenched with water (1 mL) and then partitioned between dichloromethane (200 mL) and water (100 mL). The organic phase was dried ($MgSO_4$) and

evaporated *in vacuo* leaving an oil that was crystallized (EtOAc:hexane) to give the tribenzyl compound (2.2 g, 4.8 mmol, 92 % yield).

^{1}H NMR (500 MHz, $CDCl_3$) δ_H 4.04 (1H, m), 4.30 (2H, m), 4.35 (2H, m), 4.43 (1H, m), 4.55 (6H, m), 5.52 (1H, d, 0.9 Hz), 7.31-7.34 (15 H, m)

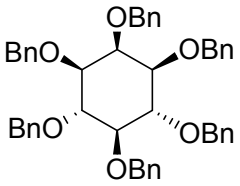

1,2,3,4,5,6-Hexa-*O*-benzyl-*myo*-inositol (13).[89]

Dichloromethane (1 mL) was added to the benzyl derivative **12** (0.76 g, 1.7 mmol) at room temperature. The solution was diluted with methanol (15 mL) and Dowex 50W-X8-100 (H^+ form, 3.5 g) was added. The suspension was stirred for 14 hours after which TLC confirmed completion of the reaction. The resin was removed by filtering the suspension and the resulting filtrate evaporated to yield a white solid. The solid was suspended in dichloromethane and evaporated three times to ensure sufficient removal of the methanol. Without further purification, the crude product was dissolved in dry DMF (20 mL) and sodium hydride (0.28 g of 60 % dispersion in oil, 7 mmol) **(Caution: evolution of hydrogen gas!)** was added. The reaction was stirred for five minutes after which benzyl bromide (0.9 mL, 7 mmol) was added dropwise followed by continuous stirring for fourteen hours. The reaction was quenched with methanol (1 mL) and the solvents removed *in vacuo* to yield an oil that was dissolved in dichloromethane (50 mL) and extracted with water (50

mL). The organic layer was then dried ($MgSO_4$) and evaporated to yield the crude **13** that was easily purified by crystallization from boiling methanol (1.12 g, 0.25 mmol, 94 % yield)

^{1}H NMR (500 MHz, $CDCl_3$) δ 3.38 (2H, dd, J = 2.16, 9.83), 3.50 (1H, t, 9.25 Hz), 4.06 (1H, m), 4.11 (1H, t, J = 9.54), 4.59 – 4.69 (5 H, m), 4.84 – 4.95 (7H, m), 7.28 – 7.31 (30 H, m).

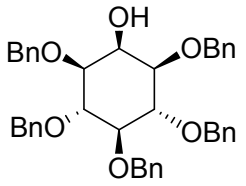

1,3,4,5,6-Penta-*O*-benzyl-*myo*-inositol (10).[89]

To a solution of **13** (0.10 g, 0.13 mmol) in dry dichloromethane under argon gas, tin (IV) chloride (0.13 mL of a 1 M solution in dichloromethane, 0.13 mmol) was added and the reaction stirred for one hour at room temperature. The reaction was diluted with dichloromethane (2 mL) then quenched with cold water (1 mL). A white precipitate formed which dissolved upon successive washes with brine (3 × 1 mL). The organic layer was dried ($MgSO_4$) and evaporated to yield a crude oil that was purified by flash chromatography (silica gel, 1:7 v/v EtOAc/toluene) to give pure **10** (0.048 g, 0.076 mmol, 55 % yield) as a white solid.

2.1.4 Racemic 3-MSI via reductive amination

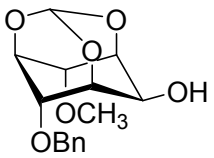

(±) 4-*O*-Benzyl-6-*O*-methyl-1,3,5-*O*-methylidyne-*myo*-inositol (14).[78] To a stirring solution of **1** (1.0 g, 5.2 mmol) in DMF (50 mL) under Argon gas, NaH (0.23 g of 60 % dispersion in oil, 5.7 mmol) **(Caution: evolution of hydrogen gas!)** was added in one portion. The mixture was allowed to stir for 20 minutes at room temperature. Iodomethane (0.35 mL, 5.8 mmol) was added dropwise and the reaction allowed to react for 16 hours. Again, NaH (0.23 g of 60 % dispersion in oil, 5.7 mmol) was added in one portion and the mixture stirred for 30 minutes at room temperature. Benzyl bromide (0.70 mL, 5.8 mmol) was added dropwise and the reaction stirred for another 16 hours. Water (1 mL) quenched the reaction followed by removal of solvents *in vacuo* to yield a brown oil. The oil was taken up in CH_2Cl_2 (50 mL), washed with water (3 × 20 mL) and dried ($MgSO_4$). The organic layer was evaporated to leave a brown oil that was purified by flash chromatography (silica gel, 1:3 v/v EtOAc/toluene) yielding **14** (0.76 g, 2.4 mmol, 47% yield) as a colourless oil.

^{1}H NMR (300 MHz, $CDCl_3$) δ_H 3.47 (3H, s), 4.12 (1H, br, s), 4.18 (1H, m), 4.27 (1H, m), 4.34 (1H, m), 4.46 (1H, m), 4.64 (2H, m), 5.49 (1H, s), 7.32-7.56 (5H, m)

^{13}C (500 MHz, $CDCl_3$) 53.80, 57.94, 61.75, 67.89, 72.03, 73.01, 73.91, 76.23, 103.76, 127.90, 128.35, 128.91, 137.99

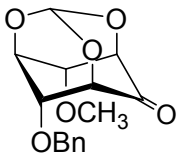

(±) 4-*O*-Benzyl-6-*O*-methyl-2-oxo-1,3,5-*O*-methylidyne-*myo*-inositol (15).[78]

To a stirring solution of oxalyl chloride (3.9 mL, 7.8 mmol) in dry CH_2Cl_2 (13 mL) maintained at -75 °C with a dry ice/acetone slurry, dimethylsulfoxide (1.2 mL) was added dropwise **(Caution: rapid evolution of gas!)**. After stirring for 10 minutes a solution of **14** (2.10 g, 7.1 mmol) in CH_2Cl_2 (8 mL) was added dropwise via cannula over the course of 5 minutes. The reaction was kept at -75 °C and allowed to stir for 1 hour after which triethylamine (5mL) was added dropwise. The solution immediately formed a precipitate and was allowed to gradually reach room temperature and subsequently diluted with diethyl ether (50 mL). The mixture was filtered through a small silica gel column (approximately an inch of silica in a column of 1 inch diameter). An additional portion of diethyl ether (50 mL) was passed through the column and combined with previous filtrate. The ether was evaporated to yield **15** (1.97 g, 94% crude yield) which was used directly without further purification.

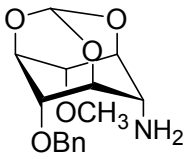

(±) 4-*O*-Benzyl-6-O-methyl-1,3,5-*O*-methylidyne-*scyllo*-inosamine (16).[85]

A solution of **15** (0.11 g, 0.38 mmol) in methanol (2 mL) was stirred at 0 °C. A portion of NH_3 in MeOH (2 M, 0.5 mL, 1.0 mmol) was added followed by acetic

acid (19 μL, 0.33 mmol) and the reaction stirred at 0 °C for ten minutes. After addition of sodium cyanoborohydride (0.070 g, 1.1 mmol) the mixture was stirred for 3 days at room temperature. The reaction was quenched with aqueous HCl (1 mL, 10% w/v) and extracted with diethyl ether (10 mL). The aqueous phase was brought to pH 10 by the addition of KOH pellets and subsequently extracted with diethyl ether (3 × 10 mL). The organic layers were collected, dried ($MgSO_4$) and evaporated to yield the amine (0.045 g, 0.15 mmol, 40%) as a colourless oil that was used without further purification.

NMR (500 MHz, $CDCl_3$) δ_H 2.10 (2H, broad s D_2O exchangeable), 3.47 (3H, s), 3.65 (1H, m), 4.16 – 4.18 (1H, m), 4.31 (2H, m), 4.34 (1H, m), 4.51 - 4.55 (1H, m) 4.64 (1H, d, J = 11.6), 4.69 (1H, d, J = 11. 3), 5.54 (1H, s), 7.29 – 7.37 (5H, m)

^{13}C NMR (75 MHz, $CDCl_3$) δ 50.5, 68.4, 71.3, 72.1, 73.7, 103.0, 128.0, 128.1, 128.7, 137.6

HRMS *m/z* cal'd for $C_{15}H_{20}NO_5$ $(M + H^+)$ 294.1341, found 294.1337 (EI)

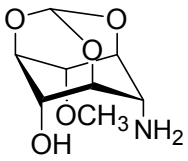

(±) 6-*O*-Methyl-1,3,5-*O*-methylidyne-*scyllo*-inosamine. In a 100 mL round bottom flask, the amine **16** (0.30 g, 1.0 mmol) was dissolved in dichloromethane (2

mL) and diluted with methanol (20 mL). Palladium on activated charcoal (10 % w/w, 0.60 g) was added. The flask was fitted with a rubber septum and its contents were subjected to three rounds of evacuation with a water aspirator followed by flushing with hydrogen gas from a balloon fitted onto a stopcock. The mixture was hydrogenated for 3 days recharging the balloon with fresh hydrogen each day. The suspension was filtered through a bed of celite and the solvents removed to yield a white solid (92 % crude yield) that was used directly in the next step.

NMR (500 MHz, D_2O) δ_H 4.14 (1H, m), 4.22 (1H, m) 4.44 (1H, m), 4.53 (1H, m), 4.58 – 4.95 (2H, m), 4.69 (3H, s), 5.63 (1H, s)

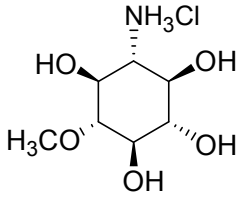

(±) 6-O-Methyl-*scyllo*-inosamine (3-MSI).

To a solution of crude amine from the above procedure (0.17 g, 0.83 mmol) dissolved in water (20 mL) Dowex resin (50WX8-100, 3.2 g) was added. The suspension was stirred for 24 hours. The mixture was then poured into a 20 mL burette plugged with glass wool forming a column of Dowex. After the Dowex settled the reaction water was allowed to elute and the column washed with another portion of water (10 mL). **3-MSI** was eluted with HCl (20 mL, 0.5 M) and isolated

as the HCL salt (0.20 g, 0.82 mmol, 82 % yield) upon removal of the solvent *in vacuo*.

^{1}H NMR (500 MHz, D_2O) δ 3.01 (1H, t, J = 10.6 Hz), 3.11 (1H, t, J = 8.8 Hz), 3.32 (2H, m), 3.38 (1H, m), 3.52 (4H, m)

^{13}C (500 MHz, D_2O) δ 56.16, 60.80, 69.82, 70.17, 72.85, 74.59, 84.52

HRMS *m/z* cal'd for $C_7H_{15}NO_5$ ($M + H^+$) 194.1023, found 194.1028 (EI)

2.1.5 Racemic 3-MSI via tin chloride deprotection

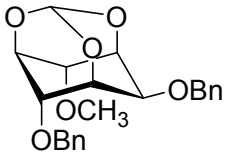

(±)2,6-Di-*O*-benzyl-4-*O*-methyl-1,3,5-*O*-methylidyne-*myo*-inositol (17). To a solution of **1** (2.0 g, 11 mmol) in dry DMF (60 mL) at room temperature and under argon was added sodium hydride (0.42 g of a 60 % dispersion in oil, 10.5 mmol) **(Caution: evolution of hydrogen gas!)**. The reaction mixture was stirred for ten minutes and then iodomethane (0.65 mL, 11 mmol) was added followed by continuous stirring for an additional 14 hours. A yellowish clear solution resulted into which another portion of sodium hydride was added (0.84 g of a 60 % dispersion in oil, 21 mmol) **(Caution: evolution of hydrogen gas!)** and allowed to react for 10 minutes. Benzyl bromide (2.5 mL, 21 mmol) was added dropwise and

the reaction stirred for another 14 hours. Water (1 mL) was used to quench the reaction and the solution was then evaporated to dryness *in vacuo* at 65 °C leaving a yellow precipitate which was dissolved in dichloromethane (20 mL), washed with water (20 mL), brine (20 mL) and dried ($MgSO_4$). The organic phase was evaporated to give a yellow oil that was purified by flash chromatography (silica gel, 1:6 v/v EtOAc/toluene) yielding **17** (2.9 g, 8.3 mmol, 75% yield) as a colourless oil.

NMR (500 MHz, $CDCl_3$) δ_H 3.41 (3H, s), 3.99 (1H, m), 4.18 (1H, m), 4.25 - 4.26 (1H, m), 4.33 – 4.34 (1H, m), 4.46 (1H, m), 4.52 (1H, d, 12.0 Hz), 4.64 (1H, d, J = 12.0 Hz), 5.57 (1H, d, 0.9 Hz), 7.30 – 7.44 (10 H, m)

^{13}C NMR (500 MHz,$CDCl_3$) δ_C 57.78, 67.94, 68.21, 70.74, 70.96, 72.05, 72.09,74.32, 76.43, 103.65, 127.92, 128.25, 128.35, 128.40, 128.72, 128.91, 138.14, 138.31

HRMS *m/z* cal'd for $C_{42}H_{44}O_6$ ($M + H^+$) 385.1646, found 385.1642 (EI)

Analysis Calculated for $C_{22}H_{24}O_6$: C, 68.74; H, 6.29, found C 67.63, H 6.09

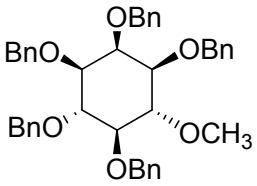

(±)1,2,3,5,6-Penta-*O*-benzyl-4-*O*-methyl-*myo*-inositol (18).

Dichloromethane (25 µL) was used to dissolve **17** (0.10 g, 0.27 mmol) at room temperature. The solution was diluted with methanol (3 mL) and Dowex 50W-X8-

100 (H^+ form, 0.5 g) was added. The suspension was stirred for 14 hours after which TLC confirmed completion of the reaction. The Dowex was removed by filtering the suspension through a disposable glass pipette plugged with glass wool and the resulting solution evaporated to yield a colourless oil. The oil was dissolved in dichloromethane and evaporated three times to ensure removal of the methanol. Without further purification, the crude oil was dissolved in dry DMF (1 mL) and sodium hydride (49 mg of a 60 % dispersion in oil, 0.11 mmol) **(Caution: evolution of hydrogen gas!)** was added. The reaction was stirred for five minutes after which benzyl bromide (0.2 mL, 2 mmol) was added dropwise followed by continuous stirring for fourteen hours. The DMF was removed *in vacuo* to yield a orange oil that was purified by flash chromatography (silica gel, 100 % toluene to 1:6 v/v EtOAc/toluene) to yield **18** as a white solid (0.165 g, 0.25 mmol, 95 % yield)

mp 72-74 ºC

NMR (500 MHz, $CDCl_3$) δ_H 3.33 (1H, dd, J = 9.85 Hz, 2.11 Hz), 3.40 (1H, dd, J = 9.83 Hz, 2.08 Hz), 3.45 (1H, t, J = 9.19 Hz), 3.74 (3H, s), 3.86 (1H, 9.49 Hz), 4.07 (1H, m), 4.11 (1H, t, J = 9.51 Hz), 4.63 – 4.73 (5H, m), 4.88 – 4.98 (5H, m), 7.33 – 7.46 (25H, m)

^{13}C NMR (500 MHz,$CDCl_3$) δ_C 61.80, 72.56, 73.16, 73.21, 74.48, 74.88, 76.28, 76.31, 81.29, 81.35, 84.11, 84.34, 127.75, 127.89, 127.94, 127.96, 128.00, 128.03, 128.23, 128.38, 128.51, 128.57, 128.75, 128.78, 128.82, 128.86, 138.86, 139.03, 139.37, 139.42

HRMS *m/z* cal'd for $C_{42}H_{44}O_6$ ($M + Na^+$) 667.3030, found 667.3031 (EI)

Analysis Calculated for $C_{43}H_{44}O_6$: C, 78.23; H, 6.88 Found C 78.05; H 6.87

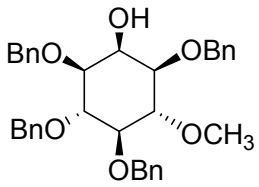

(±)1,3,5,6-Tetra-*O*-benzyl-4-*O*-methyl-myo-inositol (19).[89] A solution of **18** (0.10 g, 0.16 mmol), tin (IV) chloride (0.16 mL of a 1 M solution in dichloromethane, 0.16 mmol) in dry dichloromethane under argon gas was stirred for one hour at room temperature. The reaction was diluted with 2 mL of dichloromethane then quenched with cold water (1 mL). A white precipitate formed which dissolved upon successive washes with brine (3 × 1 mL). The organic layer was dried ($MgSO_4$) and evaporated to yield a crude oil that was purified by flash chromatography (silica gel, 1:7 v/v EtOAc/toluene) to give pure **19** (0.051 g, 0.09 mmol, 58 % yield) as a colourless oil.

NMR (500 MHz, $CDCl_3$) δ_H 2.45 (1H, s), 3.30 (1H, dd, J = 2.60 Hz, 7.03 Hz), 3.36 -3.40 (2H, m), 3.69 – 3.74 (4H, m), 3.97 (1H, t, 9.54 Hz), 4.03 (1H, m), 4.71 – 4.80 (4H, m), 4.87 – 4.92 (4H, m), 7.33 – 7.40 (20 H, m)

^{13}C NMR (500 MHz, $CDCl_3$) δ 61.83, 68.11, 73.11, 73.18, 76.30, 76.33, 80.07, 80.12, 81.47, 83.47, 83.69, 127.88, 127.96, 127.99, 128.18, 128.23, 128.25, 128.27, 128.38, 128.40, 128.75, 128.76, 128.87, 138.36, 138.52, 139.16, 139.19

Analysis Calculated for $C_{35}H_{38}O_6$: C, 75.79; H, 6.91 Found C 75.63; H 6.90

HRMS *m/z* cal'd for $C_{35}H_{38}O_6$ $(M + H^+)$ 555.2747, found 555.2754 (EI)

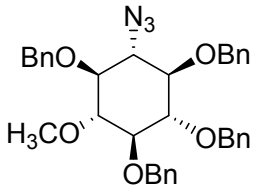

(±)2-deoxy-2-azido-1,3,5,6-Tetra-*O*-benzyl-4-*O*-methyl-*scyllo*-inositol (20).

A stirring solution of **19** (0.1 mmol) in pyridine (1 mL) was lowered partially into an ice bath. Methanesulfonyl chloride (~ 0.2 mL) was added dropwise and the reaction allowed to gradually reach room temperature. After stirring for 20 hours the solution was poured into ice water (1 mL), partitioned and the organic layer further extracted with water (2 × 1 mL), brine (2 × 1 mL) and dried (Na_2SO_4). Upon evaporation a yellowish oil remained that was redissolved in CH_2Cl_2 and evaporated once more. Without further purification, the oil was dissolved in DMF (1 mL) and treated with NaN_3 (55 mg, 0.8 mmol) and heated at 90 °C for 16 hours. The DMF was removed *in vacuo* to yield a solid that was dissolved in ethyl acetate (2 mL) and washed with water (1 mL), brine (1 mL) and dried ($MgSO_4$). Upon evaporation, a yellowish oil remained that was purified by flash chromatography (silica gel, 1:5 v/v EtOAc/hexanes) to give pure **20** as a gummy solid (40 mg, 0.07 mmol, 62 % yield).

NMR (500 MHz, $CDCl_3$) δ_H 3.26 – 3.27 (2H, m), 3.32 (2H, t, J = 9.3 Hz), 3.53 (1H, t, J = 9.0 Hz), 3.43 – 3.45 (1H, m), 3.69 (3H, s), 4.85 (8H, m), 7.32 – 7.47 (20 H, m)

^{13}C NMR (500 MHz, $CDCl_3$) δ 61.56, 61.73, 75.95, 76.00, 76.04, 81.13, 81.01, 82.68, 83.16, 127.78, 127.88, 129.99, 128.16, 128.31, 128.45, 128.51, 128.53, 128.56, 137.83, 137.90, 138.36

IR ν_{N3} 2107 cm^{-1}

Analysis Calculated for $C_{35}H_{37}N_3O_5$: C, 72.52; H, 6.43 N, 7.25 Found C 72.48; H 6.49; N, 7.05

2.2. Enzymology experimental

General

Chemical reagents including buffers, salts, (*S*)-lysine, 2-oxobutyrate and pyruvate were obtained from Sigma-Aldrich Canada, Ltd (Oakville, Ontario) or VWR CanLab (Mississaugua, Ontario) and were categorized as Molecular Biology Grade or were the highest grade available. UV-visible spectrophotometry was performed on a Beckman DU-640 spectrophotometer with a circulating-bath-controlled temperature block. Bradford assay kit was obtained from Bio-Rad and the Nanosep centrifugal devices from Pall Life Science. His-tag affinity columns were purchased from Amersham Biotech. ITC measurements were performed on a CSC ITC-4200 (Calorimetry Sciences Corp., Lindon Utah). Centrifugation was performed using either a Beckman Coulter microfuge 18 and 22R centrifuge or a Beckman J2-HS refrigerated centrifuge with a JLA-10.5 or JA-25.5 rotor. Cultures were grown in a Innova 4230 incubator shaker and were lysed using a Virosonic

600 ultrasonic cell disrupter. A BioCAD ® Sprint Perfusion Chromatography (Dr. David Sanders' laboratory, Department of Chemistry, University Of Saskatchewan, Saskatoon, SK, Canada) system was routinely used for large scale protein purifications and the BIO-RAD mini-protean 3 used to assess protein purity. Aspartate-β-semialdehyde was synthesized following the method of Morris.[44]

2.2.1 Expression of MosA

The expression vector construct containing the *mosA* gene has been described earlier.[13] A sample of the cloned BL21 cells containing the MosA gene was used to inoculate a 5 mL culture of LB broth containing 30 μg/mL of kanamycin. The culture was grown overnight, shaken at 250 rpm at 37 °C. The next day a 500 μL aliquot was used to inoculate 100 mL of LB broth containing 30 μg/mL kanamycin and incubated with shaking at 37 °C until the OD_{600} was about 0.5. After this time, isopropyl β-D-thiogalactopyranoside (IPTG) was added until a final concentration of 0.1 mM and the culture incubated overnight at 15 °C. The next day the cells were pelleted by centrifugation at 8000 rpm for 10 minutes at 5 °C in the JA-14 rotor. The media was decanted and the cells resuspended in 4 mL of binding buffer (20 mM Tris/HCl, 5 mM imidazole, 500 mM NaCl, 12.5 % glycerol, pH 7.9) and sonicated on ice fifteen times (two second bursts followed by two second cooling) at a power level of 4. The culture was left on ice for about a minute and the sonication process was repeated twice more. Insoluble material was then removed by centrifugation at 14000 rpm for 15 minutes at 5 °C using a JA-14 rotor. The solution was then decanted ready for purification.

2.2.2 Purification of MosA

Sonicated sample as described above was loaded onto a HiTrap™ Chelating HP affinity column charged with 5 column volumes of charge buffer (50 mM $NiSO_4$) and equilibrated with 3 column volumes of binding buffer. The host protein was eluted with 5 column volumes of binding buffer (20 mM Tris/HCl, 5 mM imidazole, 500 mM NaCl, 12.5 % glycerol, pH 7.9) and 5 column volumes of wash buffer (binding buffer with 60 mM imidazole and 10 mM EDTA). The histidine-tagged protein was eluted with elution buffer (binding buffer with 100 mM EDTA) collecting 1 mL fractions. Each fraction was visualized by SDS-PAGE and those pure fractions containing MosA were pooled and dialyzed into 100 mM NaCl, 20 mM Tris-HCl and 40% glycerol at pH 8 stored at –20 $^{\circ}$C.

2.2.3 Enzyme assays

Assays were performed in a 1 mL cuvette containing 100 mM imidazole buffer (pH 7.7), 10 mM K_2HPO_4, 52 nM MosA (based on monomer weight of 33341 g/mol) while maintaining a temperature of 37 $^{\circ}$C. Apparent $K_{M(Pyr)}$ values were measured at constant concentrations of 0.45 mM ASA, and apparent $K_{M(ASA)}$ values were measured at constant concentrations of 5 mM pyruvate. ASA concentrations were determined by end point assays.[13] Reaction progress was monitored spectrophotometrically @ 270 nm (formation of dihydrodipicolinate with ε_{270} = 4000 M^{-1} cm^{-1}) with measurements taken at 1 minute intervals. The spectrophotometer was blanked using assay solutions containing everything but

pyruvate and the reaction initiated with the addition of pyruvate followed by inversion of the cuvette 3 times.

2.2.4 Velocity measurements

Assays were performed as described above. Data were converted into a Microsoft Excel file using the DU600/7000 (version 1.0) file utility software provided with the spectrophotometer. This provided the data to generate a plot of absorbance vs. time; the slope of the linear portion of the graph divided by the extinction coefficient for dihydrodipicolinate (ε_{270} = 4000 M^{-1} cm^{-1}) gave initial velocities. Data were measured in duplicate and the average initial velocity values recorded.

2.2.5 Data processing

The calculated reaction rates were input into the software Leonora[90] and fitted to the Michaelis-Menten equation using a nonlinear least squares method. The program simultaneously solves for both K_M and V_{max}. The initial velocity patterns were fitted to the following equations

$$v = V_{max}A(K_M + A) \quad (2.1)$$

$$v = V_{max}A/[K_a(1 + I/K_{is}) + A] \quad (2.2)$$

$$v = V_{max}A/[K_a + A(1 + I/K_{ii})] \quad (2.3)$$

$$v = V_{max}A/[K_a(1 + I/K_{is}) + A(1 + I/K_{ii})] \quad (2.4)$$

In the above equations v is the intial velocity, V_{max} is the maximum velocity, A is the varied substrate concentration, K_M is the Michaelis constant of A the varied substrate, K_{is} and K_{ii} are the inhibition constants. Equations 2.2 – 2.4 represent competitive, uncompetitive and noncompetive inhibition respectively.

2.2.6 Inhibition of MosA with 2-oxobutyrate

Assays were performed as in the kinetic assays described above with the exception that 2-oxobutyrate was added and the solution incubated at 37 °C for 2 minutes prior to the initiation of the reaction with pyruvate. Four different concentrations of 2-oxobutyrate were used (4 mM, 1.5 mM, 1.0 mM and 0.25 mM) while varying pyruvate concentrations (0.125 mM, 0.25 mM, 0.5 mM, 1 mM and 1.5 mM) and keeping ASA concentrations constant (0.23 mM).

2.2.7 Determining effects of rhizopines on MosA-catalyzed aldolase activity

Assays were as described above with the exception that *scyllo*-inosamine was added and incubated at 37 °C for 2 minutes prior to the initiation of the reaction with pyruvate. Four different concentrations of *scyllo*-inosamine were used (0.5 mM, 2 mM, 4 mM, 10 mM) while keeping constant concentrations of pyruvate (0.5 mM) and ASA (0.23 mM).

2.2.8 Detection of imine intermediates

Three Eppendorf tubes containing 160 μL of imidazole buffer (100 mM imidazole, 10 mM KH_2PO_4, pH 7.2) and 40 μL of 2.6 mg/mL MosA (3.11 nmol) were prepared and kept on ice. A solution of pyruvate (800 mM) in imidazole buffer and a solution of 2-oxobutyrate (800 mM) were prepared. One sample labeled as the control had 2.35 μL of imidazole buffer added to it. The other two samples had 2.35 μL of the pyruvate solution (1.88 μmol) or 2.35 μL of the 2-oxobutyrate (1.88 μmol) solution added to them. After incubation of all three for 15 minutes at room temperature, 2.25 μL of freshly dissolved $NaBH_4$ (500 mM) in cold water (1.13 μmol) was introduced and the reaction allowed to sit for 1 hour on ice. After this time water (100 μL) was added and the entire solution concentrated and desalted in a Pall centrifugal concentrator. Water (100 μL) was used to dissolve the protein from the membrane and 30 μL of this was injected into a Waters 2796 Alliance Bio HPLC fitted with a C4 Symmetry 300 column (2.1 × 100 μm, 3.5 μ partical size) with UV detection at 280 nm. Mobile phases were solvent A (water with 0.1% v/v TFA) and solvent B (acetonitrile with 0.1% v/v TFA) set to the following timetable : T_{0min} 95% A, 5% B to T_{15min} 30% A, 70% B (gradient), $T_{15.01min}$ to T_{25min} 95% A, 5% B (direct). The flow rate was set at 0.5 mL/min with a column temperature of 40 °C. The HPLC was fitted with a flow splitter that allowed injection of eluent into a LCT Micromass mass spectrometer.

2.2.9 Inactivation of MosA

Samples were treated exactly as described above except that prior to concentration of the protein an overnight dialysis into imidazole buffer (100 mM imidazole, 10 mM KH_2PO_4, pH 7.2) was carried out. The protein solutions were then assayed as described above and the initial velocities compared to control enzyme.

2.2.10 HPLC investigation of MosA methyltransferase activity using 2-OB as methyl donor

Enzyme reactions were prepared containing SI (5 mM), 2-oxobutyrate (5mM), MosA (0.5 μM) in phosphate buffer (0.1 M, pH 7.0) to a final volume of 1 mL. Reactions were incubated at 37 ^{o}C with 250 μL samples removed for analysis at 1, 2 and 3 hours. Prior to derivatization, protein was removed by a Pall Life Science centrifugal concentrator following manufacturer's instructions. A 100 μL sample of the filtrate was mixed with 100 μL of 9-fluorenylmethyl chloroformate (5 mM solution in acetonitrile) and allowed to react for 15 minutes at room temperature. A 10 μL injection of the reaction mixture was injected into a HPLC fitted with a Zorbax C8 reverse phase column (250 mm × 4.6 mm I.D., 5 μm particle size) pre-equilibrated with 70 % deionized H_2O and 30 % acetonitrile. A solvent gradient to 100 % acetonitrile over 12 minutes eluted the derivatized rhizopines. The mobile phase flow rate was 1.0 mL/min, with the column temperature set at 25 ^{o}C and UV detector at 254 nm.

2.2.11 HPLC investigation of MosA methyltransferase activity using SAM as a methyl donor

Enzymatic reactions were prepared using 2.5 mM SAM, 2.5 mM *scyllo*-inosamine, 0.23 μM MosA to a final volume of 1 mL in imidazole buffer (100 mM imidazole, 10 mM KH_2PO_4, pH 7.6). A control reaction included all above reagents except MosA. Both reactions were incubated at 37 ^oC with 250 μL samples removed for analysis at 1, 2 and 3 hours. Prior to analysis protein, was removed by a Pall Life Science centrifugal concentrator following manufacturer's instructions. A 10 μL injection of the reaction mixture was injected into a HPLC fitted with a Zorbax C18 reverse phase column (250 mm × 4.6 mm I.D., 5 μm particle size) pre-equilibrated with 25 % MeOH and 75 % buffer (8 mM $CH_3(CH_2)_6SO_4Na$, 40 mM $NH_4H_2PO_4$, pH 3.0) at a flow rate of 1.0 mL/min, column temperature of 25 ^oC and UV detector set at 254 nm.

2.2.12 HPLC control reaction using COMT activity and subsequent SAH detection

Enzymatic assays were performed using phosphate buffer (200 mM NaH_2PO_4, 5 mM $MgCl_2$, pH 7.4), 100 units of catechol *O*-methyltransferase (one unit is the amount of enzyme that can catalyze the methylation of 1 nmol of 3,4-dihydroxybenzoic acid per hour at 37 ^oC), 3 mM SAM and 2 mM 3,4-dihydroxybenzoic acid. A reaction assay containing everything above except enzyme was used as a control. Both reactions were kept at 37 ^oC for 2.5 hours after

which protein was removed by a Pall Life Science centrifugal concentrator following manufacturer's instructions. A 10 μL sample was injected into the HPLC fitted with a C18 column equilibrated with 80% buffer (40 mM $NH_4H_2PO_4$, 8 mM $CH_3(CH_2)_6SO_4Na$ at pH 3.0) and 20% methanol. The parameters were a flow rate of 1.0 mL/min, 25 ^oC column temperature and UV detection at 260 nm.

2.3 Isothermal titration calorimetry

ITC measurements were performed on a CSC ITC-4200 (Calorimetry Sciences Corp., Lindon Utah) calorimeter. Purified MosA was dialyzed exhaustively against assay buffer (100 mM imidazole, 10 mM K_2HPO_4 pH 7.7) at 5 ºC. A portion of the dialysate was saved for preparation of the ligand solutions. All solutions were degassed under vacuum for a period of at least 10 minutes immediately prior to their use. A typical experiment involved 20 injections of 5 μL ligand solution (50 mM) into a sample cell containing 1.30 mL of protein solution (ca. 0.1 mM) after a stable baseline had been achieved. The sample cells were continuously stirred at 300 rpm with 3.5 minute intervals between injections. Dilution heats were determined by the area of each injection peak after saturation and subtracted from each injection. ITC data was analyzed by Bindworks 1.0 using the independent and cooperative binding models included in the software. The independent model where the analytical solution for the total heat is as follows

$$Q = V \cdot \Delta H \cdot \left[[L] + \frac{1 + [M] \cdot n \cdot K - \sqrt{(1 + [M] \cdot n \cdot K - [L] \cdot K)^2 + 4 \cdot K \cdot [L]}}{2 \cdot K} \right] \quad (2.5)$$

where V is the total volume, ΔH the enthalpy of association, K is the binding constant, n is the number of binding sites, [M] is the concentration of the macromolecule, [L] is the concentration of the ligand. A binding stoichiometry of 1.0 was input into software prior to the curve fitting for pyruvate and 2-oxobutryate. For (*S*)-lysine titrations data was fit to the cooperative binding model which assumes two binding sites on the macromolecule where the general partition function is

$$Z = 1 + \beta_1 X + \beta_2 X^2 \qquad (2.6)$$

where β are the Adair equilibrium constants ($\beta_1 = K_1$ and $\beta_2 = K_1K_2$) and X is the free ligand concentration. The degree of saturation (Y) can be expressed by

$$Y = \frac{\partial \ln Z}{\partial \ln X} = \frac{\beta_1 X + 2\beta_2 X^2}{1 + \beta_1 X + \beta_2 X^2} \qquad (2.7)$$

The total amount of ligand is

$$X_t = X + X_b \qquad (2.8)$$

where X_b is the amount of ligand bound per unit volume and free ligand can be obtained by solving

$$X = X_t - [M]Y \qquad (2.9)$$

where [M] is the concentration of macromolecule. The cumulative heat is then

$$Q = \frac{Vcell}{Z}\left(\beta_1 X \Delta H_1 + \beta_2 X^2 \Delta H_2\right) \qquad (2.10)$$

Where *Vcell* is the volume of the calorimeter cell and ΔH_1 is the enthalpy of binding for the first molecule and ΔH_2 is the enthalpy of binding for the second molecule.

3 Results

3.1 Chemical synthesis of proposed substrates of MosA

3.1.1 Synthesis of *scyllo*-inosamine

In all, three novel routes to SI were developed with variations in the protecting groups used. The first method began with the widely popular orthoformate of *myo*-inositol as shown in Scheme 3. The orthoformate **1** was an attractive structure because of the regioselectivity displayed by various protecting groups on this molecule. Since the C-2 OH of **1** required conversion to an amine, the orthoformate provided a protecting group that allowed regioselective protection of the C-2 OH through various methods. A convenient method was formation of the *tert*-butyldimethylsilyl (tBDMS) ether **2**. The reaction was done in DMF with 2,6-lutidine as a catalyst and base providing the silyl ether in 65% yield. A column purification step was required to separate the desired symmetrical compound from the 2,4- and 2,6-disilyl derivatives, the major side products of the reaction. Orthogonal protection using NaH and BnBr in DMF produced the symmetrical 4,6-dibenzyl silyl derivative **3** in 75% yield. Smooth removal of the tDBMS group using the fluoride ion in THF gave pure 4,6-dibenzyl orthoformate **4** 72% yield. Unfortunately, direct benzylation of the orthoformate using 2 equivalents of NaH and BnBr resulted in a mixture of tribenzyl, 2,4 and 4,6 dibenzyl and monobenzyl derivatives that were difficult to separate. Swern oxidation of **4** gave the ketone **5**

in 85% yield, this was followed by reductive amination using ammonia in methanol in the presence of acetic acid and $NaCNBH_3$. This reaction, after simple acid base extractions, provided **6** with the desired stereochemistry in 43% yield. Hydrogenolysis of the benzyl ethers was very slow likely due to poisoning of the Pd/C catalyst with the amino group.[91] The long reaction time was overcome by increasing the amount of catalyst to a 1:1 ratio of amine to Pd/C. Finally, hydrolysis of the orthoformate moiety with Dowex ion exchange resin 50W-X8-100 (H^+) in water and elution with 0.1 M HCl provided the desired compound with an 87% yield over both deprotection steps. **SI** was produced in 6 steps with 11% yield.

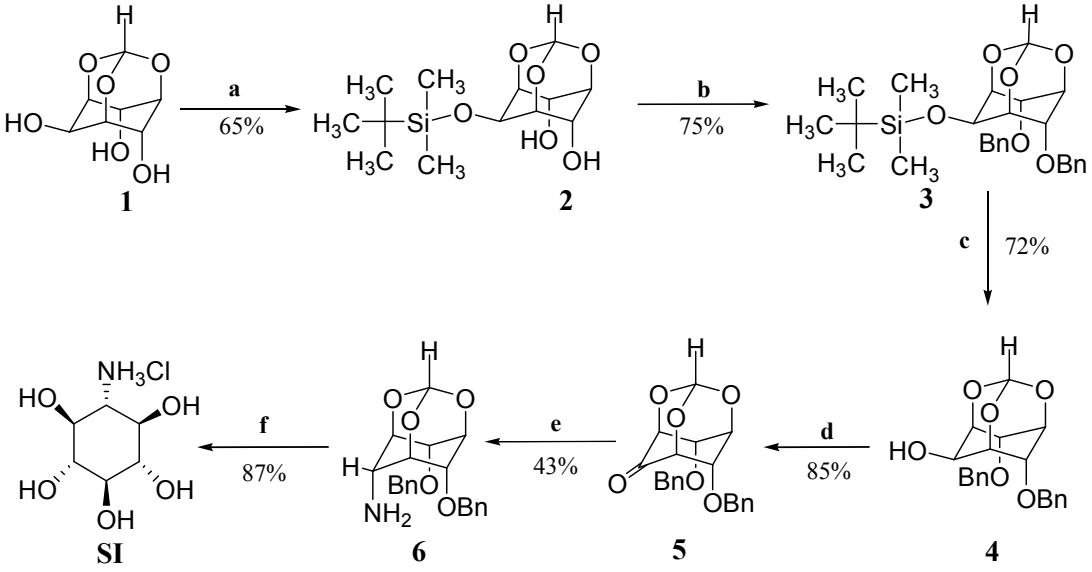

Scheme 3. Synthesis of SI from 1. Reagents and conditions: a) *t*BDMSCl, 2,6-lutidine, DMF b) NaH (2.5 equiv), BnBr, DMF c) TBAF, THF d) Oxalyl chloride, DMSO, CH_2Cl_2, TEA -60 °C f) i) Pd/C 10%, H_2, CH_3OH ii) Dowex X8-100 (H^+), H_2O

The second route developed utilized a combination of benzyl ethers and the isopropylidene of *myo*-inositol (Scheme 4). The isopropylidene **7** was produced by heating dimethoxypropane in DMSO with toluenesulphonic acid as a catalyst as described in the literature.[86] The desired compound was easily obtained on a large scale without the need for column chromatography by neutralization with triethylamine followed by the addition of ether. Perbenzylation of **7** with NaH and BnBr in DMF yielded a racemic mixture of the fully protected benzyl derivative **8** in 82% yield. The isopropylidene was removed by refluxing in CH_3OH and HCl to yield racemic tetrabenzyl **9** in 81% yield. Regioselective protection of the C-1 or C-3 OH was attempted using NaOH and BnCl in refluxing benzene[88] however, this method provided a mixture of hexabenzyl and pentabenzyl inositols. A much better method was to utilize dibutyl tin oxide in the presence of BnBr and tetrabutyl ammonium bromide in acetonitrile. The symmetrical pentabenzyl derivative was obtained in an excellent 92% yield after being easily purified by crystallization from methanol. Routine mesylation in pyridine and S_N2 azidolysis in DMF gives the protected azide **7** possessing the desired *scyllo* stereochemistry with no trace of the *myo*-isomer. Simultaneous reduction of the azide and hydrogenolysis of the benzyl groups required the *in situ* protection of the amine by incorporating $tBoc_2O$ in the reaction mixture. Without the addition of $tBoc_2O$ to the hydrogenolysis reaction, a complex mixture of partially deprotected benzyl derivatives would result independent of the amount of catalyst used and the reaction pressure. After hydrogenolysis, the carbamate was cleaved by stirring overnight with Dowex 50W-X8-100 (H^+) in water. The use of Dowex provided both the deprotection and

purification of the SI with an 81% yield. **SI** from *myo*-inositol was produced in 6 steps with a 22% overall yield.

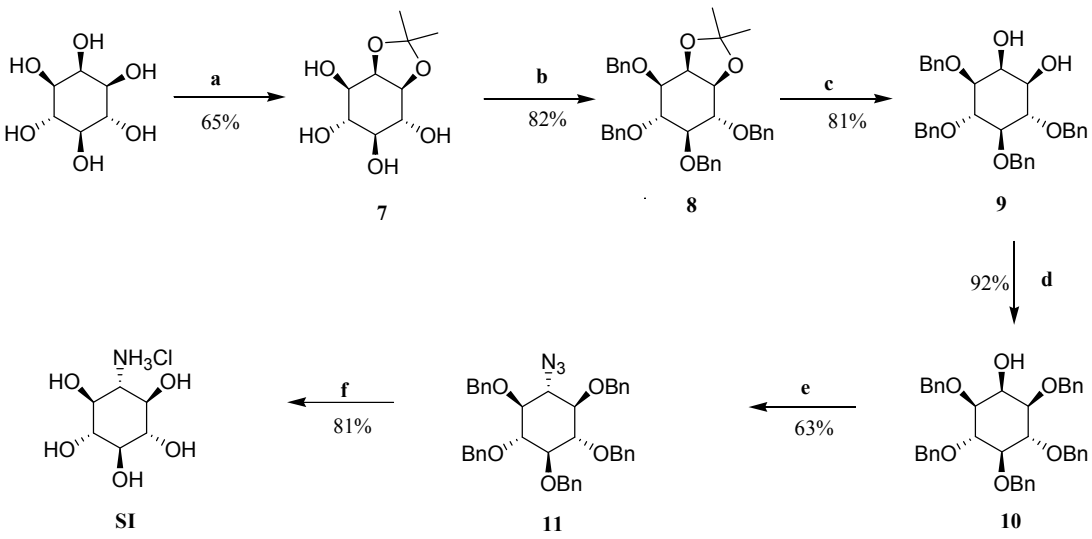

Scheme 4. Synthesis of SI from myo-inositol
Reagents and conditions: a) Dimethoxypropane, TsOH, DMSO 90 °C, b) HCl, MeOH, reflux c) NaH, BnBr, DMF d) Dibutyltinoxide, BnBr, TBAB, ACN e) i) MesylCl, Pyridine ii) NaN_3, DMF, 80 °C f) i) Pd/C 10%, H_2, CH_3OH ii) Dowex X8-100 (H^+), H_2O elute HCl

The third route shown in Scheme 5 began with the perbenzylation of **1** with NaH and BnBr in DMF to produce **12** in 92% yield. The tribenzyl ether easily crystallizes from methanol so flash chromatography is not required. The next step involves the hydrolysis of the orthoformate moiety using Dowex 50WX8-100 (H^+). A few drops of CH_2Cl_2 are added to dissolve the tribenzyl derivative followed by dilution in methanol and addition of the resin. The reaction is stirred overnight after which the Dowex is filtered and the methanol evaporated to yield tribenzyl inositol.

Perbenzylation of tribenzyl inositol in DMF using NaH and BnBr produced the symmetrical hexabenzyl **13**. Again chromatography is avoided as the hexabenzyl derivative is easily crystallized from methanol at an 88% yield for both steps. Direct perbenzylation of *myo*-inositol was reported previously, however failed to work in our hands.[89] Regioselective deprotection of the only axial benzyl group is achieved with $SnCl_4$ in CH_2Cl_2. Subsequent mesylation, azidolysis and deprotection are as described above for compound **10** to **SI**. This route produces *scyllo*-inosamine in a 5 step synthesis with an overall yield of 23%.

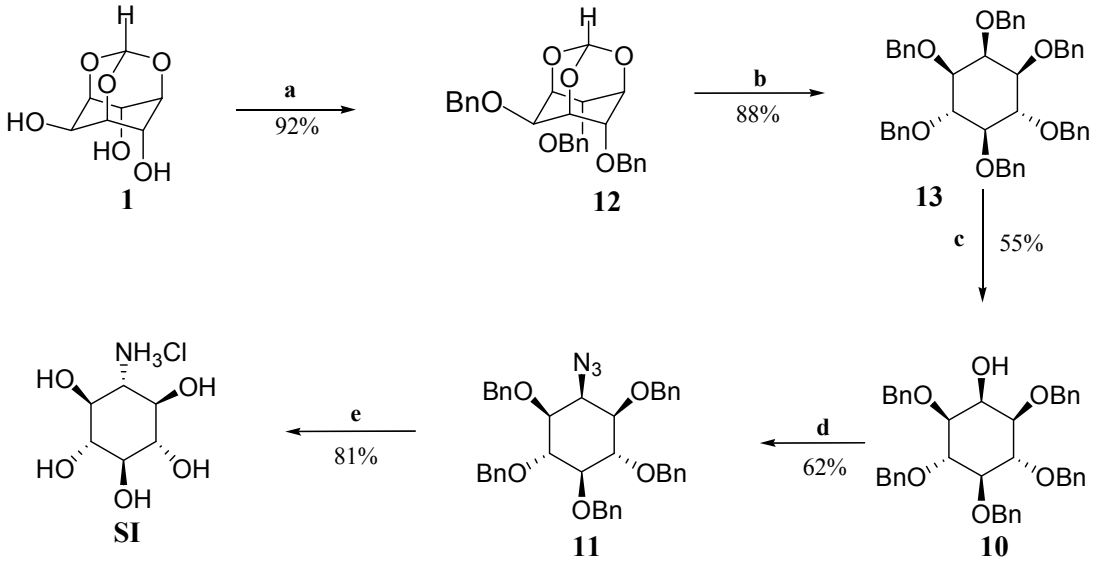

Scheme 5. Synthesis of SI via $SnCl_4$. Reagents and conditions: a) NaH, BnBr, DMF b) i) Dowex (H+) MeOH ii) NaH, BnBr, DMF c) $SnCl_4$, CH_2Cl_2 d) i) MesylCl, Pyridine ii) NaN_3, DMF, 80 °C e) *t*Boc_2O, H_2, Pd/C 10% ii) Dowex H^+, H_2O, elute HCl

3.1.2. Synthesis of racemic 3-*O*-methyl-*scyllo*-inosamine (3-MSI)

Two routes towards the synthesis of racemic 3-MSI have been developed. The first relies on the regioselective methylation of **1** using one equivalent of NaH and CH_3I in DMF followed by an additional 1 equivalent of NaH and BnBr to produce racemic **14.** This compound was purified by flash chromatography and obtained in 47% yield. Swern oxidation gave the ketone **15** in 85% yield followed by the stereoselective reductive amination to give **16** in 40% yield. Hydrogenolysis using H_2 gas and Pd/C in methanol followed by hydrolysis with Dowex 50W-X8-100 produces **3-MSI** as the HCl in 82% yield. **3-MSI** was synthesized from *myo*-inositol in 4 steps with an overall yield of 13%.

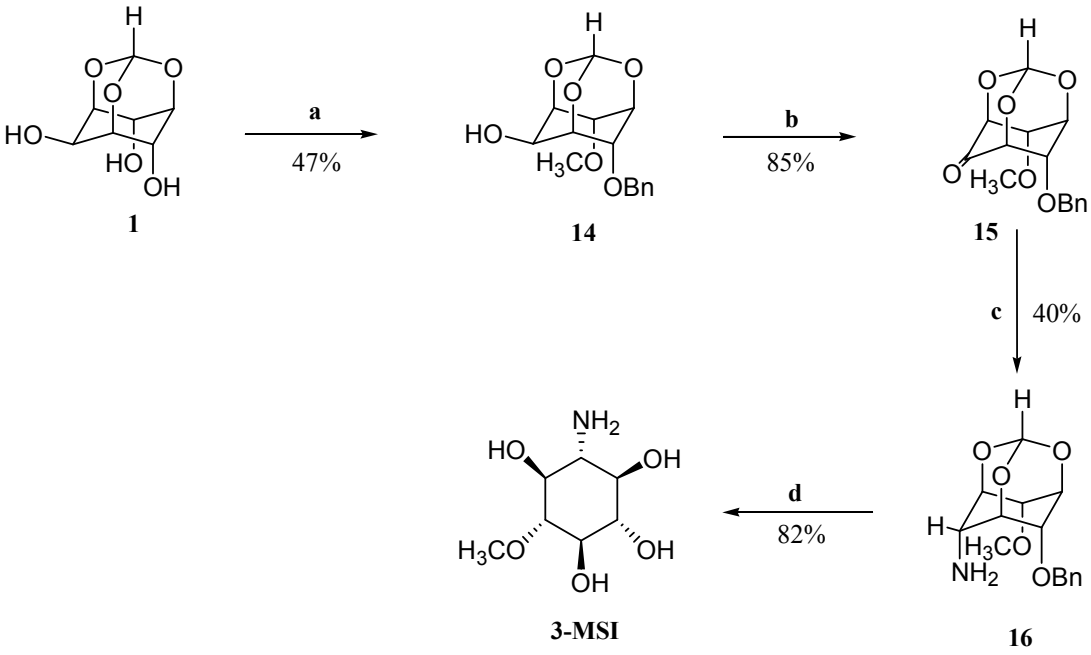

Scheme 6. Synthesis of 3-MSI via 1. Reagents and conditions a) i) 1 equiv NaH, CH_3I ii) 1 equiv NaH, BnBr, DMF b) Oxalyl chloride, DMSO, TEA, CH_2Cl_2 -60 °C c) NH_3, AcOH, $NaCNBH_3$, MeOH d) i) H_2 Pd/C MeOH ii) Dowex (H^+), H_2O elute HCl

The second route shown in Scheme 7 began with the one pot methylation and benzylation of **1** to produce racemic **17** in 72% yield. One equivalent of CH_3I and NaH in DMF was stirred overnight at room temperature followed by an additional two and a half equivalents of NaH and BnBr. Hydrolysis of the orthoformate with Dowex 50WX8-100 (H^+) followed by perbenzylation gave fully protected **18** with a 95% yield. Regioselective removal of the axial benzyl group with $SnCl_4$ in CH_2Cl_2 provided **19** in 58% yield. The free axial alcohol was mesylated in pyridine and worked up to yield an oil that was immediately subjected to azidolysis in DMF. This provided azide **20** in 62% yield with only the *scyllo* isomer detected by NMR. Simultaneous hydrogenolysis of the benzyl groups and reduction of the azide in the presence of $tBoc_2O$ protected the amine *in situ* preventing poisoning of the catalyst. Subsequent removal of the tBoc carbamate was achieved with Dowex 50WX8-100 (H^+) which also allowed purification after pouring the slurry into a column and eluting the amine with HCl (0.1M). Racemic 3-MSI was obtained in a 5 step synthesis with an overall 20% yield.

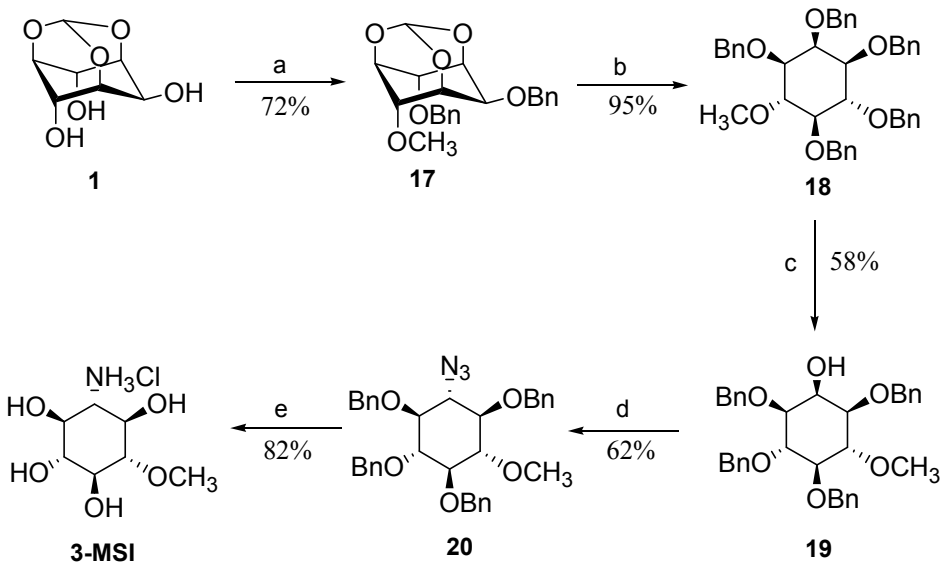

Scheme 7. Synthesis of 3-MSI via $SnCl_4$. Reagents and conditions: a) i) NaH, CH_3I, DMF ii) NaH, BnBr b) i) Dowex (H^+) MeOH ii) NaH, BnBr, DMF c) $SnCl_4$, CH_2Cl_2 d) i) MesylCl, Pyridine ii) NaN_3, DMF, 80 °C e) $tBoc_2O$, H_2, Pd/C 10%, CH_2Cl_2/MeOH ii) Dowex H^+ H_2O, elute HCl

3.2 Protein expression

3.2.1 Expression of MosA

The expression of MosA at different temperatures and various concentrations of IPTG was investigated to optimize expression yields. Unfortunately, most of the MosA overexpressed was located in the insoluble fraction after sonication and centrifugation. Experimental cultures were set up in parallel varying the concentration of IPTG from 0.1 mM to 0.5 mM and the expression temperatures at 15 and 20 °C. The results show that increasing IPTG to

concentrations greater than 0.1 mM actually lowered the amount of soluble protein. On the other hand, when kept at 0.1 mM IPTG, lowering the expression temperature had a positive effect on the amount of soluble enzyme. The optimal conditions were as follows: cultures were grown in LB media in an incubator shaker set at 250 rpm and 37 °C until reaching an optical density between 0.6 and 0.8 measured at 600 nm. The culture temperature was lowered to 15 °C, induced with IPTG to a final concentration of 0.1 mM and incubated overnight with shaker speed set at 250 rpm. Following this procedure MosA was routinely isolated with yields of ~ 10 mg protein/1L culture.

3.2.2 Purification and storage of MosA

The mosA gene was cloned by Tony Tam[13] into the pET28b expression vector. This vector contains the gene sequence for a hexahistidine tag that is expressed on the N-terminus of MosA. This allows one-step purification of MosA by using a 1 mL HiTrap chelating Sepharose FF column which coordinates nickel, a metal with a high affinity towards hexahistidine peptides. However, following the manufacturer's procedure resulted in MosA preparation being slightly contaminated with proteins endogenous to the *E. coli* BL 21 (DE3) strain that had a low affinity to the chelating column (see Figure 15).

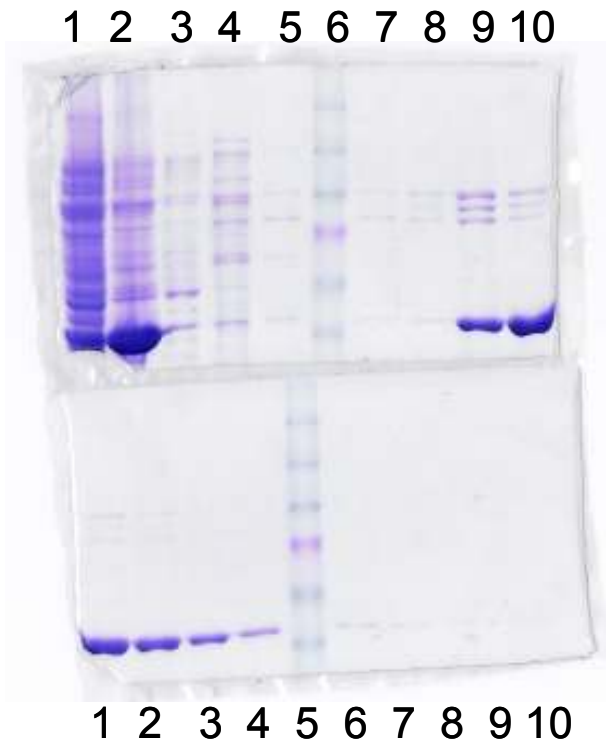

Figure 15. SDS-PAGE of optimized MosA expression and purification: Top gel: Lane 1, insoluble pellet after sonication; Lane 2, soluble fraction after sonication; Lane 3, flow fraction 1; Lane 4, binding buffer wash; Lane 5, wash buffer fraction 1; Lane 6, protein molecular weight standards (Invitrogen) - molecular weight markers from top of gel as follows 1: 181.8 kDa 2: 115.5 kDa 3: 82.2 kDa 4: 64.2 kDa* (pink band) 5: 48.8 kDa 6: 27.1 kDa; Lane 7, wash fraction buffer 2; Lane 8, elution fraction 1; Lane 9, elution fraction 2; Lane 10, elution 3; Bottom gel: Lanes 1- 4, elution fractions 4-8; Lane 5, protein molecular weight standards; Lane 6 – 8, elution fractions 8 – 10.

By washing the column with 95% washing buffer 5% elution buffer, MosA was purified almost to homogeneity. MosA was found to be active for extended periods (more than 3 months) if stored in Tris buffer (20 mM, pH 8.0), NaCl (200 mM) and glycerol (40% v/v) at -20 °C. For ITC experiments, short term storage (less than 3 days) of MosA was typically done in imidazole buffer (100 mM, 10 mM K_2HPO_4 pH 7.7) at 5 °C.

3.3. Enzyme assays

3.3.1 MosA's aldolase activity

To confirm the kinetic parameters of MosA, assays were performed at 37 ºC in imidazole buffer (100 mM imidazole, 10 mM K_2HPO_4, pH 7.7). Kinetic data were analyzed with Leonora[90] using equal weight curve fitting calculations. Apparent values were obtained by varying the concentration of one of the substrates (either pyruvate or ASA) while maintaining a constant concentration of the other. The results were an apparent $K_{M(Pyr)} = 0.58 \pm 0.03$ mM (see Figure 16) while maintaining a constant concentration of ASA (0.45 mM). For ASA an apparent $K_{M(ASA)} = 0.22 \pm 0.04$ (see Figure 17) was obtained while maintaining a constant concentration pyruvate (5 mM). Substrate inhibition was evident at higher ASA concentrations. The kinetic parameters obtained are summarized in Table 1.

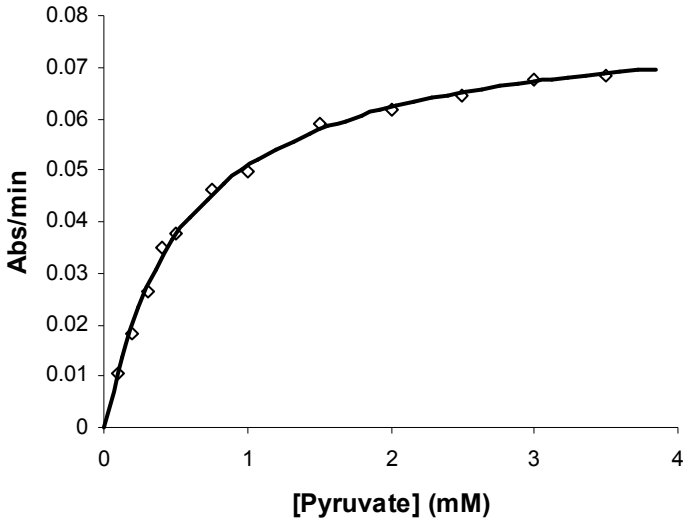

Figure 16. Initial velocity at fixed concentrations of ASA (0.45 mM) as a function of pyruvate concentration. Reactions performed in assay buffer (100 mM imidazole, 10 mM K_2HPO_4, pH 7.7) at 37ºC. The data points (◊) are experimental data while the line represents the fit from Leonora.[90]

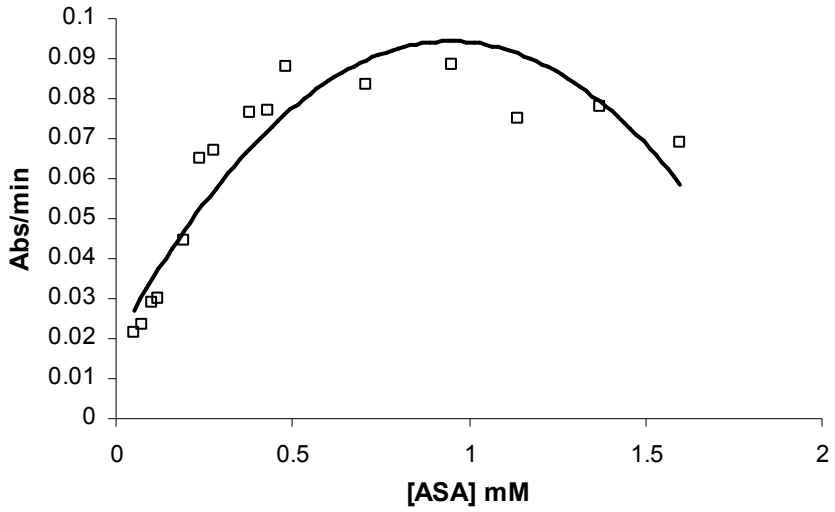

Figure 17. Initial velocity pattern at fixed concentrations of pyruvate (5 mM) while varying ASA concentration. Reactions performed in assay buffer (100 mM imidazole, 10 mM K_2HPO_4, pH 7) at 37 ºC. The data points (□) are experimental data while the line represents the fit from Leonora.[90]

Table 1. Summary of the apparent kinetic parameters determined for MosA at 37 ºC

	V_{max} (μM min^{-1})	K_M (mM)	k_{cat} (s^{-1})	k_{cat}/K_M ($M^{-1}s^{-1}$)
Pyruvate	20 ± 3	0.58 ± 0.03	6.6 ± 1	$(1.1 \pm 0.2) \times 10^4$
L-ASA	28 ± 3	0.22 ± 0.01	9.0 ± 1	$(4.1 \pm 0.1) \times 10^4$

In calculations of kinetic parameters the molar mass of MosA was taken as 33341 g/mol.

3.4 Inhibition studies

3.4.1 Inhibition of MosA's DHDPS activity by 2-OB

It has been proposed that MosA may be an O-methyltransferase catalyzing the transfer of a methyl group from 2-OB to **SI**.[17] If 2-OB was a methyl donor forming a Schiff base in analogy to pyruvate of the aldolase reaction of MosA, it would be unlikely that the active site for both reactions would reside at different locations in the enzyme. Consequently, 2-OB should affect the known DHDPS activity of MosA if it were a substrate. Kinetic data on MosA's DHDPS activity obtained in the presence of 2-OB was analyzed by Leonora.[90] The resulting patterns shown in Figure 18 fit well to that of a competitive inhibitor and a $K_I = 0.9 \pm 0.3$ mM with respect to pyruvate was determined. Extremely poor fits resulted when attempts were made to fit the kinetic data to the equations for noncompetitive and uncompetitive inhibitors.

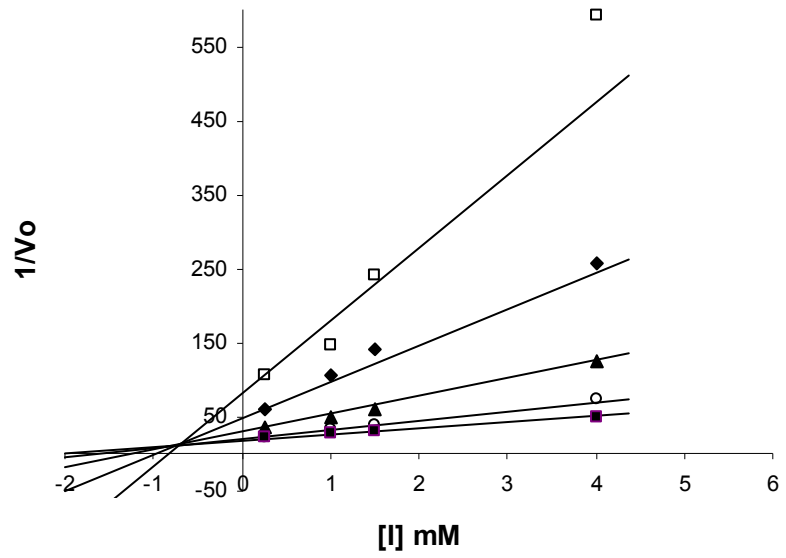

Figure 18. Dixon Plot of inverse initial velocity (1/µM/min) vs concentration of 2-OB (mM) at various concentration of pyruvate (□ 0.125 mM, ♦ 0.25 mM, ▲ 0.5 mM, ○ 1.0 mM ■ 1.5 mM). Reactions performed in assay buffer (100 mM imidazole, 10 mM K_2HPO_4, pH 7.7) at 37 ºC.

3.4.2 Inhibition of MosA's DHDPS activity with SI

The reaction mentioned by Babbitt and Gerlt shown in Figure 5[17] described SI as the potential nucleophile in the novel methyltransferase reaction with 2-OB catalyzed by MosA. Since 2-OB forms a Schiff base with MosA and is a competitive inhibitor with respect to pyruvate it is reasonable to expect the novel methyltransferase activity to share the same active site as the DHDPS reaction. Consequently, **SI** could affect MosA's DHDPS activity. Kinetic analysis plotted in Figure 19, shows that even at very high concentrations of **SI** little change is observed in the rate of the DHDPS reaction.

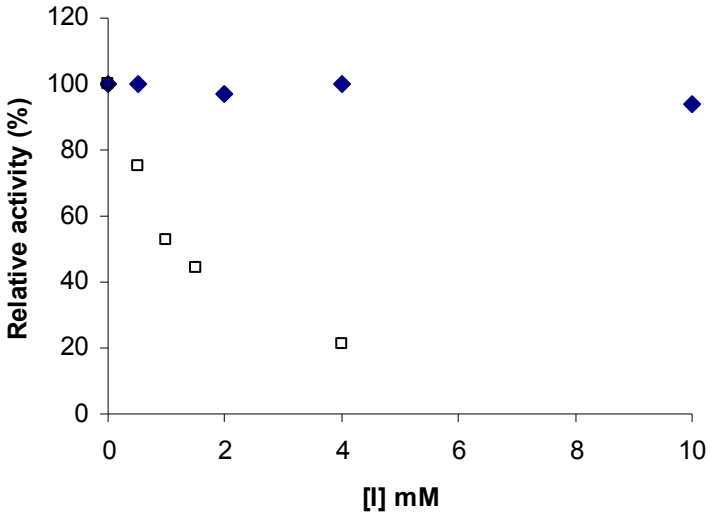

Figure 19. Inhibition of MosA's DHDPS activity by 2-OB (□) and SI (♦) at fixed concentration of pyruvate (0.5 mM) and ASA (0.22 mM). Reactions performed in assay buffer (100 mM imidazole, 10 mM K_2HPO_4, pH 7.7) at 37ºC.

3.5 Detection of imine intermediates

3.5.1 Sodium borohydride reduction of imine with 2-oxobutyrate (2-OB)

It has been shown that DHDPS from *E. coli* forms a Schiff base between pyruvate and an active site lysine (K161)[31] which can be observed by mass spectrometry.[32,92] Sequence alignments between MosA and DHPDPS show that this lysine residue is conserved in the MosA sequence. The first step in the proposed methyltransferase reaction involves the formation of a Schiff base between MosA and 2-OB. Treatment of MosA with $NaBH_4$ followed by HPLC-MS resulted in a peak corresponding to a mass of 33342 ($M + H^+$) as shown in Figure 21. This is the mass expected for MosA without any modifications, demonstrating that the reagent

itself does not affect the mass of the protein. Treatment of MosA with $NaBH_4$ in the presence of 2-OB followed by HPLC-MS resulted in a peak corresponding to a mass of 33427 ($M+ H^+$) as illustrated in Figure 22. The difference in the masses is 85 corresponding to the mass difference expected for a reduced Schiff base between MosA and 2-OB as shown in Figure 20.

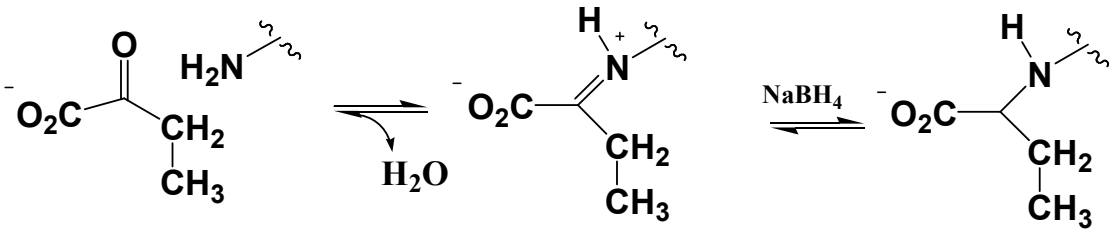

Figure 20. Formation of a Schiff base between 2-OB and lysine residue of MosA and subsequent reduction by sodium borohydride. The mass difference between modified and natural MosA would be 85 g/mol corresponding to the addition of $C_4H_5O_2$ to the protein.

3.5.2 Inactivation of MosA through reduced Schiff base intermediates

For both the control and the 2-OB samples, a portion of the solution was removed and dialyzed after treatment with $NaBH_4$. Kinetic analysis, summarized in Table 2, revealed that the treatment of MosA with borohydride had little effect on MosA's DHDPS activity. On the other hand, the protein which was modified by 2-OB and borohydride showed little activity after dialysis. This is evidence that 2-OB is forming a Schiff base in the DHDPS active site of MosA.

Table 2: Relative activity of MosA after treatment with $NaBH_4$

	MosA	MosA + $NaBH_4$	MosA + 2-OB + $NaBH_4$
Relative Activity (%)	100 %	97 %	12 %

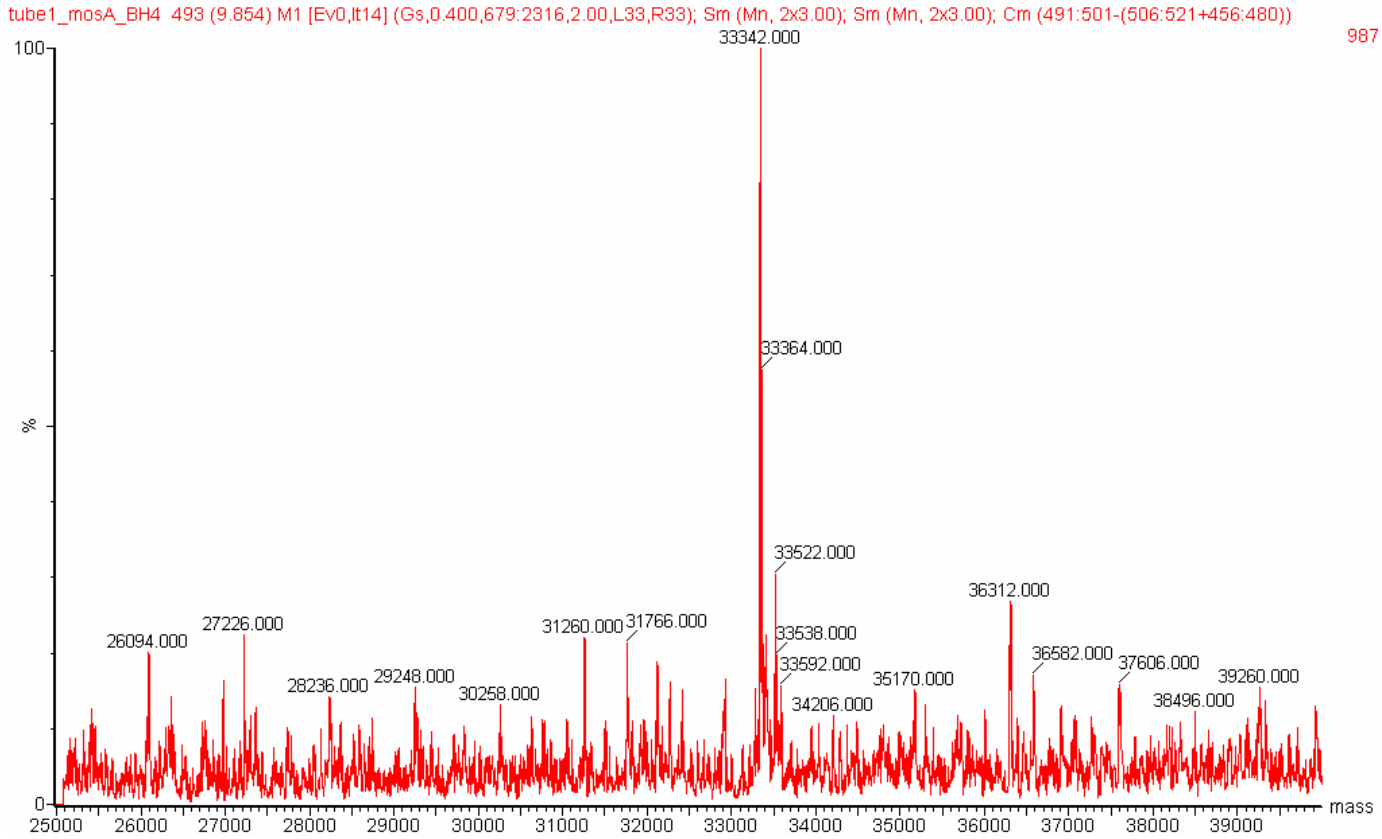

Figure 21. Control experiment for detection of a Schiff base intermediate by HPLC-MS. Mass spectrum obtained of MosA (3.11 nmol) treated with $NaBH_4$ (1.13 µmol) in assay buffer (100 mM imidazole, 10 mM KH_2PO_4, pH 7.2).

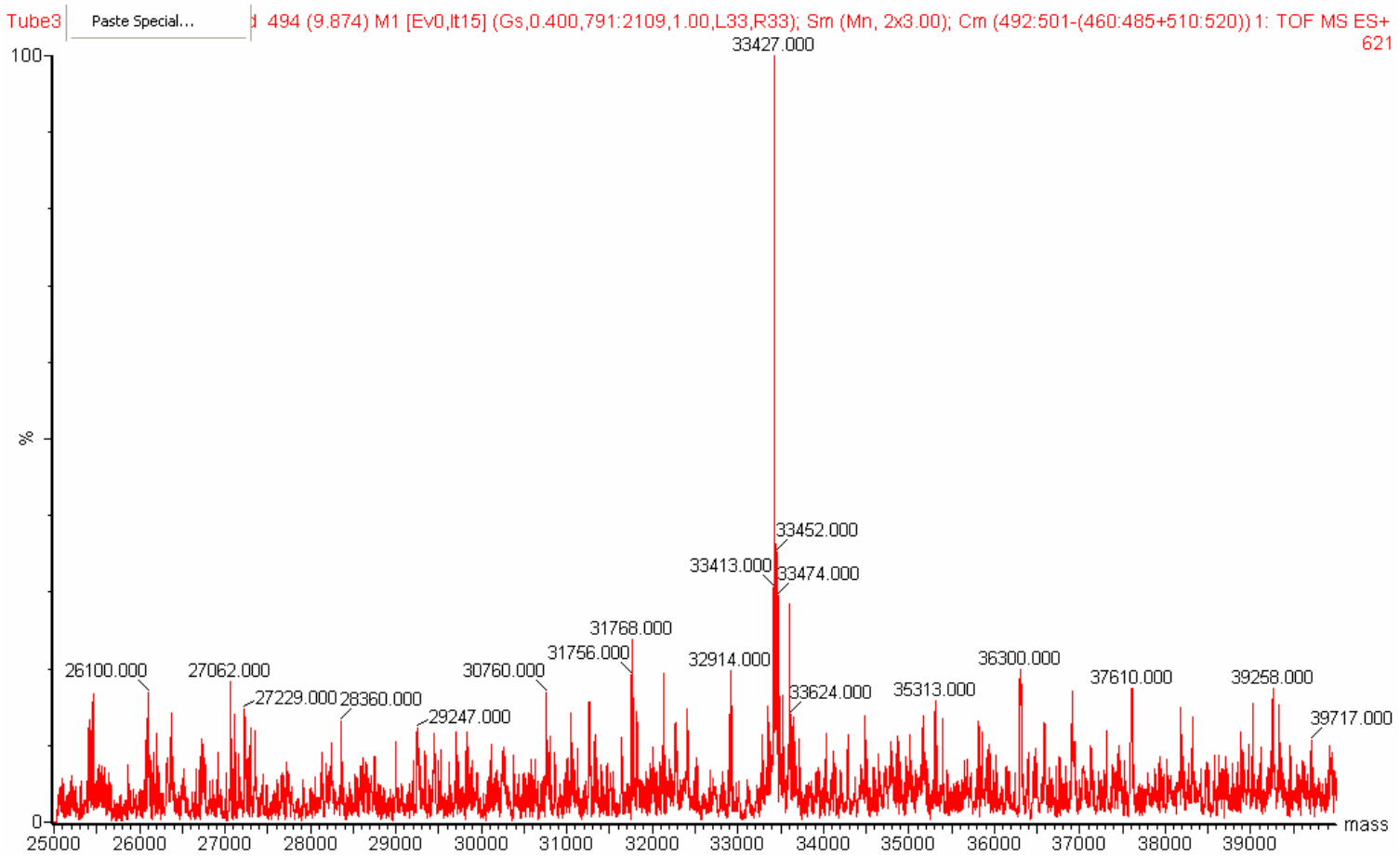

Figure 22. Detection of a Schiff base intermediate between MosA and 2-OB by HPLC-MS. Mass spectrum obtained of MosA (3.11 nmol) treated with 2-OB (1.88 µmol) and $NaBH_4$ (1.13 µmol) in assay buffer (100 mM imidazole, 10 mM KH_2PO_4, pH 7.2).

3.6 Rhizopine Assays

3.6.1 HPLC for detection of MosA's methyltransferase activity using 2-OB and SI as substrates

A search in the literature for *O*-methyltransferase assays applicable to MosA's proposed methyltransferase function proved unsatisfying. Most of the assays relied on radiolabelled SAM or substrates, HPLC, GC or TLC, none of which were directly applicable towards the investigation of MosA's methyltransfer activity. Furthermore, the high polarity and the lack of a chromophore mean that the inosamine structures required derivatization prior to reverse phase chromatography.

The novel methylation reaction involves the formation a Schiff base between 2-OB and MosA during the first step of the reaction. This provides an electron sink allowing nucleophilic attack by **SI** on the methyl group of the 2-OB-Schiff base. This reaction would result in the formation of **3-MSI** and pyruvate. Consequently, if pyruvate or 3-MSI was detected upon incubation of **SI**, 2-OB with MosA, this suggests that a methyltransferase reaction was being catalyzed.

Initial attempts to develop an assay was based on the HPLC separation of the phenylhydrazones of 2-OB and pyruvate using 2,4-dinitrophenylhydrazine as a derivatizing agent. Unfortunately, reliable and mild conditions for the derivatization procedure proved to be difficult to develop. Furthermore, HPLC analysis would be complicated by the fact that a mixture of stereoisomers is often observed in the chromatograms.[93] Consequently, the focus changed to the derivatization and

separation of SI and 3-MSI. Initial attempts to derivatize the rhizopines with phenylisothiocyanate also proved to be difficult as solubility issues complicated procedures. On the other hand, 9-fluorenylmethoxycarbonyl chloride (FMOC-Cl) a commonly used derivatizing agent for amino-sugars, dissolved in acetonitrile proved to be a very convenient and reliable method.

The FMOC derivatization of **SI** is illustrated in Figure 23. The temperature, pH and time of reaction are all important parameters in the derivatization. The most import side reaction is the hydrolysis of the FMOC-Cl by water producing FMOC-OH. Unfortunately, the rate of hydrolysis by water and the amino sugars both rise with increasing pH. Consequently, the conditions need to be explored such that hydrolysis and aminolysis rate are optimal.

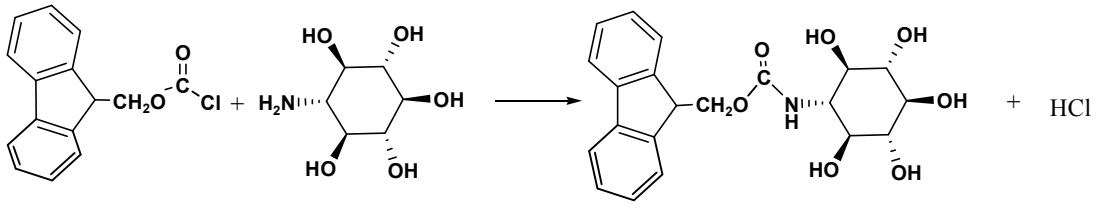

Figure 23. The derivatization reaction of SI with FMOC-Cl

A reliable method for derivatizing the rhizopines was based on that used for assaying glucosamine concentrations[94]. FMOC-Cl dissolved in acetonitrile is mixed with an equal amount of the buffered solution of the rhizopine at room temperature for at least 20 minutes. Initial attempts to perform the derivatization reaction at a pH of 8.0 in borate buffer resulted in mostly hydrolysis of the FMOC-Cl. Upon lowering of the pH to 7.0, the relative amounts of FMOC-OH to FMOC-**SI** were reasonable. Assay conditions used in MosA's DHDPS reaction were typically performed in imidazole at

pH 7.7. However, dissolving rhizopine in imidazole buffer and treatement with FMOC-Cl resulted in the exclusive hydrolysis of the reagent as imidazole was likely acting as a nucleophilic catalyst. However, changing the buffer to phosphate (pH 7.0, 0.1 M) where MosA is known to be active[13] allowed the derivatization to proceed sufficiently.

Once suitable derivatization conditions were found, retention times were determined for the compounds of interest. The FMOC derivatives of **SI** (Figure 25) and **3-MSI** (Figure 26) had retention times of 3.4 and 3.7 minutes respectively. The FMOC-Cl eluted at 10.8 minutes while the FMOC-OH at 7.1 minutes. Enzymatic assays included MosA, 2-OB and **SI** were allowed to proceed for 3 hours after which a portion of the reaction solution was removed, the enzyme filtered and the filtrate subjected to derivatization. From the resulting chromatogram shown in Figure 27 no peaks corresponding to the FMOC-**3-MSI** were detected. Conversely FMOC-**SI** was clearly present at the expected 3.4 minute elution time. To ensure that detection of FMOC-3-MSI was possible in the assay conditions, a 10% w/w spike of **3-MSI** to **SI** was introduced into the assay solution after the 3 hour incubation. A peak corresponding to FMOC-3-MSI of about 10% the area was detected in the chromatogram at 3.8 minutes as shown in Figure 28. These experiments clearly show that MosA does not catalyze the transfer of a methyl group from 2-OB to SI to produce 3-MSI. MosA is not a methyltransferase that utilizes 2-OB as a novel methyl donor in rhizopine biosynthesis.

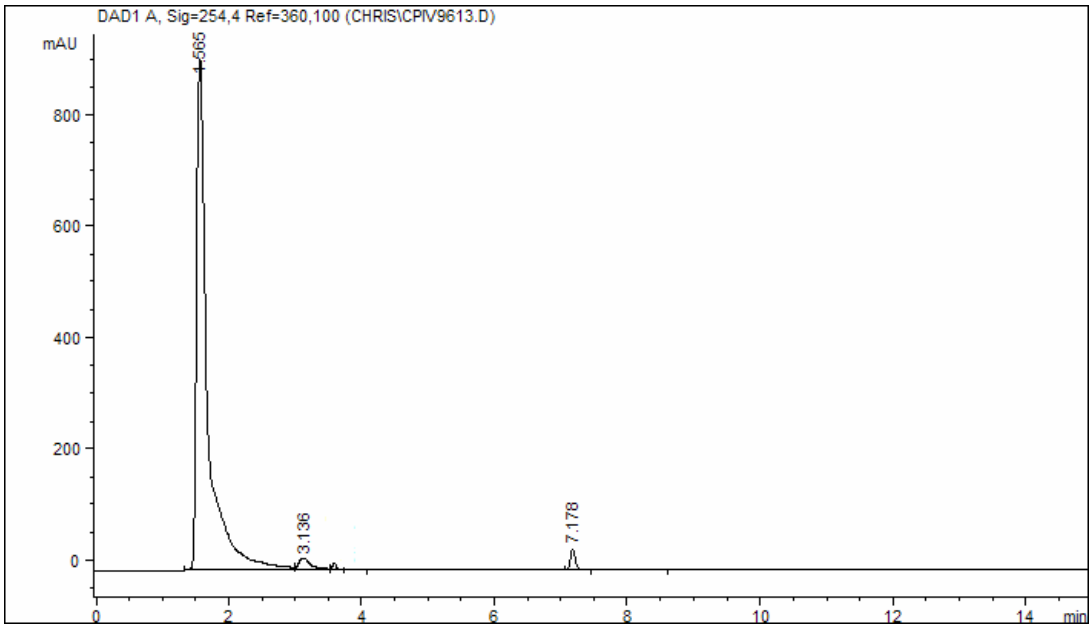

Figure 24. Chromatogram after injection of 2-OB (5mM) in phosphate buffer (0.1 M, pH 7.0)

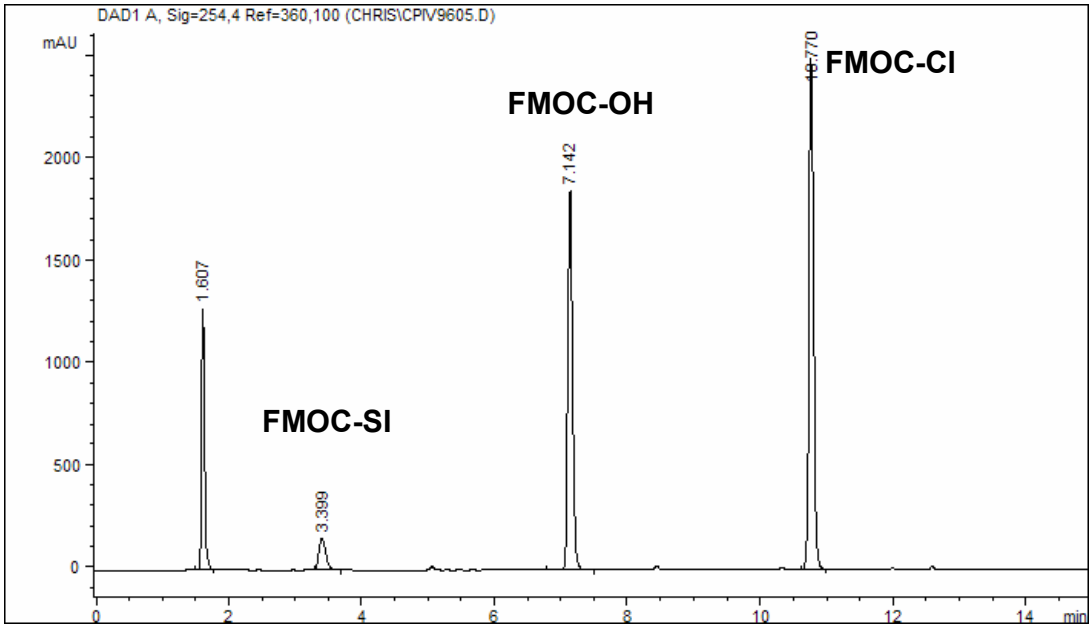

Figure 25. Chromatogram obtained by derivatization of SI in the presence of 2-OB. SI (5mM) and 2-OB (50 mM) in phosphate buffer (0.1 M, pH 7.0) after 30 minute incubation with 100 µL of FMOC-Cl (5 mM).

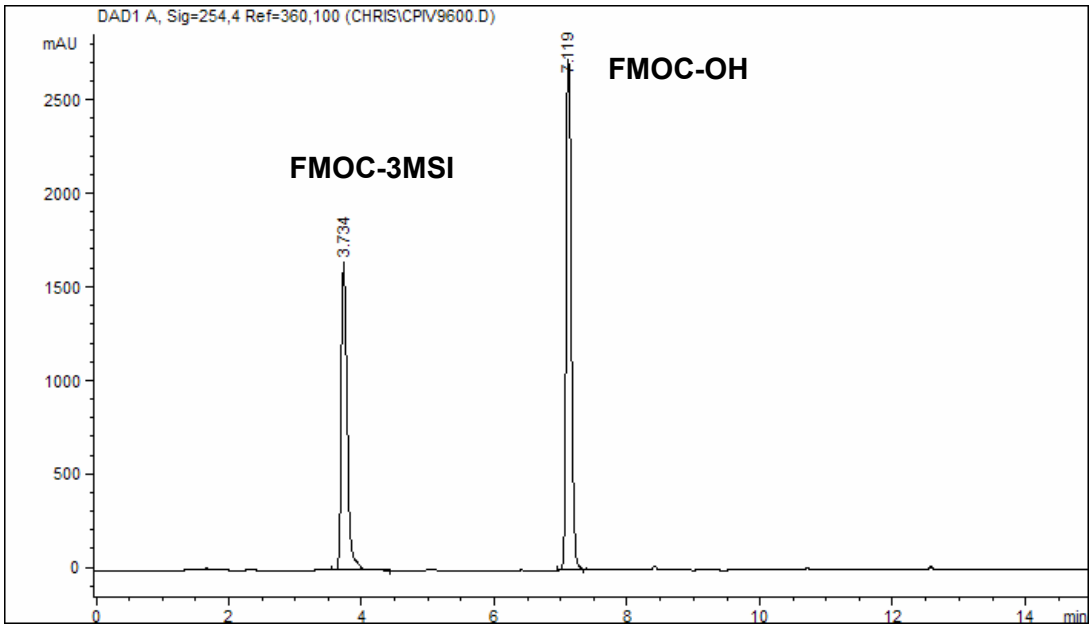

Figure 26. HPLC chromatogram of 3-MSI derivatized with FMOC-Cl.

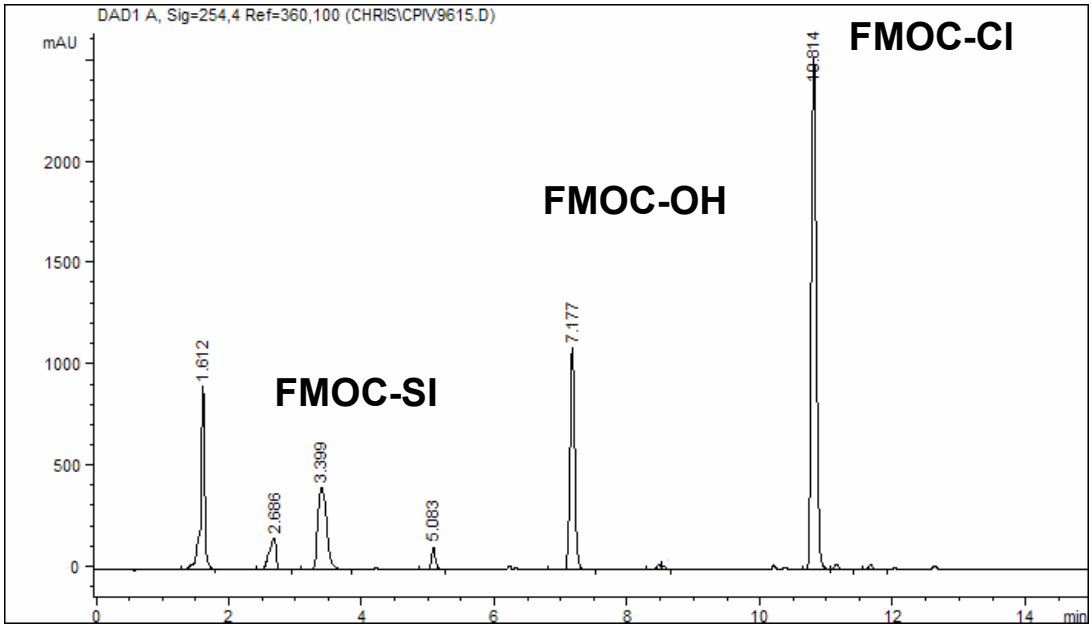

Figure 27. HPLC chromatogram of MosA displaying no methyltransferase activity using, 2-OB as a methyl donor. The assay included MosA (0.5 µM), 2-OB (5 mM), SI (5 mM) after 3 hour incubation at 37 ºC. The derivatization was accomplished after filtering off the enzyme and mixing the assay solution (100 µL) with FMOC (100 µL, 5 mM in acetonitrile) and allowing 30 minute reaction time.

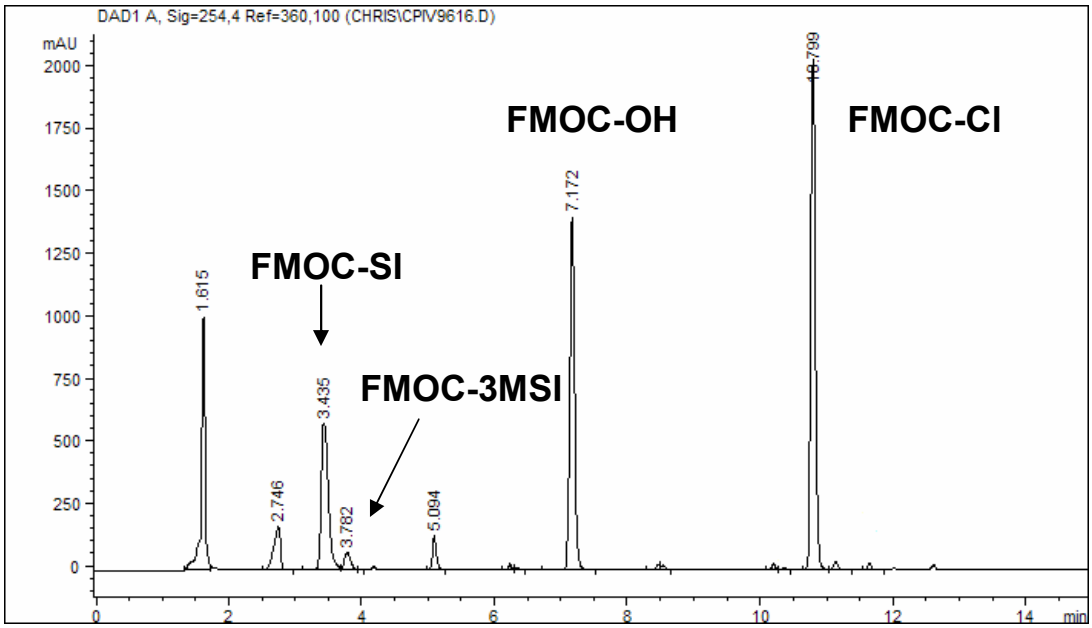

Figure 28. HPLC methyltransferase assay of MosA with a 10% spike of 3-MSI (10% that of SI) added to the derivatization mixture.

3.6.2 HPLC for detection of methyltransferase activity using S-adenosyl-methionine (SAM) and SI as substrates

Most *O*-methyltransferases in the protein database are S-adenosylmethionine (SAM) dependent. Consequently, SAM was chosen as a candidate to be tested as a methyl donor. Unfortunately, SAM-dependent reactions are often difficult to assay given that direct spectrophotometric techniques are rare. Most assays employ a separation of the products (HPLC, GC, TLC etc) and subsequent detection through a variety of methods.[9] However, most of these techniques focus on the non-cofactor substrates and products of the reaction. The possibility exists that MosA could utilize SAM as a methyl donor in the formation of **3-MSI** from **SI**. Although no known SAM binding motif is present in MosA, perhaps a novel site has evolved. HPLC experiments were designed to detect any methyltransferase reaction by monitoring the disappearance of SAM and appearance of S-adenosylhomocysteine (SAH).

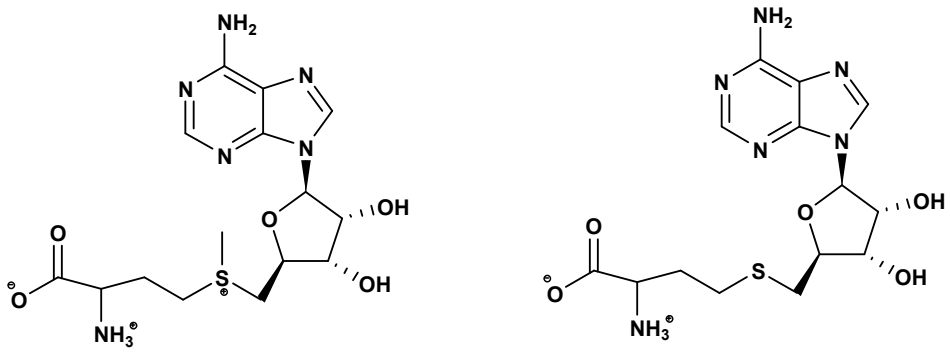

Figure 29. Structures of SAM and SAH

Commercially available SAM comes only 70% pure as shown in Figure 30. Unfortunately, one of the major decomposition products is SAH. Consequently, any HPLC assays that measured the decrease in amounts in SAM and increased amounts of SAH must take this into account. SAH on the other hand, comes very pure, simplifying its use as a standard for HPLC analysis.

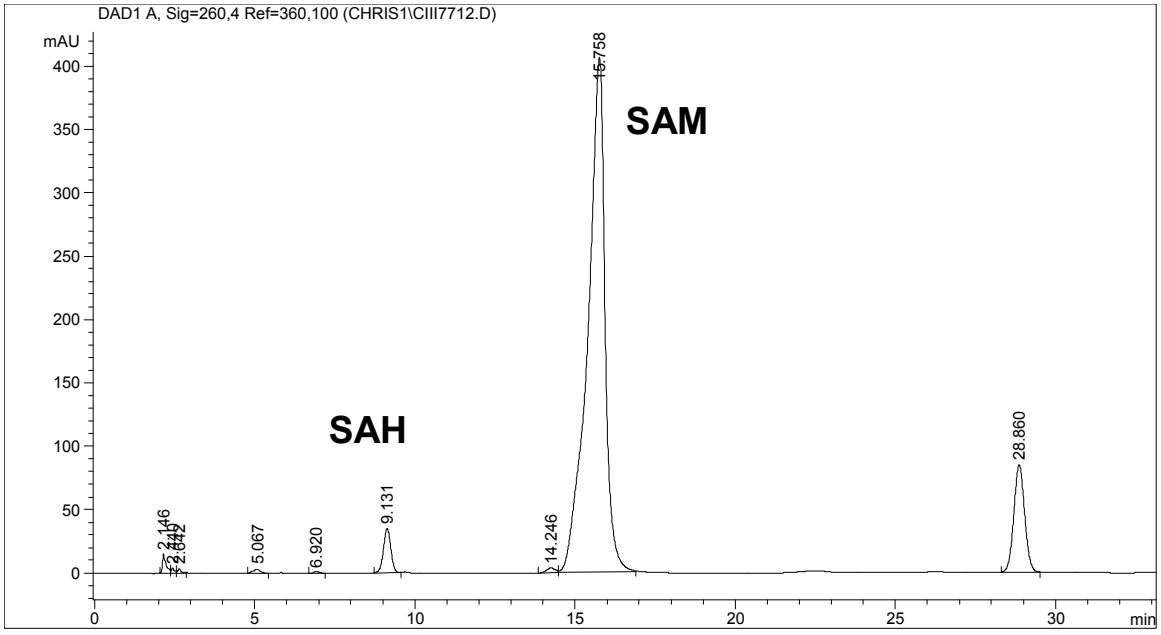

Figure 30. HPLC chromatogram of commercially available SAM demonstrating purity.

Enzymatic assays were set up at 37 ^{o}C and the samples incubated for several hours. Samples were taken, protein filtered out and aliquots injected into the HPLC fitted with a C18 column equilibrated with 80% buffer (40 mM $NH_4H_2PO_4$, 8 mM heptanesulfonic acid at pH 3.0) and 20% methanol. Detection of SAM and SAH was done at 260 nm using retention times that were determined by the commercial standards. Methyltransferase activity was qualitatively diagnosed by comparing the ratios of the areas of SAM to SAH. Comparing the relative amounts of SAM to SAH no methyltransferase activity was detected as demonstrated in Figure 31. Consequently, MosA does not utilize SAM as a methyl donor in the formation of **3-MSI** from **SI**.

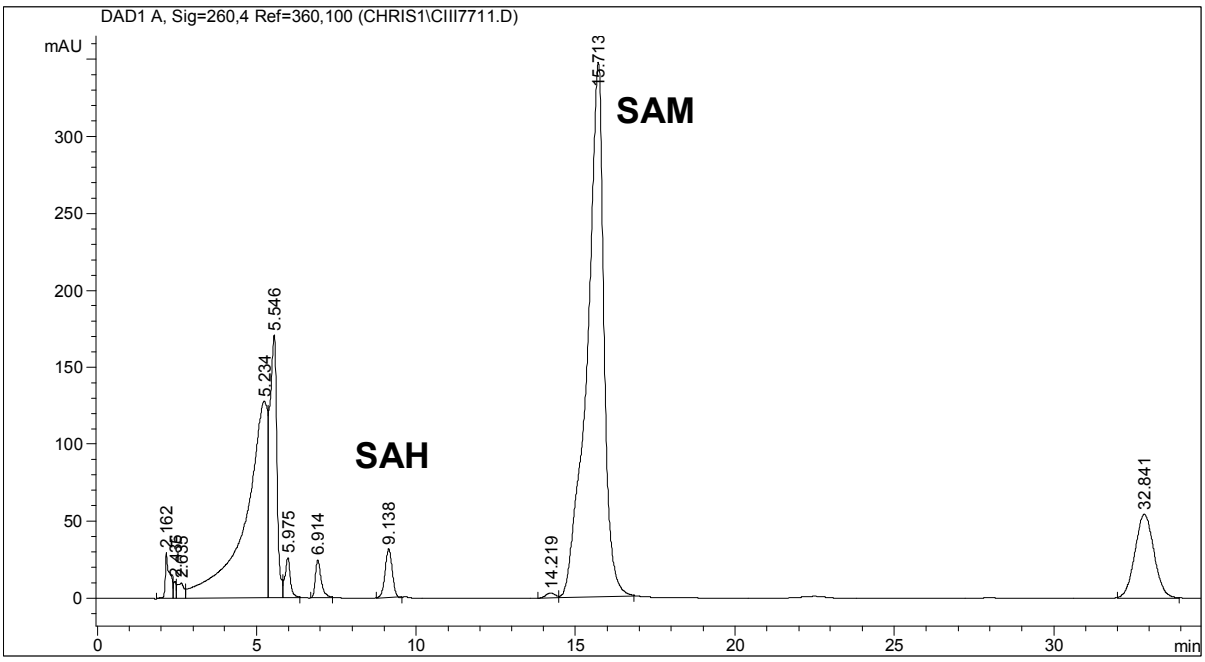

Figure 31. HPLC chromatogram of MosA displaying no methyltransferase activity using SAM as methyl donor determined by HPLC. Assay included MosA, SI (2.5 mM) and SAM (2.5 mM) and were incubated for 3 hours at 37 ºC in assay buffer (100 mM imidazole, 10 mM K_2HPO_4, pH 7.6)

3.6.3 HPLC control reaction using catechol-*O*-methyltransferase (COMT) activity

In order to determine if methyltransferase activity can be detected as described above a control assay was developed using catechol-*O*-methyltransferase (COMT). This enzyme catalyzes the transfer of a methyl group from SAM to protocatechuic acid (3,4-dihydroxybenzoic acid) as illustrated in Figure 32. HPLC assays shown in Figure 33 demonstrate that the peak corresponding to SAH is increasing with time while the peak corresponding to SAM is decreasing. Although the observed changes shown in Figure 33 are not extensive, the results allow the qualitative observation of methyltransferase activity by monitoring the disappearance of SAM and appearance of SAH.

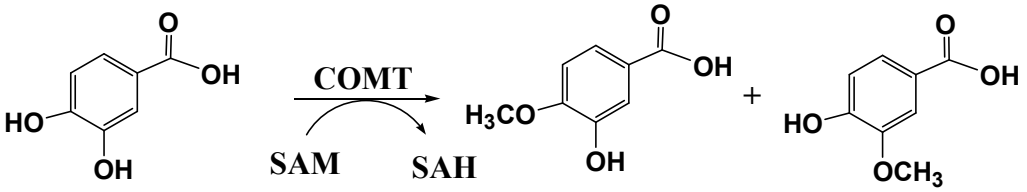

Figure 32. The reaction catalyzed by COMT

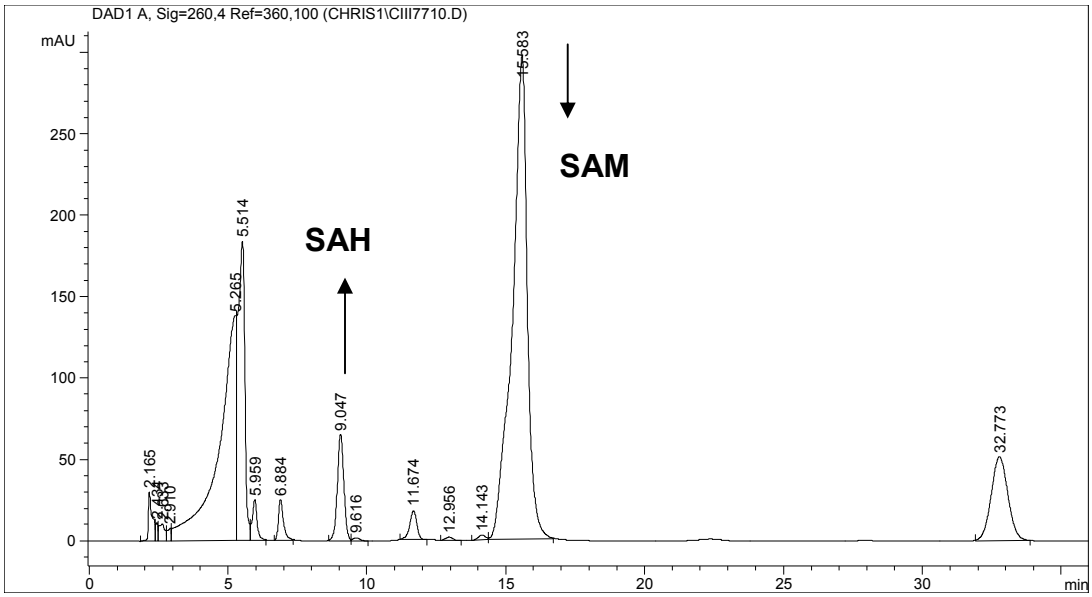

Figure 33. HPLC chromatogram of the COMT enzymatic assay. The reaction included phosphate buffer (200 mM NaH_2PO_4, 5 mM $MgCl_2$, pH 7.4), 100 Units COMT, 3 mM SAM and 2 mM 3,4-dihydroxybenzoic acid 2.5 hours, 37 ºC

The use of reverse phase HPLC to separate FMOC derivatives of the rhizopines provided direct evidence that MosA did not catalyze the transfer of a methyl group from 2-OB to **SI**. In addition, methyltransferase assays that monitored SAH production and SAM consumption failed to detect any MosA catalyzed methyl transfer from SAM to SI. Consequently, it is very likely that MosA is not the enzyme that catalyzes the formation of **3-MSI** from **SI**.

3.7 Isothermal titration calorimetry

3.7.1 Thermodynamics of pyruvate's interaction with MosA

In the inaugural report of the measurements of binding constants by ITC, Wiseman et al[95] noticed that the shape of the binding isotherm for a simple one to one binding stoichiometry changes according to the product of the association constant (*K*)

and the concentration of the macromolecule [M]. This unitless parameter has been called the Wiseman constant and it calculated as shown in equation 3.1.

$$c = [M]K_a \qquad (3.1)$$

It has been widely accepted that reliable thermodynamic data could be obtained only for those systems that the Wiseman value was $10 \leq c \leq 500$ which are characterized by sigmoidal binding isotherms.[81,95,96] For low affinity systems ITC experiments would require high concentrations of the macromolecule in order to achieve reasonable c values for extraction of accurate thermodynamic values.

When considering ITC as a tool to characterize the thermodynamic parameters of MosA, estimations of the protein concentration required to achieve suitable c values were unreasonably high (greater than 140 mg/mL for each experiment). Fortunately, Turnbull and Daranas[96] validated the accuracy of using ITC on low affinity systems by studying the thermodynamic parameters of known weakly binding systems. For low affinity systems, it is important to have a higher signal to noise ratio in order to accurately determine ΔH and K_a. Furthermore, a sufficient portion of the binding isotherm is needed for reliable data to be extracted during the fitting process. Concentrations of the ligand and macromolecule were important, easily modified experimental parameters that were taken into account when designing the ITC experiments. Consequently, experiments that had concentrations of MosA around 0.1 mM (based on monomer) and pyruvate/2-OB of 50 mM were found to provide a reasonable binding isotherm without reaching saturation amounts too quickly. At these

concentrations of MosA and pyruvate, a good signal to noise ratio was achieved with avoidance of early saturations thus satisfying suggestions outlined by Turnbull.

Sufficient time must be allowed to elapse between injections to ensure that the system reaches equilibrium after each perturbation. Equilibration times as long as 1200 seconds were reported for ITC experiments characterizing the binding of an aldehyde analogue of Biocyclomycin to Rho protein.[97] For pyruvate titrations into MosA, injection times were varied between 200 – 300 seconds ensuring that equilibrium was reached. Equilibrium was easily achieved within 200 seconds between injections as this reaction is catalyzed by MosA. It is also important to note that the MosA-imine with pyruvate is likely a reversible process, an obvious requirement for determination of equilibrium constants. Equilibrium conditions imply reversibility of the chemical process. Evidence to support reversibility comes from the fact that $NaBH_4$ is required to form the covalent intermediate between MosA and pyruvate. Furthermore, if imine formation was irreversible, then saturation should be reached after the second injection. This would have introduced more than one equivalent of pyruvate to MosA monomer. In addition, since water is the first product of the reaction between MosA and pyruvate in an aqueous environment, it seems unlikely that this process is entirely irreversible. It has been noted that details of the catalytic mechanism of DHDPS in *E. coli* are a bit unclear as kinetic changes are observed at different pH's of enzymatic assay.[34]

From the ITC data, a hyperbolic isotherm was obtained as shown in Figure 34. Using Bindworks software and assuming stoichiometry of n = 1.0, the thermodynamic parameters obtained for pyruvate binding to MosA are given in Table 3.

From Table 3, a few interesting observations can be noted. To begin with, K_d was found to be 0.39 ± 0.5 mM which is reasonably close to the Michaelis constant for pyruvate of $K_{M(Pyr)}$ = 0.19 mM. Additionally, the formation of the imine between MosA and pyruvate has favorable contributions from both enthalpy and entropy with values of ΔH = -3.8 ± 0.6 kJ/mol and $T\Delta S$ = 16 ± 1 kJ/mol. The errors measured in this data were obtained by standard deviation of experiments done in triplicate.

Table 3. Thermodynamic parameters of MosA-2-oxo-acid interactions

Ligand	K_d (mM)	ΔH (kJ/mol)	ΔG (kJ/mol)	$T\Delta S$ (kJ/mol)	Wiseman constant, *c*
Pyruvate 25ºC[a]	0.4 ± 0.1	-3.8 ± 0.6	-19.8 ± 0.5	16 ± 1	0.3
Pyruvate 15ºC[a,b]	0.5 ± 0.1	-3.7 ± 0.1	-19.1 ± 0.5	16 ± 1	0.2
Pyruvate Tris[c]	0.5	-3.7	-19	15	0.1
2-OB[a]	2 ± 1	-3 ± 2	-15 ± 2	12 ± 3	0.1

[a]Experiments performed in imidazole buffer (100 mM, pH 7.7). Values are an average of three independent trials ± standard deviation unless otherwise indicated [b]Values are an average of two independent trials ± standard deviation [c]Experiments performed in Tris buffer (100 mM, pH 7.7). Values are based on one trial.

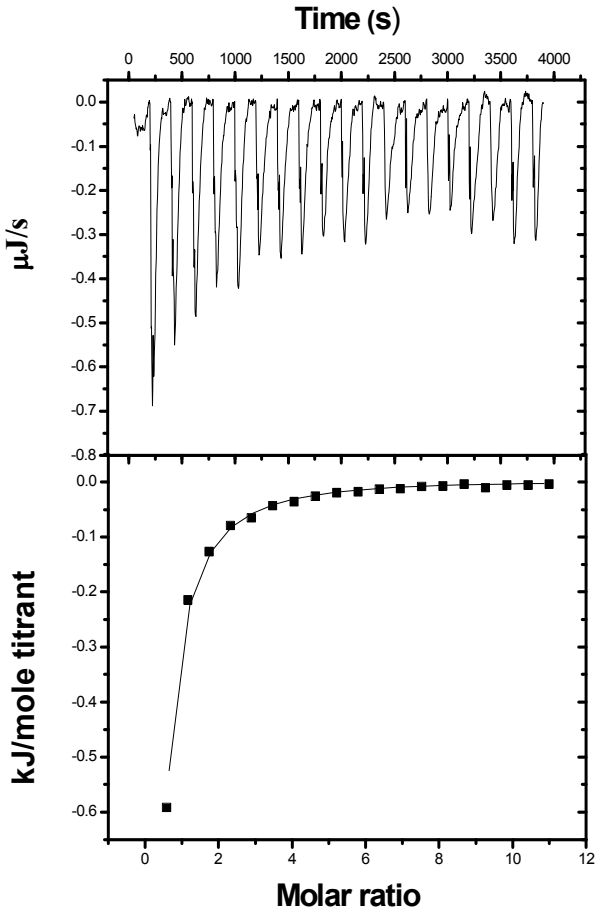

Figure 34. ITC titrations of pyruvate into buffered MosA solutions. Top graph shows the raw data for 19 injections (5 µL) of pyruvate (50 mM) into an imidazole buffered MosA solution (0.07 mM based on monomer molar mass) at 15 ºC. The bottom graph shows data points as energy (as kJ/mol titrant) as a function of molar ratio with the solid line representing the fit to the 1:1 binding model from Bindworks 1.0.

In addition to obtaining the thermodynamic parameters, ITC is also useful in providing evidence as to whether or not protons are released into the aqueous media upon binding or reaction. Release of protons is diagnosed by performing identical experiment in different buffers of varying ionization enthalpy and comparing the

enthalpy of binding values obtained.[81] In the case of pyruvate, similar values were obtained from ITC experiments when Tris (the ionization enthalpy of Tris $\Delta H \approx$ -47 kJ/mol) was used as the buffer system instead of imidazole (the ionization enthalpy of imidazole $\Delta H \approx$ -36 kJ/mol) at pH 7.7. This suggests that no protons were released to or removed from the aqueous solution during the binding process.

The measurements of ΔH and $T\Delta S$ at different temperatures are used to determine changes in heat capacity of the system. Changes in heat capacity, ΔC_p can provide information about the mechanism of the binding event.[98] For example, hydrophobic binding interactions are often characterized by small (frequently positive) enthalpy changes, large positive entropy changes and a negative contribution to ΔC_p. On the other hand, factors that often contribute to a positive value of heat capacity are : 1) changes in ligand conformation 2) changes in protein conformation 3) interactions between the side chains and the protein with solvent 4) interactions between the solvent and ligand.[99] The thermodynamic parameters of pyruvate's interaction with MosA showed no significant dependence on temperature suggesting no large changes in heat capacity for those experiments done at 15 ºC and 25 ºC. These findings may be due to limitations of the instrument on a low affinity system rather than a ΔC_p actually being 0, especially given that pyruvate binding is dominated by entropy.

3.7.2 Thermodynamics of 2-oxobutyrate's interaction with MosA

Earlier in this dissertation it was shown that 2-OB forms a Schiff base with MosA. Furthermore, kinetic studies indicate that 2-OB is a competitive inhibitor with respect to pyruvate on MosA's DHDPS activity. ITC gave the in data shown in Figure 35 with the thermodynamic parameters of binding of 2-OB to MosA outlined in Table

3. Similar to pyruvate's binding to MosA, 2-OB's interaction with MosA is entropically driven; $T\Delta S = 12 \pm 3$ kJ/mol, and a slightly favorable enthalpy with $\Delta H = -3 \pm 2$ kJ/mol is obtained. Furthermore a $K_d = 2 \pm 1$ mM was consistent with $K_i = 1.0 \pm 0.3$ mM that was determined kinetically.

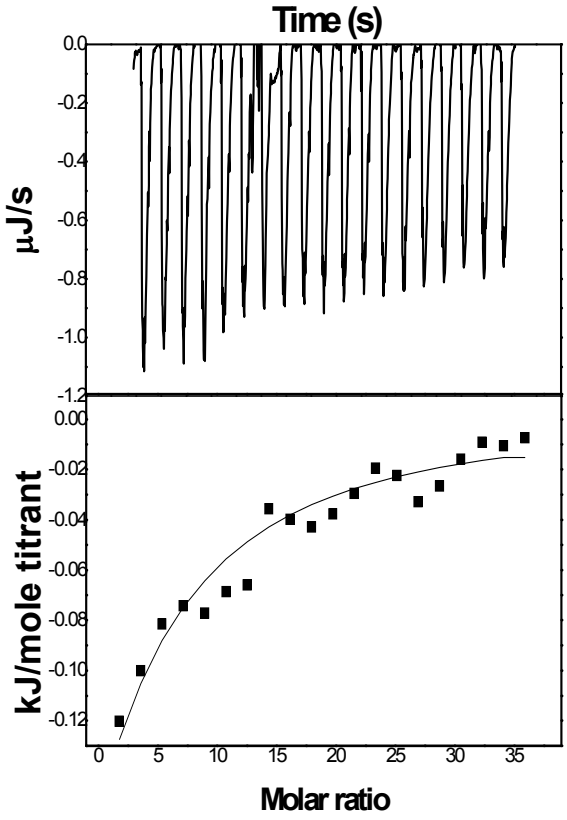

Figure 35. ITC titrations of 2-OB into buffered MosA solution. Top graph shows the raw data for 20 injections (5 µL) of 2-OB (50 mM) into a buffered solution of MosA (0.11 mM based on monomer molar mass) at 25 ºC. The bottom graph shows data points as energy (as kJ/mol titrant) as a function of molar ratio with the solid line representing the fit to the 1:1 binding model from Bindworks 1.0.

3.7.3 Thermodynamics of (*S*)-lysine's interaction with MosA in the presence of pyruvate

It is known that (*S*)-lysine is an allosteric feedback inhibitor of the dihydrodipicolinate synthases (DHDPS) in plants[100] and *E. coli*.[34] However, the exact mechanism of (*S*)-lysine inhibition is unclear. Initial work done on DHDPS from *E. coli* suggested that (*S*)-lysine is an uncompetitive inhibitor with respect to pyruvate and noncompetive with respect to ASA.[34] More recently, Gerrard has shown that (*S*)-lysine displays partial mixed inhibition with respect to pyruvate meaning that (*S*)-lysine has some effect on the first half reaction.[40]

ITC experiments performed on MosA should help determine the nature of (*S*)-lysine's inhibition. Titrations of (*S*)-lysine (50 mM) into imidazole buffered solutions of MosA (≈ 0.1 mM) were done both in the presence and absence of pyruvate. The data resulted in isotherms with a high signal to noise ratio. Using the software Bindworks, a cooperative binding model fit the data, well, supporting the previously suggested notion that (*S*)-lysine binds to MosA in a cooperative manner, as suggested previously.[13] Neither the independent nor the multiple independent models built into the Bindworks software provide reasonable fits to the data.

In constrast to the 1:1 binding model, the cooperative binding model assumes two molecules of ligand bind to two interacting binding sites. The crystal structure of DHDPS from *E. coli* with bound (*S*)-lysine, has two lysine molecules bound at the dimer-dimer interface. The binding site of the second molecule of (*S*)-lysine is within the coordination sphere of the first lysine molecule, explaining the cooperativity

observed. Consequently, concentrations of MosA used in curve fitting by Bindworks were based on the molar mass of the dimer. Furthermore, Hill plots gave Hill coefficients all greater than 1, supporting the conclusion that (*S*)-lysine binds to MosA in a cooperative manner.[13]

From the data shown in Figure 36 obtained by titrating (*S*)-lysine (50 mM) into buffered solutions of MosA and pyruvate, thermodynamic values for the first and second binding events were determined, as outlined in Table 4. The binding of the first (*S*)-lysine displayed a weak affinity with a $K_d = 0.4 \pm 0.1$ M and $\Delta G_1 = -2.3 \pm 0.6$ kJ/mole. A slightly favorable enthalpy of $\Delta H_1 = -2.2 \pm 0.4$ kJ/mole and a small change in entropy of $T\Delta S_1 = 0.2 \pm 0.6$ kJ/mole was extracted. For the second molecule of (*S*)-lysine a much higher affinity was determined with a $K_d = 2.2 \pm 0.7$ μM and $\Delta G_2 = -32 \pm 6$ kJ/mole. A favorable $\Delta H_2 = -21 \pm 2$ kJ/mole and a favorable change in entropy of $T\Delta S_2 = 11 \pm 6$ kJ/mole contributed to the higher affinity binding.

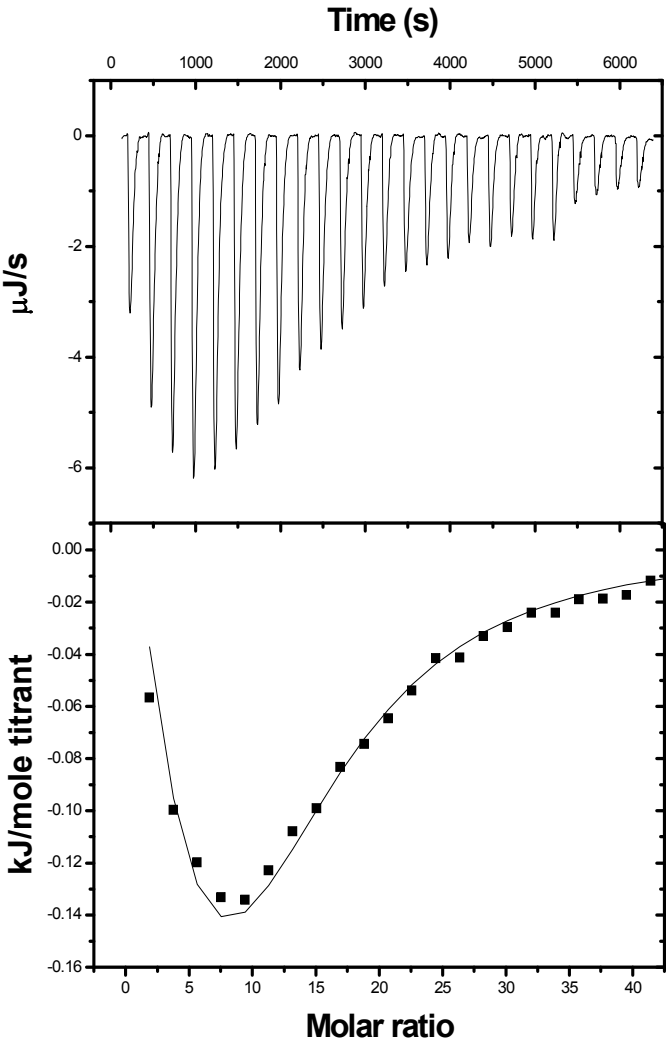

Figure 36. ITC titrations of (*S*)-lysine into a buffered pyruvate/MosA solution. Top graph shows the raw data for 20 injections (5 µL) of (*S*)-lysine (50 mM) into a buffered solution of MosA (0.055 mM based on dimer molar mass) saturated with pyruvate at 15 ºC. The bottom graph shows data points as energy (as kJ/mol titrant) as a function of molar ratio with the solid line representing the fit to the cooperative binding model from Bindworks 1.0.

Table 4. Thermodynamic parameters of (*S*)-Lysine association with MosA at 25 ºC

Ligand (enzyme form)	K_{d1} (M)	K_{d2} (μM)	ΔH_1 (kJ/mol)	ΔH_2 (kJ/mol)	ΔG_1 (kJ/mol)	ΔG_2 (kJ/mol)	$T\Delta S_1$ (kJ/mol)	$T\Delta S_2$ (kJ/mol)
(*S*)-lys[a] (MosA + pyruvate)	0.4 ± 0.1	2.2 ± 0.7	-2.2 ± 0.4	-21 ± 2	-2.3 ± 0.6	-32 ± 6	0.2 ± 0.6	11 ± 6
(*S*)-lys[b] (apo-MosA)	0.4 ± 0.1	3.2 ± 0.7	-0.8 ± 0.5	-3.3 ± 0.1	-2.5 ± 0.5	-31 ± 7	2 ± 1	28 ± 7
(*S*)-lys[a] (MosA + 2-OB)	0.3 ± 0.1	10 ± 3	-0.3 ± 0.1	-14 ± 1	-3.4 ± 1	-28 ± 8	3 ± 1	14 ± 8

[a]Experiments performed in imidazole buffer (100 mM, pH 7.7). Values are an average of at least three independent trials ± standard deviation unless otherwise indicated [b]Values are an average of two independent trials ± standard deviations.

3.7.4 Thermodynamics of (*S*)-lysine's binding to MosA in the absence of pyruvate

As discussed in section 3.7.3, it is not entirely clear whether or not (*S*)-lysine binds to DHDPS in the absence of pyruvate. Initial reports by Karsten[34] suggested that (*S*)-lysine was uncompetitive with respect to pyruvate meaning that pyruvate must occupy the active site prior to the binding of (*S*)-lysine. Alternatively Gerrard reported[29] that (*S*)-lysine was a mixed inhibitor with respect to pyruvate thus binding to MosA regardless of the occupancy of the pyruvate in the active site of MosA. In both reports, these interpretations were made by the analysis of kinetic data. ITC, on the

other hand, measures the heat released or absorbed upon the association of two interacting species making the technique very useful in determining the nature of (*S*)-lysine inhibition. Consequently, ITC experiments were performed by titrating (*S*)-lysine into solutions of MosA in imidazole buffer (pH 7.7) in the absence of pyruvate.

ITC isotherms in Figure 37 clearly indicate that an interaction between MosA and (*S*)-lysine was occurring without the requirement of pyruvate in the enzyme solution. The thermodynamic data obtained (outlined in Table 4) reveals no significant differences K_{d1} or K_{d2}. However, significant changes in enthalpy and entropy are observed such that a complete reversal of the dominating forces of binding is observed. The enthalpy value for the second (*S*)-lysine drops from $\Delta H_{2(Pyr)}$ of -21 ± 2 kJ/mol to a much lower $\Delta H_{2(Apo)}$ of -3.3 ± 0.1 kJ/mol. The entropy values for $T\Delta S_2 = 11 \pm 6$ kJ/mole increased significantly giving $T\Delta S_{2(Apo)} = 28 \pm 7$ kJ/mol. The resulting increase in entropy compensated for the unfavorable enthalpy keeping the binding constants for the second (*S*)-lysine relatively unchanged in the absence of pyruvate. Since the enthalpy term for the binding of the second lysine increased significantly (became less favorable) the loss of some important intermolecular interactions must be occurring during the binding event in the absence of pyruvate. This, however, was compensated for by an increase in the entropy, allowing the affinity constants to remain relatively unchanged.

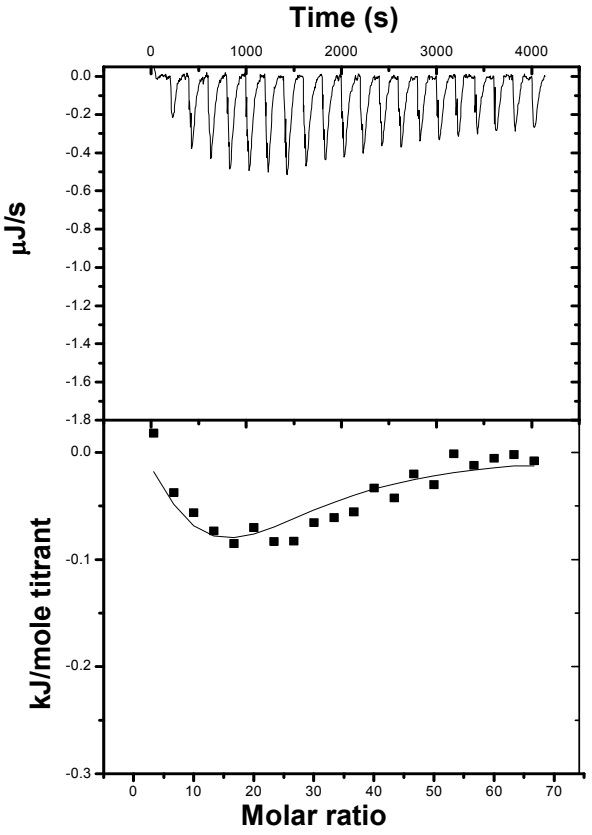

Figure 37. ITC titrations of (*S*)-lysine into buffered MosA solution. Top graph shows the raw data for 20 injections (5 µL) of (*S*)-lysine (50 mM) into a buffered solution of MosA (0.05 mM based on dimer molar mass) at 25 ºC. The bottom graph shows data points as energy (as kJ/mol titrant) as a function of molar ratio with the solid line representing the fit to the cooperative binding model from Bindworks 1.0.

3.7.5 Thermodynamics of (*S*)-lysine binding to MosA in the presence of 2-OB

The interaction of 2-OB with MosA has been thermodynamically characterized by ITC supporting the fact that 2-OB interacts with MosA in an analogous way to pyruvate. However, 2-OB only appears to be an inhibitor of MosA and does not appear to be a substrate of MosA. To examine whether or not 2-OB can influence the binding of (*S*)-lysine to MosA, ITC experiments were performed. The binding isotherm in Figure 38 resulted from titrations of (*S*)-lysine into 2-OB saturated solutions of MosA. The resulting thermodynamic parameters are outlined in Table 4. The binding thermodynamics of the first (*S*)-lysine did not significantly change in the presence of 2-OB. This was also the case for those experiments done in the absence of pyruvate. For the second (*S*)-lysine a slightly higher dissociation constant was observed compared to the $K_{d(Pyr)}$ suggesting a slightly lower affinity in the presence of 2-OB. The most significant changes came from comparison of the enthalpy and entropy values. The observed enthalpy in the presence of pyruvate changed from $\Delta H_{2(Pyr)}$ of -21 ± 2 kJ/mol to $\Delta H_{2(2\text{-}OB)}$ of -14 ± 1 kJ/mol in the presence of 2-OB. Entropy, on the other hand, changed from $T\Delta S_{2(Pyr)}$ = 11 ± 6 kJ/mole in MosA/pyruvate solution to $T\Delta S_{2(2\text{-}OB)}$ of 14 ± 8 kJ/mol. Again, enthalpy-entropy compensation kept the dissociation constant fairly constant in all three cases.

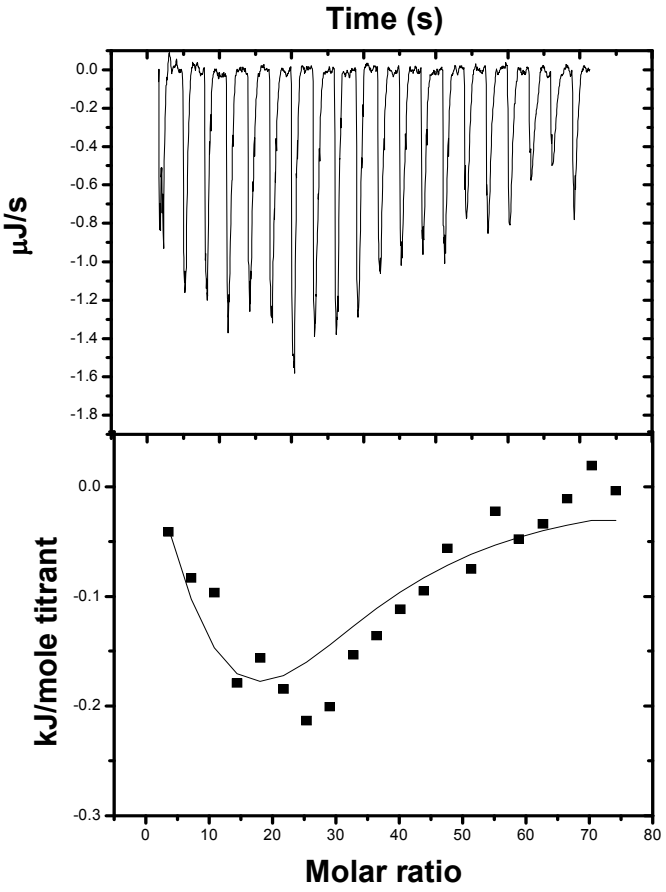

Figure 38. Titrations of (*S*)-lysine into a buffered 2-OB/MosA solution. Top graph shows the raw data for 20 injections (5 µL) of (*S*)-lysine (50 mM) into a buffered solution of MosA (0.052 mM based on dimer molar mass) saturated with 2-OB at 25 ºC. The bottom graph shows data points as energy (as kJ/mol titrant) as a function of molar ratio with the solid line representing the fit to the cooperative binding model from Bindworks 1.0.

3.7.6 Heat capacity changes upon (*S*)-lysine's binding to MosA

Changes in heat capacity provide useful information about the release of solvent upon binding of a ligand to a protein.[101] Unlike enthalpy, entropy and free energy, heat capacity changes can distinguish between effects caused by polar and nonpolar hydration.[102] Change in heat capacity is expressed as

$$\Delta C_p = \mathrm{d}\Delta H/\mathrm{d}T \qquad (3.2)$$

This expression relates changes in enthalpy with respect to changes in temperature assuming that no change in heat capacity occurs over the range of temperatures examined. An influential paper by Sturtevant listed six possible sources of heat capacity change involving proteins in aqueous solutions: 1) exposure of hydrophobic groups to aqueous solvent, 2) exposure of electrostatic charges to aqueous solvent, 3) hydrogen bond formation, 4) conformational changes to protein or interacting molecules, 5) changes in intramolecular vibrations, 6) changes in equilibria due to temperature changes.[101] During the association of a ligand to a protein, these sources all contribute to a change in the heat capacity of the system which can make ΔC_p positive, negative or zero. Other events such as proton uptake or release into the solvent also must be considered when interpreting data.[103]

Titrations of (*S*)-lysine into buffered solutions of MosA and pyruvate were performed at 15, 18, 20 and 25 ºC. The data summarized in Table 5 demonstrate that no

temperature dependent trends were observed for the binding of the first (*S*)-lysine. However, this may be due to the low and scattered enthalpic values for this ligand making any relationship difficult to diagnose. On the other hand, the thermodynamic data obtained for the second lysine reveal a linear relationship between Gibbs free energy, enthalpy, entropy and temperature. Plots of ΔH_2 versus temperature are shown in Figure 39. An estimate of ΔC_p = 1 kJ/mol K was obtained by determining slope of the linear relationship between ΔH_2 and T. Large positive heat capacity changes upon intermolecular associations involving proteins are rare although several cases have been reported in the literature.[103-106]

Table 5. Thermodynamic parameters obtained for the binding of (*S*)-lysine to MosA in pyruvate saturated solutions at 20, 18 and 15 ºC

Ligand	K_{d1} (M)	K_{d2} (μM)	ΔH_1 (kJ/mol)	ΔH_2 (kJ/mol)	ΔG_1 (kJ/mol)	ΔG_2 (kJ/mol)	$T\Delta S_1$ (kJ/mol)	$T\Delta S_2$ (kJ/mol)
(*S*)-lys[a] 20ºC	0.4 ± 0.1	2 ± 0.6	-3.7 ± 0.1	-28 ± 1	-4.9 ± 1.2	-33 ± 10	1 ± 1	5 ± 10
(*S*)-Lys[a] 18 ºC	0.2 ± 0.1	1 ± 0.3	-2.0 ± 1.2	-28 ± 2	-4.0 ± 2	-34 ± 10	2 ± 2	6 ± 10
(*S*)-Lys[b] 15 ºC	0.8 ± 0.1	0.6 ± 0.1	-2.2 ± 0.2	-32 ± 1	-0.6 ± 0.4	-35 ± 6	-2 ± 1	3 ± 6

[a]Experiments performed in imidazole buffer (100 mM, pH 7.7). Values are an average of at least two trials ± standard deviation
[b]Values are an average of two independent trials ± standard deviation

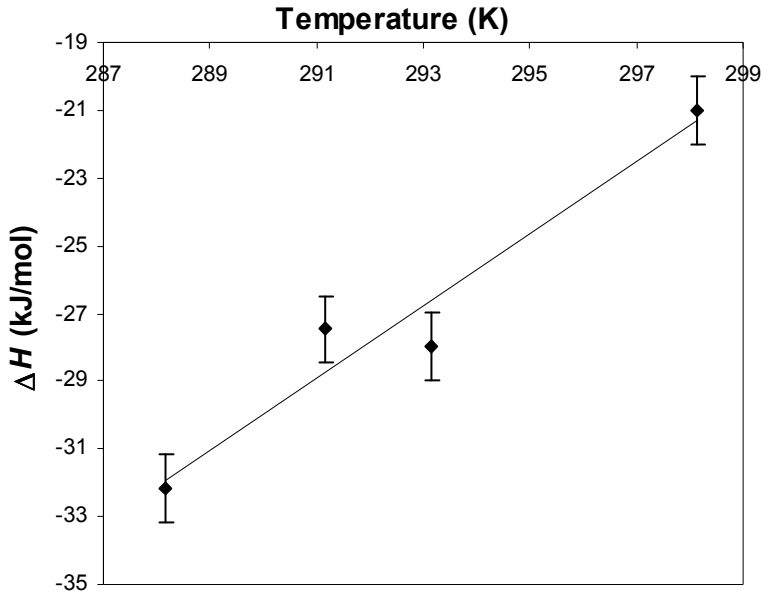

Figure 39. Temperature dependence of ΔH_2 (♦) for the binding of the second (*S*)-lysine to MosA in the presence of pyruvate. Estimation of ΔC_p was obtained by the slope of the linear relationship between ΔH_2 and temperature.

For the binding parameters of the second (*S*)-lysine, enthalpy and entropy are temperature dependent whereas Gibbs free energy shows little dependence at the temperatures studied. Gibbs independence of temperature is typically found in protein-ligand associations and is a reflection of the basic fact that stronger noncovalent bonds (enthalpically favorable) is compensated by a loss of degree of freedom (entropically disfavorable) or vice versa.[107] A plot of ΔH_2 versus $T\Delta S_2$ usually yields a linear relationship that provides the extent of enthalpy-entropy compensation. A slope equal to one is considered complete compensation, a slope greater than 1 is enthalpically dominant and less than one is entropically dominant.[108] However, the large error associated with the $T\Delta S_2$ for the binding of the second (*S*)-lysine values do not allow a meaningful plot of enthalpy-entropy compensation. However, from examining the

thermodynamic parameters outlined in Table 5, enthalpy and entropy compensation is likely occurring.

3.7.7 Thermodynamics of the interactions of the rhizopines and SAM with MosA

ITC experiments were performed by injecting **SI** or **3-MSI** into buffered solutions of MosA. The heats of each injection were corrected for dilution and normalized with respect to moles of titration as shown in Figure 40 A and B. The energy associated with the raw data peaks were consistent in their magnitudes corresponding to an average energy release of -51.6 μJ per injection for SI and -54.1 μJ per injection for 3-MSI. Titrations into the sample cell containing only dialysis buffer (i.e. no enzyme) produced average dilution heats of -53.5 μJ per injection for SI and -54.6 μJ for 3-MSI. Once dilution heats were subtracted from the rhizopine-MosA titration data, it was clear that no interaction was detected, calorimetrically. Additionally, no interaction was observed upon titrations of **SI** into 2-OB saturated solutions of MosA as shown Figure 40 C. It is unlikely that the novel methyltransferase reaction is occurring without any observable enthalpy changes.

In attempt to detect any interactions between MosA and the ubiquitous methyl donor SAM, ITC experiments were performed. Titrations of SAM into buffered solutions of MosA produced peaks that, once dilution heats were subtracted from the data, failed to detect any association. The enthalpy values corrected for dilution heats were normalized with respect to moles of titrant and plotted in Figure 40 D.

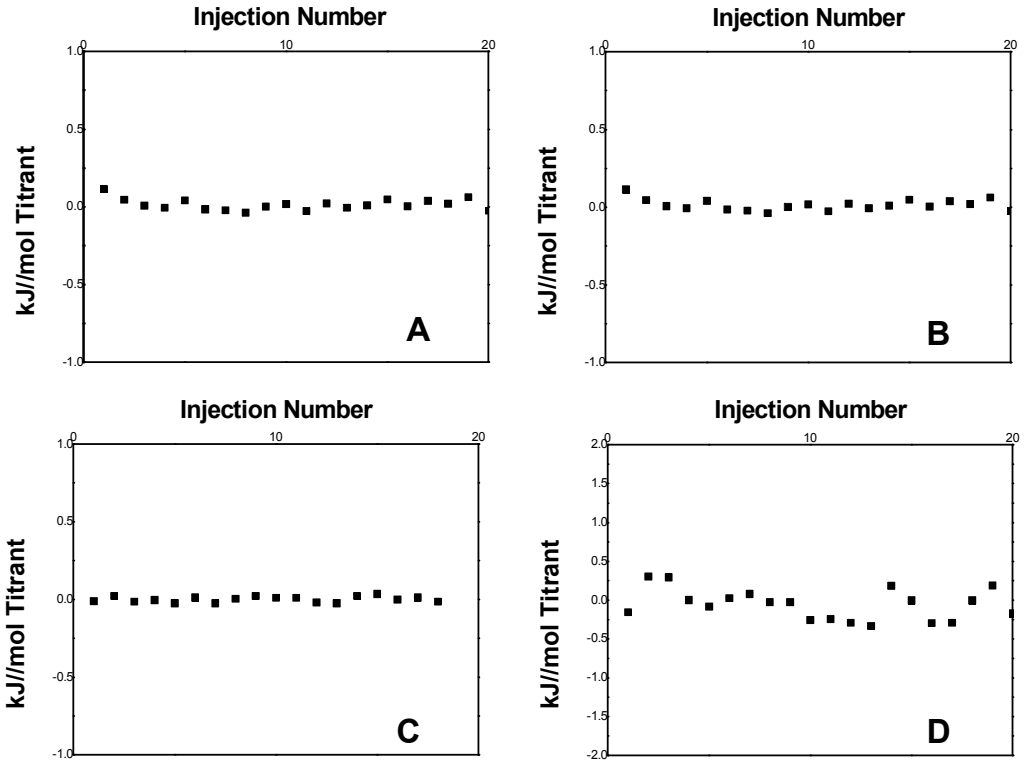

Figure 40. ITC titrations of SI, 3-MSI and SAM into a buffered MosA solution and SI into a buffered 2-OB/MosA solution. A) Graph shows the data obtained for 20 injections (4 μL) of SI (25 mM) into a buffered solution of MosA (0.1 mM based on monomer molar mass) at 15 ºC. Dilution heats were subtracted and the energy per injection normalized with respect to moles of titrant. **B)** Graph shows the data obtained for 20 injections (4 μL) of 3-MSI (25 mM) into a buffered solution of MosA (0.1 mM based on monomer molar mass) at 15 ºC. Dilution heats were subtracted and the energy per injection normalized with respect to moles of titrant. **C)** Graph shows the data obtained for 17 injections (5 μL) of SI (25 mM) into a buffered solution of MosA (0.12 mM based on monomer molar mass) saturated with 2-KB at 15 ºC. Dilution heats were subtracted and the energy per injection normalized with respect to moles of titrant. **D)** Graph shows the data obtained for 20 injections (4 μL) of SAM (25 mM) into a buffered solution of MosA (0.09 mM based on monomer molar mass) at 15 ºC. Dilution heats were subtracted and the energy per injection normalized with respect to moles of titrant.

The difference between the ITC data of an interaction known to occur versus the data obtained for rhizopine titrations is quite significant and is illustrated in Figure 41. This graph directly compares the enthalpy values obtained for titrations of (*S*)-lysine into pyruvate saturated solutions of MosA with titrations of 3-MSI into MosA. This

figure further demonstrates that ITC technique failed to detect any interactions between the rhizopines and MosA.

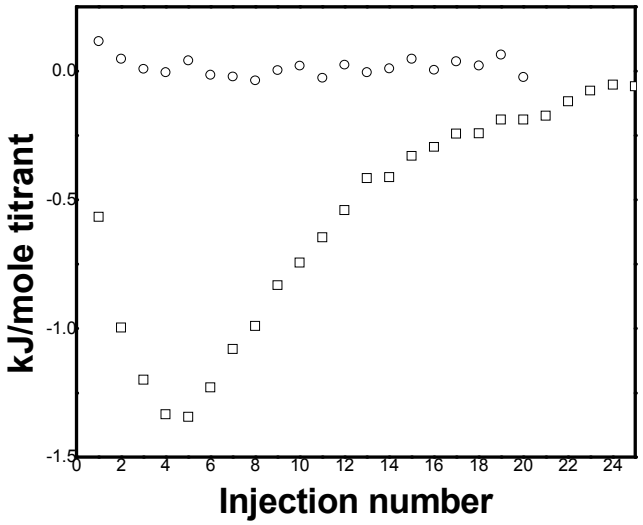

Figure 41. For comparison purposes: normalized heat as a function of injection for ITC titrations of 3-MSI into a buffered MosA solution versus 25 injections of (S)-lysine into a buffered pyruvate/MosA solution. 3-MSI (25 mM denoted by ○) into a buffered solution of MosA (0.1 mM based on monomer molar mass) and 25 injections of **(*S*)**-lysine (50 mM denoted by □) into pyruvate saturated solutions of MosA (0.12 mM based on monomer molar mass). Both experiments were done at 15 °C.

These results clearly indicate that the binding thermodynamics of MosA with its substrates and inhibitors was effectively determined by the ITC technique. The association between MosA and pyruvate and MosA and 2-OB was entropically driven as shown in Table 3. In addition, the binding isotherms produced by titrating (*S*)-lysine in pyruvate saturated solutions of MosA fit well to the cooperative binding model. As in Table 4, clear differences in the calorimetrically determined values of enthalpy and entropy were observed depending on the presence and absence of pyruvate in the MosA solution. In addition, the thermodynamic parameters extracted from titrating (*S*)-lysine

into 2-OB saturated solutions of MosA demonstrated that 2-OB evoked similar changes in MosA such that more exothermic binding was observed for the second (*S*)-lysine. This provides strong evidence that Schiff base formation between 2-OB and MosA is occurring at the active site of MosA. A large positive heat capacity was determined for the binding of the second (S)-lysine to MosA demonstrating the importance of solvent in this interaction. Additionally, the ITC technique proved very effective in determining that no associations between MosA and the rhizopines were occuring. Consequently, MosA does not use **SI** as a substrate in the production of **3-MSI** using either 2-OB or SAM as a methyl donor as no assocations between these molecules and MosA was detected**.**

3.8 Summary of Results

The results obtained from the above experiments are as follows:

- **SI** was chemicall synthesized via three separate routes with yields of 11%, 22% and 23%
- Two synthetic routes were developed to produce racemic **3-MSI** with yields of 13% and 20%
- MosA was expressed in good yields and purified using nickel affinity chromotagraphy
- Assays of MosA's aldolase activity provided kinetic parameters summarized in Table 1 and are consistent with DHDPS from *E. coli*

- 2-OB is a competitive inhibitor of MosA's DHDPS activity
- Schiff base trapping experiments using $NaBH_4$ and HPLC-MS demonstrated that 2-OB forms a Schiff base with MosA and once reduced diminishes the DHDPS activity
- **SI** had no significant effects on the DHDPS reaction nor could 2-OB replace pyruvate as the substrate for the aldolase chemistry catalyzed by MosA
- MosA does not catalyze the transfer of a methyl group from 2-OB to SI as determined by HPLC which separated FMOC derivatives of the rhizopines
- MosA does not catalyze the transfer of a methyl group from SAM to **SI** as observed by monitoring levels of SAM and SAH using HPLC
- COMT was used as a model enzyme to validate the HPLC method used in detecting possible methyltransferase activity of MosA
- ITC failed to detect any associations between **SI**, **3-MSI**, SAM and **SI** in the presence of 2-OB and MosA
- ITC was used to determine the binding thermodynamics of pyruvate and 2-OB to MosA (Table 3)
- ITC was used to support the fact that (*S*)-lysine binds cooperatively to the MosA-pyruvate complex with the thermodynamic parameters determined for the binding of the first and second (*S*)-lysine summarized in Table 4
- ITC was used to demonstrate that (*S*)-lysine is a cooperative non-competitive inhibitor of MosA with respect to pyruvate and the thermodynamic parameters summarized in Table 4

- The binding of the second (*S*)-lysine to the MosA-pyruvate complex was characterized by a large positive heat capacity change and the resulting thermodynamic parameters obtained at different temperatures are summarized in Table 5
- Titrations of (*S*)-lysine into 2-OB/MosA solutions produced more exothermic enthalpy values for the binding of the second inhibitor compared to those values obtained for (*S*)-lysine titrations into MosA alone.

4. Discussion

4.1 Chemical synthesis of proposed substrates of MosA

Over the course of this work, three novel synthetic routes were developed for the chemical synthesis of **SI**. The first method shown in Scheme 3 relies on the popular use of the 1,3,5-monoorthoformate of *myo*-inositol **1**. Since the C-2 OH of *myo*-inositol was required to be converted to an amine, the orthoformate was an obvious starting point due to known reactions which allowed orthogonal protection at the C-2 and C-4/6 positions. Formation of the C-2 *t*-BDMS ether was reportedly obtained in 48% yield by using imidazole as the nucleophilic catalyst and base in DMF.[84] However, our lab and others[61] upon attempting to follow the procedure, obtained a mixture of mono- and di-silylated derivatives which lowered the overall yield and complicated purification. This problem was overcome by replacing the imidazole with 2,6-dimethylpyridine. This served to increase the steric hindrance of the nucleophilic catalyst, improving the regioselectivity such that 65% of pure **3** was obtained.[61] Compound **3** was then benzylated, followed by removal of the silyl group with fluoride ion to produce **4**. A reported procedure described the direct protection of the C-4 and C-6 hydroxyl groups of the orthoformate using 2.1 equivalents of NaH and p-methoxybenzylbromide in 40% yield.[109] However, inconsistent yields resulted upon replacement of *p*-methoxybenzyl bromide with benzyl bromide when attempting to synthesize **4** directly from **1**.

In order to synthesize **SI**, the C-2 OH requires conversion to an amine while simultaneously inverting the substituent to the axial position. Several synthetic routes can be envisaged; however, the most obvious choice would be S_N2 displacement of a tosyl or mesyl group with NaN_3 followed by reduction to the amine. However, the rigid orthoformate structure is remarkably resistant to S_N2 reactions. This is not surprising considering its structural similarity to adamantane, a molecule that has been shown to undergo solvolysis of tosylate or bromide derivatives with retention of configuration.[110] Furthermore, addition of an ether in place of a methylene group within the adamantane ring led to a higher proportion of products formed via the S_N1 mechanism**.**[111] This resistance to substitution reactions has enabled tosyl, mesyl and camphorsulfonyl groups to be conveniently used in the regioselective protection of the orthoformate.[60,63,112]

Another route to synthesis of the amine is the stereoselective reductive amination of a ketone derivative of the orthoformate. A similar reaction was previously reported using CH_3NH_2 and $NaCNBH_3$ on an oxidized orthoformate derivative to give a secondary amine possessing the *scyllo*- configuration.[85] In an attempt to follow a similar strategy of reductive amination, Swern oxidation of **4** produced the symmetrical ketone **5**. It was important to avoid water when working up this reaction due to the formation of a stable hydrate between water and the ketone. In fact, stable hydrates have been crystallized from stirring a related compound in wet THF.[109] Sufficiently pure **5** is easily obtained by simply passing the crude reaction mixture, diluted in ether, through a small column of silica gel (~ 1- 2 inches of silica). Without further purification **5** is reductively aminated using a 2 M solution of ammonia in MeOH and acetic acid in the

presence of $NaCNBH_3$. Following this procedure amine **6** is obtained in 43% yield.

Typically, ammonia is not used for reductive aminations because the primary amine product formed is often more nucleophilic than the ammonia. As a result, the aminated substrate often reacts with another molecule of unreacted ketone. To circumvent this, ammonia is held in large excess therefore minimizing the probability of this occurring. Furthermore, inductive effects and steric hindrance of the orthoformate derivative may have reduced the reactivity of **6**. The stereoselectivity of the reductive amination may be explained by steric hindrance of the benzyl ethers at C-4 and C-6 preventing the borohydride from donating the hydride ion from that side of the structure. Other examples of stereoselective reduction of protected inositols resulting in the *scyllo* configuration are known.[85,113] The frequently observed long range coupling between the orthoformate hydrogen and the proton at C-2[61,114] characteristic of the *myo*-isomer, is not observed in the NMR spectrum of compound **6**, supporting the assignment of the *scyllo*- configuration.

Hydrogenolysis of the benzyl groups of **6** using hydrogen gas and Pd/C (10%) as a catalyst proved to be difficult. Normally, hydrogenolysis of benzyl ethers are carried out smoothly with catalytic amounts of the Pd/C under an atmosphere of hydrogen. However, the presence of an amine in the inositol structure likely resulted in poisoning of the Pd catalyst.[91] Fortunately, this problem was overcome by increasing the amount of catalyst in the reaction.

Hydrolysis of orthoformate derivatives typically requires strongly acidic conditions such as trifluoroacetic acid or aqueous HCl. However, our lab began using Dowex 50W-X8 100 (H^+) ion exchange resin to hydrolyze the orthoformate moiety.

The use of Dowex in water has provided a convenient and simple method of removing the orthoformate moiety in our lab on many different compounds.[115] By simply filtering off the resin and evaporating the solvent after overnight stirring at room temperature, inositol derivatives that were sufficiently pure for further reactions are easily obtained. Furthermore, in the case of the inosamines, hydrolysis and purification can be achieved in one step by pouring the slurry into a small column plugged with glass wool, washing the column of resin with water and eluting **SI** with 0.1 M HCl.

The second route towards **SI** shown in Scheme 4, began with the isopropylidene protected *myo*-inositol **7**. This reaction was easily performed on large scale and did not require chromatography as the product would precipitate out of solution upon partial neutralization with TEA and dilution of the reaction solution with ether.[86] Simultaneous protection of the C-1/C-3 and C-2 hydroxyl groups allowed perbenzylation of the inositol frame under routine conditions, producing **8,** which upon hydrolysis produces racemic **9**. The regioselective protection of the equatorial C-1 (or C-3) hydroxyl group of **9** provides the symmetrical **10** keeping the hydroxyl group at C-2 open to derivatization. Previous reports suggest that compound **10** can be synthesized by refluxing **9** in a mixture of benzyl chloride and NaOH in benzene.[116] In our hands these conditions proved inefficient, producing mostly hexabenzyl inositol with a mixture of the symmetrical and unsymmetrical benzyl ethers.

The reaction of diols with dibutyltin oxide to produce stannylene acetals is routinely used in carbohydrate chemistry.[117] Stannylene acetals are well known for undergoing regioselective alkylation and acylation reactions of nonsymmetrical diols.[118] As shown in Figure 42, the regioselectivity is believed to arise from the formation of

dimers in solution which result in one of the two oxygen atoms from the parent diol being coordinated to two tin atoms in the equatorial position of the coordination polyhedron.[119] The other oxygen from the parent diol, in the apical position, maintains its nucleophilicity as it is coordinated to one tin atom leading to the regioselectivity often observed.

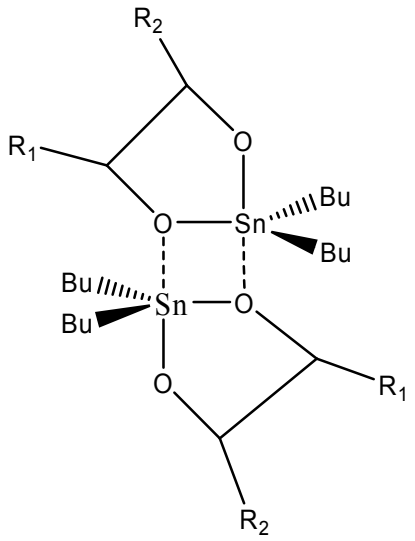

Figure 42. Dimer formation of stannylene acetals rationalizing the regioselectivity observed. The oxygen atoms in the apical position of each Sn maintain their nucleophilicity and are selectively alkylated. This diagram is adapted from reference 119.

Recently, the stringent conditions typically required for stannylene formation and subsequent alkylation was challenged.[120] For example, the azeotropic removal of water via Dean-Stark apparatus, typically described as necessary for stannylene formation, was shown to be redundant in some cases. Furthermore, use of the inexpensive tetrabutylammonium bromide (TBAB) in place of the more expensive and typically used tetrabutylammonium iodide provided good yields. Following the modifications suggested above, pentabenzyl **10** is easily obtained by refluxing **9** with dibutyltin oxide and benzyl bromide in the presence of TBAB in ACN. The reaction

showed high regioselectivity with excellent efficiency as **10** was obtained in 92% yield. Furthermore, purification was easily achieved by crystallization from hot methanol.

Once the symmetrical alcohol was obtained routine mesylation and S_N2 azidolysis produced the protected azide possessing the desired *scyllo*- with no trace of the *myo*-isomer. Support for the *scyllo* configuration comes from the ^{1}H NMR spectrum which displays coupling constants of approximately 9 Hz. This is consistent with the axial-axial coupling constants characteristic of ring protons possessing a dihedral angle of about 180º. Simultaneous reduction of the azide and routine hydrogenolysis of the benzyl groups proved difficult in our hands, possibly due to poisoning of the catalyst. Unfortunately, increasing the amount of catalyst did not produce successful results as in the hydrogenolysis of **6**. The problem was later overcome by *in situ* protection of the amine by inclusion of $tBoc_2O$ in the hydrogenolysis mixture.[121] Once the hydrogenolysis was complete, stirring overnight in Dowex (H^+) followed by loading the suspension into a small column and elution with 0.1 M HCl provided the amine **1** as the HCl salt, with spectroscopic properties identical to **SI** produced previously.

The third route towards synthesizing **SI** shown in Scheme 5 relies on the regioselective deprotection of hexabenzyl **13**. A previously reported procedure to directly benzylate *myo*-inositol was ineffective in our hands.[89] A much more convenient route was developed by perbenzylation of the orthoformate producing **12,** which after routine work up and dissolution of the crude solid in methanol, crystallized out of solution. Dowex hydrolysis and subsequent perbenzylation provided the hexabenzyl **13** in excellent yields with no chromatography required for any step.

The most important reaction of this route was the use of tin (IV) chloride in CH_2Cl_2 to regioselectively remove the axial benzyl group of **13**.[89] Two drawbacks of this reaction are its sensitivity to water and the resulting mixture of benzyl inositols that require careful separation by column chromatography. The mechanism of this reaction has been proposed[122] to begin with the coordination of two suitably located oxygen atoms from the benzyl ethers to the $SnCl_4$. Upon coordination of a third oxygen atom, one of the chlorides on the tin atom displaces the benzyl group of the inositol resulting in benzyl chloride and a tin-alkoxy complex as shown in Figure 43.

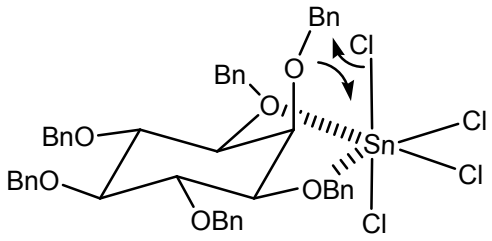

Figure 43. Regioselective removal of the axial benzyl ether of compound 13. Diagram adapted from reference 122.

The tin-alkoxy derivative is then hydrolyzed upon quenching the reaction with water to yield symmetrical **10**. Once **10** is obtained, an identical procedure as described above produces **11** and **SI.** Although this route provides **SI** in 5 steps and 23% yield, the use of $SnCl_4$ limited the convenience of the route due to the stringent conditions and difficult separation required.

Two routes towards the synthesis of racemic **3-MSI** were developed. The first route shown in Scheme 6 began with the regioselective methylation and benzylation of **1** to produce racemic **14**. The regioselectivity of these reactions has been suggested to be due to the pK_a of the C-4 and C-6 protons being lowered by intramolecular hydrogen

bonding between C-4 and C-6 hydroxyl groups. In addition, it has been suggested that small metal ions such as sodium form stable chelates (see Figure 12) that contribute to the selectivity.[58] It is vital to maintain the order of alkylation such that the methyl ether is formed prior to the benzylation in this one pot reaction. Placement of a benzyl ether at the C-4 or C-6 hydroxyl groups leads to subsequent alkylation preferentially occurring at the C-2 position and loss of the desired regioselectivity.[78] Once racemic **14** is obtained, an identical procedure is used, as discussed for synthesis of the intermediate compounds **5** and **6** to form **SI**.

The second route shown in Scheme 7 described for synthesis of **3-MSI** relied on the ability of $SnCl_4$ to remove the axial benzyl group of the fully protected compound **18** regioselectively. This procedure is identical to that described for compound **13** as discussed for synthesis of **SI**. Fortunately, the replacement of a benzyl group with methyl group at the C-4/C-6 position in **18** did not affect the regioselectivity of this reaction. Once the tetrabenzyl derivative **19** was synthesized, identical reactions were used as discussed for **10** to **SI**. In summary, two routes were developed for the synthesis of **3-MSI** starting from the orthoformate of *myo*-inositol with overall yields of 13% and 20%, respectively.

4.2 MosA does not display any methyltransferase activity

4.2.1 Catalysis and inhibition of the DHDPS reaction of MosA

The assignment of MosA as a methyltransferase is controversial due to the fact that its amino acid sequence is highly related to that of dihydrodipicolinate synthase (DHDPS) from *E. coli*. In fact, MosA is more closely related to DHDPS from *E. coli*

than DHPDS's from other organisms are to each other (see Figure 4).[18] Once MosA was cloned, expressed and purified[13] in our lab it was shown that MosA is a DHDPS catalyzing the condensation between pyruvate and ASA with Michaelis constants similar to that of the DHDPS from *E. coli*.[18] Additionally, the turnover number and specificity constants shown in Table 1 are too high to be associated with a side reaction.

In 1997, Babbitt and Gerlt mentioned the possibility of a novel methyl transferase reaction illustrated in Figure 5 that explains MosA's role in rhizopine biosynthesis without ignoring its similarity to DHDPS.[17] The proposed mechanism, in analogy to DHDPS, forms an imine between 2-OB and an active site lysine providing an electron sink for nucleophilic attack by **SI** on the terminal methyl of the imine. This would result in the release of **3-MSI** and pyruvate into solution. No known methyltransferase reactions that proceed through an aldol-like mechanism have ever been observed in nature.

The finding that MosA has DHDPS activity seriously calls into question its implication in rhizopine biosynthesis but does not rule it out. The proposed methyltransferase function of MosA is easier to accept considering the subtle differences between 2-OB and pyruvate in the first half of the reaction. Furthermore, experimental evidence has been provided to suggest that MosA is possibly a methyltransferase. Considering both the similarity of the proposed mechanism and the existing rhizopine evidence, *in vitro* observation of MosA's catalytic promiscuity is important to investigate this interesting issue.

In order to possess the methyltransferase activity proposed, MosA would be required to catalyze Schiff base formation between the active site lysine and 2-OB.

Schiff base trapping experiments using $NaBH_4$ in the presence of MosA and 2-OB demonstrated that 2-OB does indeed form a Schiff base with MosA. As shown in Figure 22 a major peak corresponding to the mass expected for a reduced imine between 2-OB and MosA was found by HPLC-MS. Incubation of $NaBH_4$ with MosA in assay buffer did not alter the mass of the protein. Despite the fact that MosA forms a Schiff base with 2-OB, it is still unclear whether or not this is occurring at the active site or at some other lysine near the surface of the enzyme.

However, after Schiff base trapping experiments were performed, dialysis of the modified MosA resulted in enzyme with significantly reduced DHDPS activity (see Table 2), suggesting that the modification was occurring at the active site. A control reaction, in which MosA was treated with $NaBH_4$ and dialyzed, determined that aldolase activity was not affected by the reducing agent in the absence substrate. This confirms that the $NaBH_4$ did not react with MosA destroying aldolase activity, and that the reduction of the active site imine to the amine was most likely responsible for loss in MosA's aldolase activity.

Previously, it was reported that 2-OB is a competitive inhibitor of DHDPS from *E. coli*.[34] Since 2-OB competes with pyruvate for the active site of DHDPS from *E. coli*, it is reasonable to expect the same for MosA. Kinetic analysis in Figure 18 suggested that 2-OB is a competitive inhibitor of MosA with respect to pyruvate. A K_i of approximately 1 mM was determined, revealing that both pyruvate and 2-OB have similar affinities to MosA. It is also plausible that 2-OB participates in the condensation reaction with ASA forming a dipicolinic acid derivative with an additional methyl group. However, no aromatic dipicolinate derivatives are detected

spectrophotometrically upon replacement of pyruvate with 2-OB in the DHDPS assays. This was also the case in *E. coli* DHDPS.[31]

The Schiff base reaction between MosA and 2-OB is likely occurring. This is supported by the fact that HPLC-MS detected a 2-OB-MosA Schiff base and that 2-OB is a competitive inhibitor of the DHDPS activity of MosA. However two important points should be considered when reflecting upon these results; 1) just because 2-OB forms a Schiff base with MosA does not mean it is a methyl donor and 2) 2-OB and pyruvate are structurally similar so that discrimination by the active site is unlikely. Consequently, 2-OB may form a Schiff base in the active site of MosA, but no subsequent aldolase or methyl transfer is catalyzed. One important difference may be the tautomerization of the 2-OB-lysine imine to form the enamine. Since 2-OB does not replace pyruvate in the aldol part of the DHDPS reaction, it is possible that the enamine is not forming in the active site. Steric hindrance of the C-4 methyl group of 2-OB may be preventing enamine formation. Alternatively, the enamine may be forming but the C-4 methyl group of 2-OB is preventing the approach of ASA and the aldol chemistry from occurring**.**

There are many examples of enzymes that cannot exclusively distinguish pyruvate from 2-OB as substrates, including lactate dehydrogenase,[123] pyruvate oxidase[124] and 2-oxo-acid:ferrodoxin oxoreductase.[125] This was an unfortunate finding because a coupled assay that detected pyruvate in the presence of 2-OB would be useful in monitoring the proposed methyltransferase activity of MosA. Based on the number of enzymes that use both pyruvate and 2-OB as substrates it should not be surprising that MosA interacts with 2-OB in a way analogous to pyruvate.

The first experiments done involving **SI** were to determine if the presence of this molecule affected MosA's DHDPS activity. A graph of the initial velocity vs inhibitor concentrations demonstrated that at high concentrations of **SI** (~10 mM) little change is observed in the DHDPS activity of MosA as illustrated in Figure 19. In other words, **SI** does not seem to strongly interact with the active site that MosA uses to catalyze the DHDPS reaction. Any effects seen at high concentrations of **SI** are likely due to spontaneous imine formation between the **SI** and the pyruvate in solution, thereby lowering concentrations of free pyruvate and hence slowing down enzymatic activity. If MosA is a methyltransferase that catalyzes two reactions in the same active site, one would expect the presence of **SI** to effect DHDPS activity. However, the absence of inhibition does not rule out the possibility that MosA has two functions.

4.2.2 HPLC assays fail to detect methyltransferase activity of MosA

In order to observe methyltransferase activity catalyzed by MosA, an HPLC assay is required. Developing such a method was challenging as the assays needed to distinguish 2-OB from pyruvate and **3-MSI** from **SI** after enzymatic treatment. Furthermore, all analytes involved were polar, charged molecules (at pH's required for activity) and did not possess chromphores required for immediate UV-Vis detection. Consequently, pre-column derivatization would be necessary for both the detection and separation of pyruvate from 2-OB and **SI** from **3-MSI**.

Initial efforts to develop an assay focused on the separation and detection of pyruvate and 2-OB. Historically, derivatization of carbonyl containing compounds with 2,4-dinitrophenylhydrazine has been used for over 80 years.[126] This reagent forms phenylhydrazones with the carbonyl reactant which would provide a nonpolar and chromophoric group necessary for reverse-phase chromatography and spectrophotometric detection. However, the lack of recent literature examples and the harsh conditions often employed for the derivatization reaction limited the desirability of this route. Additionally, phenylhydrazones exist as a mixture of interconverting isomers, often suffering from instability which would potentially complicate the analysis.[93,127,128] After only a few attempts to develop a reliable, convenient and compatible procedure it was clear that the rhizopines were the better choice for derivatization and subsequent detection in an HPLC assay.

A significant amount of work has been done on the derivatization and HPLC separation of hexosamines such as glucosamine and galactosamine. Being structurally similar to the rhizopines, the literature describing the derivatization and quantification of amino sugars provided excellent insight into designing a method for observing methyltransfer activity of MosA.[129] Several reagents have been used in the derivatization of various amino sugars and primary amines. These include phenylisothiocyanate (PITC),[130,131] o-phthaldehyde (OPA)[132] and fluorenylmethylcarboxy chloroformate (FMOC-Cl).[133-135] These reagents react with primary and secondary amines which would serve to reduce the overall polarity and basicity of the molecules allowing separation on a reverse phase column. Furthermore, all possessed aromatic functional groups allowing UV detection.

Despite the fact that OPA and PITC serve to introduce some of the chemical properties desired for the assay, they were not without drawbacks. To begin with, OPA is an unstable reagent that needs to be prepared daily. Furthermore, the separation of OPA derivatized compounds has been shown to be heavily influenced by inorganic cations.[136] On the other hand, PITC required inconvenient, time consuming derivatization procedures lowering the attractiveness of the reagent.[130]

Recent papers have been published that quantitatively analyzed glucosamine concentrations using HPLC and pre-column derivatization with FMOC-Cl.[94,137] Due to the ease of derivatization and stability of both the reagent and the derivatized products, FMOC-Cl was the best choice for derivatizing the rhizopines. However, one issue associated with FMOC-Cl was the spontaneous hydrolysis of the reagent to produce the acid FMOC-OH.[129] The ratio of amine attack versus water attack was influenced heavily by pH and temperature.[94] In addition, the derivatization of the rhizopines was to be performed in the presence of buffers which could also influence the derivatization reaction.

Initial attempts to react rhizopines with FMOC-Cl were done in borate buffer at pH 9.0.[133] However, derivatization at this high pH resulted in almost exclusive hydrolysis of the FMOC-Cl forming FMOC-OH from nucleophilic attack by hydroxide. However, upon lowering the pH to 7.0, a favorable ratio of derivatized rhizopine to hydrolysis product was obtained.

In addition to the issues at high pH, choice of buffer is also an important factor. MosA has been shown to be active in imidazole, phosphate and Tris buffers.[13] However, when the rhizopines are dissolved in imidazole, the derivatization reaction

resulted in exclusive formation of FMOC-OH. This is not surprising as imidazole is likely to act as a nucleophilic catalyst or general base leading to the hydrolysis of the FMOC-Cl. Fortunately, the rhizopines dissolved in phosphate buffer at pH 7.0 resulted in significant formation of both FMOC-**SI** and FMOC-**3-MSI**. The effects of temperature and reaction time on the derivatization of the rhizopines was similar to those found for glucosamine.[138]

MosA assays were set up using MosA, 2-OB and **SI** in phosphate buffer at pH 7.0. At 1, 2 and 3 hours a 100 μL aliquot was removed, filtered to remove MosA and subjected to derivatization with FMOC-Cl. The chromatogram shown in Figure 27 revealed a peak corresponding to the retention time of FMOC-**SI** with no peaks corresponding to the FMOC-**3-MSI**. To be sure that the peaks corresponding to FMOC-**3-MSI** and FMOC-**SI** were distinguishable after assay conditions, a 10% spike of **3-MSI** was included in the derivatization after 3 hours. As shown in Figure 28, the derivatized rhizopine peaks were easily resolved and eluted at the retention times determined from control reactions. Consequently, no methyltransferase activity by MosA was observed using 2-OB as a methyl donor to **SI** in the formation of **3-MSI**.

S-Adenosyl methionine (SAM) is a ubiquitous methyl donor required by the vast majority of methyltransferases throughout nature. These enzymes catalyze the formation of methyl ethers, methylthio ethers, methyl amines, methyl esters and methyl amides most of which rely on SAM for methyl donation.[139] Upon donation of the methyl group, *S*-adenosyl homocysteine (SAH) and the corresponding methylated product are formed. Due to the widespread use of SAM for methyltransferase enzymes it is reasonable to suggest that MosA may utilize SAM despite the fact that the sequence

of MosA does not reveal any known SAM binding sites. Consequently, HPLC assays were developed to detect any methyltransferase activity MosA may have on **SI** using SAM as a methyl donor. Interestingly, no known assays have been developed to monitor concentration changes of the cofactors SAH and SAM over the course of an enzymatic reaction.

HPLC methods have been developed that allow reverse phase HPLC to separate and quantify both SAM and SAH.[140] Since both molecules are charged at assay pH, ion pairing agents were included to ensure retention onto the nonpolar column. Commercially available SAM and SAH were obtained so that retention times of these cofactors could be determined. Unfortunately, SAM is available only 60% pure from the manufacturer with SAH being one of the contaminants in the preparation. This complicates matters if our goal was to detect SAH in an enzymatic assay. Fortunately, the ratio of SAM to SAH remained constant throughout control reactions. This allows detection of methyltransferase activity by monitoring an increase in the amounts of SAH and corresponding decreases in SAM.

Enzymatic assays containing MosA, SAM and **SI** were incubated in imidazole buffer for 3 hours. The chromatogram in Figure 31 show that the ratio of SAM to SAH did not change over the course of the reaction time. This suggests that MosA does not utlize SAM as a methyl donor in rhizopine formation. In an attempt to simplify the analysis, the reverse reaction containing MosA, SAH and **3-MSI** was analyzed. The appearance of a peak corresponding to the retention time of SAM would suggest the reverse methyltransferase reaction is occurring. Aliquots removed at 1, 2 and 3 hours

failed to detect the presence of SAM; thus, no reverse methyltransferase activity was observed by MosA on **3-MSI** and SAH.

To be certain that the method of measuring the relative amounts of SAH to SAM to detect methyltransferase activity was valid, a control reaction was sought. The highly studied, commercially available, SAM-dependent enzyme catechol *O*-methyltransferase (COMT) was an ideal candidate. This enzyme catalyzes the transfer of a methyl group from SAM to one of the hydroxyls of various catecholamines, including the neurotransmitters dopamine, epinephrine and norepinephrine. In addition, COMT is involved in the metabolism of dietery catechols and catecholic drugs such as those in the treatment of hypertension, asthma and Parkinson disease.[141]

There have been many assays developed in the characterization of this enzyme, none of which directly determined SAM/SAH levels to monitor enzymatic activity. Over the course of a three hour reaction, 100 μL aliquots were withdrawn, filtered to remove enzyme and the filtrate analyzed by HPLC. The chromatogram in Figure 33 clearly detects changes in the relative amounts of SAM to SAH over the assay time validating this method. Although these assays may not be the best choice for determination of accurate kinetic parameters, they are sufficient to observe methyltransferase activity qualitatively, as the COMT experiments demonstrate.

4.2.3 ITC does not detect any interactions between the rhizopines and MosA

Isothermal titration calorimetry is a valuable technique for thermodynamically characterizing biomolecular associations. In a single experiment ΔH, K_a, ΔG, ΔS and n can be determined making this technique extremely valuable in biological chemistry.

ITC is a very attractive tool for investigation of MosA's role in rhizopine biosynthesis as it should detect any specific intermolecular interactions between **SI** and **3-MSI** with MosA.

Titrations of **SI**, **3-MSI** and SAM into buffered solutions of MosA produced peaks of similar magnitude throughout each experiment. Titration of those molecules into identical buffer produced heats of dilution which once subtracted from the data obtained, resulted in effectively canceling out the heats determined for each titration of the rhizopines and SAM into MosA (Figure 40). Consequently, no interactions between MosA and the rhizopines or SAM were detected by ITC. Furthermore, titrations of **SI** into 2-OB-saturated solutions of MosA produced heats consistent with dilution heats obtained without enzyme. The failure to detect interactions between MosA and the rhizopines and SAM strongly supports the conclusion that MosA is only a DHDPS and not an *O*-methyltransferase in the production of **3-MSI** from **SI**.

The reaction in Figure 5, although hypothetically possible, has to my knowledge never been observed as part of an enzymatic or nonenzymatic mechanism. It was an exciting possibility that seemed to be supported by initial findings that 2-OB interacted with MosA. The interaction of 2-OB with enzymes that use pyruvate as a substrate is not uncommon due to the structural similarity of the two 2-oxo acids. Furthermore, since the aldolase reaction requires close juxtaposition of the aldehyde carbonyl of ASA to the pyruvate enamine, there should be enough room to accommodate the presence of a longer alkyl tail as in 2-OB. In fact, other long chain 2-oxo acids, as well as succinic acid semialdehyde, are inhibitors of DHDPS from *E. coli*, with several published crystal structures containing these molecules in the active site.[33] It has been shown previously

that 2-OB is a competitive inhibitor of DHDPS from *E. coli*[34] and in agreement with MosA, no aldolase product is detected upon replacement of 2-OB in the DHDPS assay. This may be due to steric hindrance of the C-4 carbon of 2-OB preventing the electrophilic carbon of ASA from getting close enough for the aldol reaction. Alternatively, the tautomerization of the Schiff base to the enamine is not occurring within the active site. The C-4 methyl group of the 2-OB may sterically clash with active site residues of MosA preventing tautomerization and subsequent aldolase activity. No evidence for either of these scenarios was obtained. Another important point to consider is that **SI** had almost no effect on the DHDPS reaction. If **SI** was indeed a substrate of MosA sharing the same active site as the aldol reaction, one would expect it affect the DHDPS activity. However, little effect was observed by **SI** on the DHDPS reaction catalyzed by MosA. In addition, no calorimetrically detected interactions were observed to occur between the rhizopines and MosA.

In light of the evidence that MosA is only a DHDPS, how does one explain the results observed in rhizopine biosynthesis? To begin with, all of the rhizopine experiments provided indirect evidence that MosA was a methyltransferase. The first hint that MosA may be involved in **3-MSI** biosynthesis comes from *Sm* 220-3, a strain closely related to *Sm* L5-30. In *Sm* 220-3 the mos locus shares extensive similarity to that of the mos locus of *Sm* L5-30 with the exception that it lacks the mosA gene. In *Sm* 220-3 only **SI** is produced suggesting that MosA must be involved in **3-MSI** biosynthesis. However, this is only indirect evidence as discussed by the authors themselves.[15] Furthermore, *Sm* 220-3 and *Sm* L5-30 are only related strains of bacteria

meaning other, perhaps important genetic differences exist, limiting the extent of the conclusions.

In addition to global genetic differences between the two strains, differences in the mos genes also exist. For example, the MosB protein from *Sm* 220-3 has 5 amino acids different from that of the MosB from L5-30. Although the function of this protein has yet to be demonstrated *in vitro* its amino acid sequence suggests it is likely an inososе-aminotransferase.[13] Although it is unlikely that the differences in 5 amino acids would significantly alter the substrate specificity or catalytic activity of MosB, it must be considered. On the other hand, MosC which is believed to be a transport protein, has 26 amino acids differing between *Sm* 220-3 and L5-30. This indicates genetic variations between the two strains that must be considered. For example, transport of rhizopine precursors into and out of the cell could be influencing production of **3-MSI**. Metabolic comparison of the two bacterial strains is valid although conclusions must be considered carefully due to the genetic differences between the two strains.

Additional evidence that MosA was a methyltransferase was obtained by the use of a plasmid that contained a truncated mosA gene. Restriction enzymes were used to cut a 771 bp internal fragment from the mosA gene creating a plasmid that would not express a functional MosA protein. This plasmid was then introduced into *Sinorhizobium meliloti* 1021 (*Sm* 1021), a strain that does not produce rhizopines. In the newly transformed *Sm* 1021 containing the truncated mosA, only **SI** was produced apparently confirming that MosA was a methyltransferase. However, this again is only indirect evidence that MosA is a methyltransferase. It is noteworthy that the rhizopine produced by this strain is identified by a very weak spot roughly corresponding to the

position of **SI** using high voltage paper electrophoresis.[15] A significant reduction in **SI** amounts was observed and this was suggested to be due to the small non-functional upstream reading frame (*i.e*. the truncated mosA gene) that may be reducing expression levels of the Mos proteins and affecting rhizopine production.[142] This brings into question what effects the presence of the disrupted mosA gene may have had on **3-MSI** production by influencing the expression of other closely linked proteins such as MosB or MosC. Interestingly, two other gene sequences encoding proteins homologous to MosA have been identified in the genome of *Sm* 1021. One of the proteins shares 59% identity to MosA and is very likely a DHDPS.[13] Since the expression of this protein would not have been affected by the truncation of MosA, changes in the rhizopine production actually resulting from removal of the catalytic enzyme is puzzling.

The *in vitro* investigation of MosA's role in rhizopine biosynthesis failed to observe methyltransferase activity. It is very likely that MosA is only a DHDPS that may somehow affect the production of **3-MSI** indirectly. Perhaps biosynthesis of (*S*)-lysine affects these pathways influencing methyltransferase activity. Alternatively, MosA may have nothing at all to do with rhizopine biosynthesis and is only an isozyme of DHDPS that belongs to the NAL sub-family of enzymes and a member of the metabolic pathway producing (*S*)-lysine in sinorhizobia.

4.3 The binding thermodynamics of substrate and inhibitors to MosA

Prior to the use of ITC to investigate rhizopine interactions with MosA, it was decided to characterize the thermodynamics of associations between MosA and known

substrates and inhibitors. Consequently, titrations of pyruvate, 2-OB or lysine into buffered solutions of MosA would allow us to evaluate the practicality of applying this technique to the rhizopine investigation. Additionally, ITC could provide interesting thermodynamic insight into the binding forces driving the interactions between MosA and its substrates and inhibitors. Once the characterization of the known associations was accomplished, experiments to detect any interactions between MosA and the rhizopines could be pursued with confidence.

Dissection of the thermodynamic parameters upon biomolecular associations is important in understanding binding affinity.[80] In general, binding interactions that are exothermic are due to the formation of hydrogen bonds, van der Waals forces and electrostatic interactions stronger or more numerous than those that existed prior to the binding event. These enthalpic contributions can arise from ligand-protein, protein-solvent and ligand-solvent interactions.[81] Entropy, on the other hand, is more complicated due to the importance of solvent effects arising from the degree of hydration of the protein and ligand.[82] Furthermore, during a binding event, contributions to entropy come from overall rotational and translation degrees of freedom of both protein and ligand. A third contribution includes both internal rotational and vibrational entropy of both ligand and protein plus any changes upon ionization.[101] During a typical association between a ligand and protein, positive contributions to entropy are usually due to release of solvent from protein and ligand upon binding while negative contributions usually occur from loss of translational, vibrational and rotational entropy of both protein and ligand.[101] The overall result for

the binding enthalpy and entropy is a collection of all the contributions that result in the thermodynamic values for the association.

It has been shown that MosA catalyzes the formation of a Schiff base between pyruvate and most likely an active site lysine.[13] As shown in Figure 34, binding isotherms from ITC experiments of pyruvate titrations into MosA determined that the interaction was characteristic of a low affinity system. Typically, low affinity systems cannot be accurately studied with ITC as discussed by Wiseman in the inaugural ITC report.[95] Recently, Turnbull[96] showed that reliable binding data can be obtained for low affinity systems if the following four criteria are met: 1) the binding stoichiometry is known, 2) a sufficient portion of the binding isotherm is used for the analysis, 3) accurate determinations of the concentrations of both ligand and macromolecule, and 4) adequate signal to noise ratio. All four of these criteria were met with the MosA-pyruvate system.

In order to extract reliable data from ITC it was important that the binding stoichiometry was known prior to the curve fitting process. Results from Schiff base trapping experiments of MosA in the presence of pyruvate and $NaBH_4$ indicated that one molecule of pyruvate was bound per monomer of MosA. Furthermore, the crystal structure of MosA that contained pyruvate in the active site confirmed the stoichiometry. This stoichiometry was also assumed for 2-oxobutyrate titrations into MosA. Prior to the curve fitting, a stoichiometry of n = 1.0 was input into the Bindworks software while ΔH and K_a were allowed to vary. For pyruvate titrations into MosA, a hyperbolic isotherm characteristic of low affinity systems was observed. The

thermodynamic parameters obtained are reproducible with MosA remaining visually soluble over the course of the experiments.

The thermodynamic values obtained for Schiff base formation between MosA and pyruvate, summarized in Table 3, indicate the process is entropically driven. This is not surprising as the burial of the negatively charged pyruvate into the active site of MosA should release water from both the surface of pyruvate and the MosA active site with favorable entropy. Furthermore, since the reaction itself involves MosA and pyruvate forming the MosA-pyruvate Schiff base and water, no large decrease in rotational and translational entropy is expected.

In addition to the favorable entropy, the enthalpy term of this reaction is also favorable likely due to the formation of the imine and some favorable interactions in the active site of MosA. Similar thermodynamic values were obtained by ITC for Rho protein covalently binding an inhibitor through a Schiff base formed between a binding site lysine and an aldehyde group.[97] The K_d extracted for pyruvate's interaction with MosA was quite close to the K_M of pyruvate, determined kinetically, supporting that the ITC technique and the criteria outlined for low affinity systems was applicable in this case. This research represents the first reported example of an enzyme-covalent intermediate which has been thermodynamically characterized by ITC.

In addition to providing binding information, ITC is also useful in diagnosing the release of protons to or from the solvent during a protein-ligand association. This is achieved by performing the ITC experiments in different buffers that vary in their ionization enthalpy. Since the enthalpy of proton transfer to and from buffer molecules contributes to the enthalpy of binding, proton transfers in different buffer systems

would result in significantly different overall enthalpy. Pyruvate titrations into MosA buffered with imidazole at pH 7.7 (the ionization enthalpy of imidazole $\Delta H \approx$ -36 kJ/mol[143]) did not produce thermodynamic parameters significantly different from those titrations buffered with Tris at pH 7.7 (the ionization enthalpy of Tris $\Delta H \approx$ -47 kJ/mol[143]) suggesting net proton exchange is not occurring upon formation of the Schiff base. Furthermore, if a proton was released into the solvent during the formation of the pyruvate-MosA Schiff base, it is reasonable to expect much larger enthalpy values per injection than those experimentally observed. For example, a typical ITC experiment had approximately 0.07 μmoles of MosA monomer buffered with imidazole. Upon injection of pyruvate, assuming all of the MosA monomer is forming a Schiff base with pyruvate and releasing a proton, one would expect to see approximately 2500 μJ of heat released from ionization of imidazole. Experimentally, each injection was about 100 μJ for the first few titrations which represent the largest heats of the experiment. This is significantly lower than expected if proton release and ionization of buffer molecules was occurring. Additionally, the mechanism of Schiff base formation does not require the net release or uptake of protons into the solvent, justifying this observation.

To characterize further the covalent interaction between MosA and pyruvate, heat capacity changes were examined by comparing enthalpy values extracted from experiments done in the range 15 ºC - 25 ºC. The thermodynamic parameters (Table 3) obtained did not differ significantly between the two temperatures suggesting small changes in heat capacity for this system. Heat capacity changes offer insight into the participation of solvent in the association of two molecules and is further discussed below.

In analogy to pyruvate, 2-OB's interaction with MosA was examined by ITC. The thermodynamic values for the interaction between 2-OB and MosA were quite similar to those values obtained from the MosA-pyruvate system suggesting similar chemistry is taking place (see Table 3). As with pyruvate, entropy is the dominant parameter with a slightly favorable contribution from enthalpy. However, both enthalpy and entropy changes for 2-OB were slightly less favorable compared to the values determined for pyruvate. Kinetically-determined K_i values of 2-OB were approximately 1 mM which compared favorably to dissociation constants of about 2 mM as determined by ITC. The resulting isotherms plotted for the 2-OB/MosA system, shown in Figure 35, demonstrate that we are approaching the detection limits of the ITC instrument. This is reflected in the scatter of data thus increasing the errors associated with the thermodynamic parameters for 2-OB. The general thermodynamic trends observed between pyruvate and 2-OB interactions with MosA are most important. However, the accuracy of the calorimetrically determined dissociation constants for the pyruvate/2-OB and MosA system is supported by kinetically determined K_i and K_M values.

The next set of ITC experiments were designed to characterize thermodynamically the cooperative association of (*S*)-lysine and MosA which should provide insight into the allosteric inhibition of the DHDPS enzymes. The residues involved in binding of (*S*)-lysine to DHDPS from *E. coli* have been studied by X-ray crystallography and discussed in section 1.3.1. The inhibition of DHDPS from *E. coli* by (*S*)-lysine was initially reported to be uncompetitive with respect to pyruvate.[34] The labeling of (*S*)-lysine as an uncompetitive inhibitor implies that it binds only after

pyruvate has occupied the active site in DHDPS. However, Gerrard has recently reported that (*S*)-lysine is a mixed inhibitor; binding to DHDPS in the presence or absence of pyruvate.[40] Direct measurement of the binding parameters of (*S*)-lysine to MosA in the presence and absence of pyruvate would directly determine the nature of the inhibition. In addition to the binding issues, the mechanism through which (*S*)-lysine exerts its influence on DHDPS activity is unknown. Consequently, ITC can provide thermodynamic insight into the inhibition of MosA leading to further understanding of DHDPS's from other organisms.

ITC experiments were conducted by titrating (*S*)-lysine into pyruvate-saturated solutions of MosA. The resulting isotherm shown in Figure 36. The thermodynamic parameters summarized in Table 4 illustrate a very strong cooperativity of binding that exists between the first and second (*S*)-lysine. The thermodynamic parameters obtained for binding of the first inhibitor molecule revealed the association is driven by a favorable enthalpy with a negligible change in entropy. Thermodynamic parameters extracted for the second (*S*)-lysine revealed the association is largely dominated by an exothermic enthalpy with further contribution from a favorable entropy. With both enthalpy and entropy driving the association, MosA has a much higher affinity for the second (*S*)-lysine compared to the first.

Rationalization of the thermodynamic parameters in Table 4 is a bit difficult as no crystal structure of MosA simultaneously bound to pyruvate and (*S*)-lysine is available. However, some general suggestions can be proposed to rationalize the thermodynamics observed. To begin with, (*S*)-lysine is a highly charged zwitterionic molecule with four relatively non-polar methylene groups and one methyne group.

Consequently, upon binding to MosA, ordered water should be freed from both the surface of (*S*)-lysine and the binding site. However, for the binding of the first (*S*)-lysine we observe a negligible entropy change, suggesting that the entropy gained from the release of water into the bulk is cancelled out by a loss in conformational and internal rotational freedom of the protein and the ligand itself. The enthalpy term is slightly favorable and is the dominant parameter driving the weak association. The relatively low enthalpic values are due to the overall contributions made from the noncovalent interactions in the partially formed binding site being effectively cancelled out by the enthalpic cost of shedding the binding site and the ligand of solvent.

For the second (*S*)-lysine, a much more favorable enthalpy is not surprising for this association as the first (*S*)-lysine completes the binding pocket. This is reflected in the observed exothermicity and is likely a consequence of the formation of the hydrogen bonds, dipole and ionic interactions in the (*S*)-lysine-MosA complex. These are significantly stronger than those noncovalent associations formed between the solvent and ligand and between the solvent and binding site. A portion of this enthapic gain may be due the first (*S*)-lysine diminishing the degree of solvation in the binding site. Consequently, the association of the second inhibitor would lead to a more negative value of change in enthalpy as no strong interactions between the solvent and the binding site would require breaking upon ligand association. In addition, any conformational changes of the enzyme structure associated with the binding of the second inhibitor would contribute to more favorable entropy. However, this could potentially be partially cancelled out by increased solvent exposure to protein structure resulting in ordering of water.

As discussed above, the exact nature of the inhibition of DHDPS from *E. coli* by (*S*)-lysine was debated in the literature. ITC experiments performed on MosA in the absence of pyruvate would shed light on the nature of (*S*)-lysine's inhibition of DHDPS. If one could detect any interactions between MosA and (*S*)-lysine in the absence of pyruvate one could conclude that (*S*)-lysine is a mixed inhibitor with respect to pyruvate. ITC revealed in Figure 37 that indeed (*S*)-lysine did interact with MosA without the need to bind pyruvate first. Interestingly, values shown in Table 4 for the dissociation constants for both the first and second (*S*)-lysine molecules were relatively independent of pyruvate. The thermodynamic parameters were not significantly different for the binding of the first (*S*)-lysine; however significant changes were observed in the enthalpy and entropy terms for the binding of the second lysine. In the presence of pyruvate, the binding of the second (*S*)-lysine is dominated by a very large exothermic value of -21 kJ/mol. However, without pyruvate, this value drops to -3.3 kJ/mol but is compensated for by a large increase in the entropy. This observation may be due to the presence of pyruvate ensuring that favorable enthalpic contacts are being formed between the enzyme and the second (*S*)-lysine that are lost without pyruvate. Without pyruvate, a slight change in the structure of the protein may prevent the formation of one or more hydrogen bonds upon inhibitor binding, leading to the less favorable enthalpic values.

Despite the lower enthalpy changes without pyruvate, the binding affinity remains relatively unchanged due to a significant increase in entropy. One possible explanation for this gain in entropy could be a relative decrease in exposure of the protein to water upon inhibitor binding. With pyruvate in the active site, slight changes

in the protein structure upon inhibitor binding may lead to increased exposure to water. This would result in favorable contributions to enthalpy and unfavorable contributions to entropy. In the absence of pyruvate, the active site is filled with water molecules. Therefore, binding of the second (*S*)-lysine may not result in a significant change in hydration of the active site. This would preserve the entropy gains from removal of solvent from the surface of (*S*)-lysine and the inhibitor binding site without being partially cancelled out by active site exposure to water. The crystal structure of MosA with both pyruvate and (*S*)-lysine bound compared to a structure of MosA bound only to (*S*)-lysine will determine any changes in protein structure upon inhibitor binding. Any differences between the two structures will allow a complete understanding of the thermodynamic differences of (*S*)-lysine binding to MosA in the presence and absence of pyruvate as observed by ITC.

Titrations of (*S*)-lysine into 2-OB-saturated solutions of MosA also produced interesting results and the resulting isotherm is shown in Figure 38. The parameters extracted (see Table 4) for the binding of the first (*S*)-lysine did not differ significantly from previous experiments. On the other hand, the second (*S*)-lysine showed a favorable enthalpy of -14 kJ/mol, a value in between the -21 kJ/mol in the presence of pyruvate and -3.3 kJ/mol for the apo-enzyme. The favorable enthalpic interactions that are being formed upon the binding of (*S*)-lysine are only partially contributing to the enthalpy compared to when pyruvate is bound. The entropy values, as with enthalpy, are in between those for MosA-pyruvate and apo-enyzme. Since MosA has less affinity for 2-OB, the weaker association is reflected in the binding of the second (*S*)-lysine suggesting important linkage between the two sites. Additionally, since the presence of

2-OB produces similar thermodynamic results as the presence of pyruvate upon the binding of (*S*)-lysine, this is strong evidence that 2-OB is interacting at the active site of MosA.

It is difficult to interpret the results obtained upon binding due to the complexity of the events, especially in the absence of structural data. However, it is clear that upon introduction of pyruvate or 2-OB into the active site of MosA, a significantly more enthalpically favorable interaction is occurring upon binding of the second (*S*)-lysine. In addition to local changes in the binding and active site structures, more global changes in the protein structure could occur. As mentioned above, one could imagine "loosening" of the active site upon inhibitor binding, influencing catalytic activity while simultaneously exposing protein groups to the solvent. If the presence of a 2-oxo acid increased exposure of protein groups to solvent upon binding of the second (*S*)-lysine, this should be reflected in heat capacity changes at different temperatures.

Changes in heat capacity (ΔC_p) upon intermolecular associations provide information regarding molecular interactions with aqueous solvent upon binding. Although the interpretation of such data is not always straightforward,[144] it typically provides valuable insight into the mechanism by changes in hydration levels of solutes.[145] For example, exposure of hydrophobic and polar solutes are accompanied by changes in heat capacity, but of opposite sign.[102] In 1977 Sturtevant reported several aspects of binding involving proteins that can affect heat capacity changes. These were described as 1) hydrophobic interactions, 2) electrostatic interactions, 3) hydrogen bonds, 4) intramolecular vibrations, 5) changes in equilibria, and 6) temperature-dependent conformational changes.[101] Consequently, biophysical analysis of protein-

ligand interaction at different temperatures can provide insight into the mechanisms dominating the interaction.

The vast majority of ΔC_p data on protein-ligand interactions are characterized by a negative heat capacity change.[144] This value is typically dominated by "hydrophobic interactions" which display more favorable enthalpic and less favorable entropic effects at higher temperatures. Although uncommon, positive heat capacity changes associated with binding between proteins and small molecules are known[99,103,105,106,146] and typically result from exposure of hydrophobic surfaces to solvent,[147] dehydration of polar surfaces[148] or structural transitions of the protein-ligand complex.[144]

ITC experiments of titration of (*S*)-lysine into pyruvate-saturated solutions of MosA at 15, 18, 20 and 25 ºC revealed a large positive ΔC_p of approximately 1 kJ/mol/K indicating the importance that solvent plays in the binding of (*S*)-lysine to MosA (see Table 5). During this event the burial of a highly charged molecule into a polar-charged binding site on MosA would contribute positively to ΔC_p. This positive contribution to heat capacity has been suggested to be due to increased thermal motion disordering the ions' double layer resulting in a smaller decrease in entropy at higher temperatures.[102] However, the contributions from removal of ions would not entirely account for the magnitude of the heat capacity observed. Heat capacities of hydration for the ammonium ion were experimentally found to be -28.9 J/mol/K and for the carboxylate ion, -46 J/mol/K.[102] Consequently, the burial of (*S*)-lysine at 25 ºC would approximately contribute 104 J/mol/K to the ΔC_p, assuming the values are additive. Furthermore, this is ignoring the hydrophobic interactions that methylene groups of (*S*)-lysine would have with water that should contribute negatively to the ΔC_p possibly

canceling out this effect. On the other hand, the binding site on MosA which already has one (*S*)-lysine and several other charged groups would require desolvation upon binding of the second inhibitor, contributing positively to the ΔC_p.

A common source of positive ΔC_p is conformational changes upon association of a ligand and a protein. Often, loosening of the protein structure results in exposure of hydrophobic and hydrophilic residues to the solvent as seen with some antibody-antigen interactions.[99] In the case of hydrophobic residues, this would have the opposite effect of hydrophobic interactions leading to a positive heat capacity change. With DHDPS from *E. coli*, the binding of (*S*)-lysine did not bring about large conformational changes although several small changes were observed.[29] However, the crystal structure solved was of DHDPS bound to (*S*)-lysine without pyruvate present. ITC experiments clearly illustrated the thermodynamic differences upon binding (*S*)-lysine to MosA in the presence and absence of pyruvate. Consequently, any inferences made regarding the interaction of DHDPS and (*S*)-lysine on apo-enzyme may only provide part of the story in attempts to rationalize the inhibition observed.

The positive heat capacity changes are indicative that solvent plays an important role in the binding of (*S*)-lysine with pyruvate in the active site. This confirms part of the previous discussion suggesting the importance of solvent behind the thermodynamics of MosA's association with (*S*)-lysine. This would create an enthalpically favorable contribution from the ordered water making the overall enthalpy more exothermic as observed. Alternatively, entropically unfavorable solvent-protein interactions would lead to a decrease in the overall entropy gains from desolvation of the inhibitor and its binding site. Consequently, we observe an enthalpically dominant

driving force with a favorable but less dominant value for entropy. In addition, any changes in protein structure that lead to an increase in the number of soft internal vibrations will contribute positively to heat capacity.[101,104] Thus, upon binding of the second (*S*)-lysine with pyruvate present in the active site, a loosening of protein structure may lead to an increase in the number of easily accessible vibrational states contributing to the positive heat capacity observed.

Systems that display large heat capacity changes are often subject to entropy-enthalpy compensation. This is typical of many protein-ligand interactions and seems evident in the binding of MosA to the second (*S*)-lysine in the presence of pyruvate. However, due to the large degree of error in the values of entropy, a linear equation is impossible to fit. As illustrated in Figure 39, the enthalpy component of the interaction decreases significantly with increasing temperature. The data suggests that this is compensated by more favorable entropy with increasing temperature keeping ΔG relatively unchanged. The compensation phenomenon has been suggested to be due to a natural consequence of any system that relies on non-covalent interactions over the course of an association and is a source of frustration when dissecting binding forces of protein-ligand interactions.[144] In processes that display entropy-enthalpy compensation, a plot of ΔH vs $T\Delta S$ typically reveals a linear relationship. If the slope of this relationship is about 1.0 this implies the compensation is complete and ΔG is independent of temperature. From the data of MosA binding the second (*S*)-lysine, it appears that the enthalpy of this interaction is not fully compensated by entropy. A more dominant enthalpy term may suggest an efficient displacement of water from the

(*S*)-lysine binding site[149] which is supported by crystal structures of the DHDPS from *E. coli*.

Isothermal titration calorimetry experiments have proved valuable in understanding the thermodynamics of the interactions between pyruvate, 2-OB and (*S*)-lysine and MosA. Furthermore, the inhibition displayed by (*S*)-lysine has been determined to be mixed as binding of the inhibitors clearly takes place prior to and after the binding of pyruvate. Exactly how (*S*)-lysine affects MosA during its inhibition is still unclear; however, ITC data suggests the importance of slight protein structural changes that lead to the inhibition. A crystal structure of the MosA-pyruvate-(*S*)-lysine complex would help determine exactly how the inhibitor exerts its influence on MosA.

5. Conclusions

The main goal of this thesis was to determine if MosA, a dihydrodipicolinate synthase, is also an *O*-methyltransferase catalyzing the formation of **3-MSI** from **SI**. Prior to the investigation three synthetic routes towards **SI** were developed with yields of 11%, 22% and 23%. In addition, two synthetic routes were developed to produce racemic **3-MSI** with yields of 13% and 20%. Once these compounds were in hand the focus turned to finding evidence that MosA may be a methyltransferase.

The rhizopine investigation began with the finding that 2-OB may be a substrate of MosA. Using kinetic analysis it was determined that 2-OB is a competitive inhibitor of MosA's DHDPS activity. Furthermore, HPLC-MS demonstrated that 2-OB forms a Schiff base with MosA; however, no methyltransferase activity was observed in HPLC assays. Interestingly, **SI** had no significant effects on the DHDPS reaction nor could 2-OB replace pyruvate as the substrate for the aldolase chemistry catalyzed by MosA. In addition, the ubiquitous methyl donor SAM failed to provide MosA with any methyltransferase activity observable by HPLC. ITC also failed to provide any evidence that **SI**, **3-MSI**, SAM and **SI** in the presence of 2-OB formed any significant associations with MosA. Consequently, MosA is a DHDPS and not an *O*-methyltransferase as this research has failed to provide any *in vitro* evidence to suggest otherwise. In addition, it is likely that MosA is a member of the (*S*)-lysine biosynthetic pathway in Sinorhizobia due to the structural and enzymatic characteristics of MosA

being so similar to that of DHDPS from *E. coli*. Experimental evidence, such as the Michaelis constants associated with the DHDPS activity and the (*S*)-lysine inhibition, strongly support this conclusion.

ITC was used to determine that the binding of pyruvate and 2-OB to MosA was largely entropically driven. This was the first time an enzyme-covalent intermediate has been observed by ITC. In addition, (*S*)-lysine was found to bind cooperatively to MosA with binding constants determined for the second association of inhibitor to MosA significantly higher than the first. Furthermore, (*S*)-lysine was found to be a non-competitive inhibitor of MosA with respect to pyruvate as binding constants were measurable for associations between the inhibitor and the enzyme in the presence and absence of pyruvate. Interestingly, MosA solutions saturated with pyruvate demonstrated that (*S*)-lysine binding was dominated by enthalpy. However, without pyruvate in the enzyme solution, the binding affinity remained similar but now the association was largely dominated by entropy. Consequently, the presence of the substrate significantly influenced the binding thermodynamics of (*S*)-lysine's association with MosA. Similar effects were observed when pyruvate was replaced with 2-OB in the enzyme solution. This clearly demonstrates the aldolase active site and the lysine binding site possesss significant linkage that allow control of the enzymatic activity. The importance of solvent in the association between the pyruvate-MosA complex and the second (*S*)-lysine was revealed by a large positive heat capacity change. This heat capacity change was likely due to removal of lysine ions out of the aqueous solution and slight conformational changes to MosA upon inhibitor binding. This would lead to protein structural changes that increased hydration levels of nonpolar

groups and hence the positive heat capacity change. The thermodynamic parameters obtained in this research have provided valuable insight into understanding binding affinity of MosA to its substrates and inhibitors. Furthermore, this research resulted in the groundwork for an understanding of the mechanism of the inhibition of MosA by (*S*)-lysine. This thermodynamic data will prove to be extremely useful when used in conjunction with X-ray crystallographic studies of MosA with the inhibitors and substrates bound.

6. Future work

The future work of this project would be to finally settle the issue of rhizopine biosynthesis by finding the protein or proteins responsible for the production of **3-MSI** and **SI**. A good place to start would be MosB, a protein found in the mos operon that shares identity with StsC; an amino acid-inosose aminotransferase. It is likely that this enzyme could produce either **SI** or **3-MSI**. In addition, the thermodynamic parameters determined for the association between MosA and (*S*)-lysine will lead to an understanding of the binding affinity and provide interesting insight into the mechanism of inhibition. However, this will require the direct comparison of the crystal structures of the MosA/(*S*)-lysine complex with and without pyruvate bound. Changes observed between the two structures can be used to rationalize the thermodynamic differences of (*S*)-lysine binding in the presence and absence of pyruvate. Furthermore, since MosA is a DHDPS and can be studied using ITC, this may be a suitable system for the calorimetry assisted development of potent inhibitors of DHDPS's from *E. coli*. The design of good inhibitors of the DHDPS enzyme has eluded researchers thus far despite receiving significant attention. With the exception of our group, none of the active DHDPS researchers have elicited the use of ITC to understand binding affinity of small molecules to these aldolases.

7. Bibliography

(1) Murphy, P. J.; Heycke, N.; Banfalvi, Z.; Tate, M. E.; de Bruijn, F.; Kondorosi, A.; Tempe, J.; Schell, J. *Proc. Natl. Acad. Sci. U S A* **1987**, *84*, 493-497.

(2) Beringer, J. E.; Brewin, N.; Johnston, A. W.; Schulman, H. M.; Hopwood, D. A. *Proc. R. Soc. Lond. B Biol. Sci.* **1979**, *204*, 219-33.

(3) Vance, C. P. *Annu. Rev. Microbiol.* **1983**, *37*, 399-424.

(4) Sprent, J. *Nature* **2003**, *422*, 672-674.

(5) Murphy, P. J.; Wexler, M.; Grzemski, W.; Rao, J. P.; Gordon, D. *Soil. Biol. Biochem.* **1995**, *27*, 525-529.

(6) Thompson, J.; Donkersloot, J. A. *Res. Microbiol.* **1992**, *143*, 127-31.

(7) Dessaux, Y.; Petit, A.; Tempe, J. *Phytochemistry* **1993**, *34*, 34-38.

(8) Wexler, M.; Gordon, D.; Murphy, P. J. *Soil. Biol. Biochem.* **1995**, *27*, 531-535.

(9) Gordon, D. M.; Ryder, M. H.; Henrich, K.; Murphy, P. J. *Appl. Environ. Micrbobiol.* **1996**, *62*, 3991-3996.

(10) Charles, T. C.; Finan, T. M. *Genetics* **1991**, *127*, 5-20.

(11) Murphy, P. J.; Heycke, N.; Trenz, S. P.; Ratet, P.; de Bruijn, F. J.; Schell, J. *Proc. Natl. Acad. Sci. U S A* **1988**, *85(23)*, 9133-7.

(12) Murphy, P. J.; Trenz, S. P.; Grzemski, W.; De Bruijn, F. J.; Schell, J. *J. Bacteriol.* **1993**, *175(16)*, 5193-204.

(13) Tam, P. H. *Master's Thesis* **2003**, *Department of Biochemistry, University of Saskatchewan*.

(14) Saint, C. P.; Wexler, M.; Murphy, P. J.; Tempâe, J.; Tate, M. E. *J. Bacteriol.* **1993**, *175(16)*, 5205-15.

(15) Rao, J. P.; Grzemski, W.; Murphy, P. J. *Microbiology* **1995**, *141*, 1683-90.

(16) Lawrence, M. C.; Barbosa, J. A. R. G.; Smith, B. J.; Hall, N. E.; Pilling, P. A.; Ooi, H. C. *J. Mol. Biol.* **1997**, *266*, 381-389.

(17) Babbitt, P. C.; Gerlt, J. A. *J. Biol. Chem.* **1997**, *272*, 30591-4.

(18) Tam, P. H.; Phenix, C. P.; Palmer, D. R. *J. Mol. Biol.* **2004**, *335*, 393-7.

(19) Hutton, C. A.; Southwood, T. J.; Turner, J. J. *Mini Rev. Med. Chem.* **2003**, *3*, 115-127.

(20) Miflin, B. J.; Napier, J.; Shewry, P. R. *Nat. Biotchnol.* **1999**, *17*, 13-14.

(21) Frisch, D. A.; Gengenbach, B. G.; Tommey, A. M.; Sellner, J. M.; Somers, D. A.; Myers, D. E. *Plant Physiol.* **1991**, *96*, 444-452.

(22) Dereppe, C.; Bold, G.; Ghisaba, O.; Ebert, E.; Schar, H. P. *Plant Physiol.* **1992**, *98*, 813-821.

(23) Yugari, Y.; Gilvarg, C. *J. Biol. Chem.* **1965**, *240*, 4710-4716.

(24) Bakhiet, N.; Forney, F.; Stahly, D.; Daniels, L. *Curr. Microbiol.* **1984**, *10*, 195-198.

(25) Bartlett, A.; White, P. *J. Gen. Microbiol.* **1986**, *132*, 3169-3177.

(26) Hoganson, D.; Stahly, D. *J. Bacteriol.* **1975**, *124*, 1344-1350.

(27) Cremer, J.; Eggeling, L.; Sahm, H. *Mol. Gen. Genet.* **1990**, *229*, 478-480.

(28) Tosaska, O.; Takinami, K. *Agric. Biol. Chem.* **1978**, *42*, 95-100.

(29) Dobson, R. C.; Griffin, M. D.; Jameson, G. B.; Gerrard, J. A. *Acta Crystallogr. D Biol. Crystallogr.* **2005**, *61*, 1116-24.

(30) Richaud, F.; Richaud, C.; Ratet, P.; Patte, J. C. *Bacteriol.* **1986**, *166*, 297-300.

(31) Laber, B.; Gomis-Ruth, F. X.; Romao, M. J.; Huber, R. *Biochem. J.* **1992**, *288 (Pt 2)*, 691-5.

(32) Borthwick, E. B.; Connell, S. J.; Tudor, D. W.; Robins, D. J.; Shneier, A.; Abell, C.; Coggins, J. R. *Biochem. J.* **1995**, *305 (Pt 2)*, 521-4.

(33) Blickling, S.; Renner, C.; Laber, B.; Pohlenz, H.-D.; Holak, T. A.; Huber, R. *Biochemistry* **1997**, *36*, 24-33.

(34) Karsten, W. E. *Biochemistry* **1997**, *36*, 1730-1739.

(35) Voet, D.; Voet, J. G. *Biochemistry*; 2nd ed.; John Wiley & Sons, 1995.

(36) Dobson, R. C.; Valegêard, K.; Gerrard, J. A. *J. Mol. Biol.* **2004**, *338(2)*, 329-39.

(37) Dobson, R. C.; Devenish, S. R.; Turner, L. A.; Clifford, V. R.; Pearce, F. G.; Jameson, G. B.; Gerrard, J. A. *Biochemistry* **2005**, *44(39)*, 13007-13.

(38) Mirwaldt, C.; Korndorfer, I.; Huber, R. *J. Mol. Biol.* **1995**, *246*, 227-239.

(39) Wierenga, R. K. *FEBS Lett.* **2001**, *492*, 193-198.

(40) Dobson, R. C.; Griffin, M. D.; Roberts, S. J.; Gerrard, J. A. *Biochimie* **2004**, *86(4-5)*, 311-5.

(41) Humphrey, W., Dalke, A., Schulten, K.; Elsevier: Urbana, IL, 1996.

(42) POV-RayTeam www.povray.org, 2003.

(43) Blickling, S.; Beisel, H.-G.; Bozic, D.; Knablein, J.; Laber, B.; Huber, R. *J. Mol. Biol.* **1997**, *274*, 608-621.

(44) Roberts, S. J.; Morris, J. C.; Dobson, R. C.; Gerrard, J. A. *Bioorg. Med. Chem. Lett.* **2003**, *13(2)*, 265-7.

(45) Dobson, R. C.; Gerrard, J. A.; Pearce, F. G. *Biochem. J.* **2004**, *377(Pt) 3*, 757-62.

(46) Brosnan, J. T.; Brosnan, M. E. *J. Nutri.* **2006**, *136*, 16365-16405.

(47) Bruice, P. Y. *Organic Chemistry*; 4th ed.; Pearson Prentice Hall: Upper Saddle River, NJ, 2004.

(48) Depeint, F.; Bruce, R. B.; Shangari, N.; Mehta, R.; O'Brien, P. J. *Chemico-Biological Int.* **2006**, *163*, 113-132.

(49) Jeffrey, C. J. *Trends Biochem. Sci.* **1999**, *24*, 8-11.

(50) O'Brien, P. J.; Herschlag, D. *Chem. Biol.* **1999**, *6*, R91-R105.

(51) Palmer, D. R.; Garrett, J. B.; Sharma, V.; Maganathan, R.; Babbitt, P. C.; Gerlt, J. A. *Biochemistry* **1999**, *38*, 4252-4258.

(52) Billington, D. C. *The inositol phosphates, Chemical synthesis and biological significance*; 1st ed.; VCH: New York, 1993.

(53) Sureshan, K. M.; Shashidhar, M. S.; Praveen, T.; Das, T. *Chem. Rev.* **2003**, *103*, 4477-4503.

(54) Takahashi, H.; Kittaka, H.; Ikegami, S. *J. Org. Chem.* **2001**, *66*, 2705-2716.

(55) Angyal, S. J. *Carbohydr. Res.* **2000**, *325*, 313-320.

(56) Uhlmann, P.; Vasella, A. *Helv. Chim. Acta* **1992**, *75*, 1979-1995.

(57) Billington, D. C.; Baker, R.; Kulagowski, J. J.; Mawer, I. M.; J.P., V.; deSolms, S. J.; Huff, J. R. *J. Chem. Soc. Perkin Trans. I* **1989**, 1423-1429.

(58) Shashidhar, M. S. *ARKIVOC* **2002**, *VII*, 63-75.

(59) Samanta, U.; Puranick, V. G.; Charkrabarti, P.; Thoniyot, P.; Shashidhar, M. S. *Acta Cryst.* **1998**, *C54*, 1289-1291.

(60) Sureshan, K. M.; Shashidhar, M. S.; Praveen, T.; Gonnade, R. G.; Bhadbhade, M. M. *Carbohydr. Res.* **2002**, *337*, 2399-2410.

(61) Baudin, G.; Glanzer, B. I.; Swaminathan, K. S.; Vasella, A. *Helv. Chim. Acta* **1998**, *71*, 1367-1378.

(62) Flores-Mosquera, M.; Martin-Lomas, M.; Chiara, J. L. *Tetrahedron Lett.* **1998**, *39*, 5085-5088.

(63) Sureshan, K. M.; Das, T.; Shashidhar, M. S.; Gonnade, R. G.; Bhadbhade, M. M. *Eur. J. Org. Chem.* **2003**, 1035-1041.

(64) Fried, J.; Boyack, G. A.; Wintersteiner, O. *J. Biol. Chem.* **1946**, *162*, 391-392.

(65) Jaines, B. H.; Elliott, N. C.; Schicho, D. L. *J. Antibiot.* **1992**, *45*, 1705-1707.

(66) Lillelund, V. H.; Jenesen, H. H.; Liang, X. F.; Bols, M. *Chem. Rev.* **2002**, *102*, 515-553.

(67) Egido-Gabas, M.; Serrano, P.; Casas, J.; Llebaria, A.; Delgado, A. *Org. Biomol. Chem.* **2005**, *3*, 1195-1201.

(68) Carter, H. E.; Clark, R. K.; Lytle, B.; McCasland, G. E. *J. Biol. Chem.* **1948**, *175*, 683-690.

(69) Hansen, C. A.; Dean, A. B.; Draths, K. M.; Frost, J. W. *J. Amer. Chem. Soc.* **1999**, *121*, 3799-3800.

(70) Anderson, L.; Lardy, H. A. *J. Amer. Chem. Soc.* **1950**, *72*, 3141-3147.

(71) Suami, T.; Lichtenthaler, F. W.; Ogawa, S. *Bull. Chem. Soc. Jpn.* **1966**, *39*, 170-178.

(72) Ogawa, S.; Isaka, A. *Carbohydr. Res.* **1991**, *210*, 105-123.

(73) Yu, J.; Spencer, J. B. *Tetrahedron Lett.* **2001**, *42*, 4219-4221.

(74) Guedat, P.; Spiess, B. *Tetrahedron Lett.* **1994**, *35*, 7375-7378.

(75) Serrano, P.; Llebaria, A.; Delgado, A. *J. Org. Chem.* **2005**, *70*, 7829-7840.

(76) Sanfilippo, C.; Patti, A.; Piatelli, M.; Nicolosi, G. *Tetrahedron: Asymmetry* **1998**, *9*, 2809-2817.

(77) Jaramillo, C.; Chiara, J. L.; Martin-Lomas, M. *J. Org. Chem.* **1994**, *59*, 3135-3141.

(78) Krief, A.; Dumont, W.; Billen, D.; Letesson, J.; Lestrate, P.; Murphy, P. J.; Lacroix, D. *Tetrahedron Lett.* **2004**, *45*, 1461-1463.

(79) CSC; 1.1 ed.; Calorimetry Sciences Corporation: Utah, 1998.

(80) Velazquez-Campoy, A.; Leavitt, S.; Freire, E. *Methods Mol. Biol.* **2004**, *261*, 35-54.

(81) Talhout, R.; Villa, A.; Mark, A. E.; Engberts, J. B. F. N. *J. Amer. Chem. Soc.* **2003**, *125*, 10570-10579.

(82) Campoy, A. V.; Freire, E. *Biophys. Chem.* **2005**, *115*, 115-124.

(83) Leavitt, S.; Freire, E. *Curr. Opin. Struct. Biol.* **2001**, *11*, 560-566.

(84) Kishi, Y.; Lee, H. W. *J. Org. Chem.* **1985**, *50*, 4402-4404.

(85) Brown, C. J.; Kirby, A. J. *J. Chem. Soc., Perkin Trans. 2* **1997**, 1081-1093.

(86) Desai, T.; Gigg, J.; Gigg, R.; Martin-Zamora, E.; Schnetz, N. *Carbohydr. Res.* **1994**, *258*, 135-144.

(87) Gigg, J.; Gigg, R.; Payne, S.; Conant, R. *Carbohydr. Res.* **1985**, *142*, 132-134.

(88) Angyal, S. J.; Tate, M. E. *J. Amer. Chem. Soc.* **1965**, 6949-6955.

(89) Koto, S.; Hirooka, M.; Yoshida, T.; Takenaka, K.; Chizuru, A.; Nagamitsu, T.; Sakuma, H.; Sakurai, M.; Mitsuo, K.; Sato, T.; Shonosuke, Z.; Yago, K.; Tomonaga, F. *Bull. Chem. Soc. Jpn.* **2000**, *73*, 2521-2529.

(90) Cornish-Bowden, A.; Oxford University Press: New York, 1995.

(91) Surfraz, M. B.; Akhtar, M.; Alleman, R. K. *Tettrahedron Lett.* **2004**, *45*, 1223-1226.

(92) Shneier, A.; Kleanthous, C.; Deka, R.; Coggins, J. R.; Abell, C. *J. Amer. Chem. Soc.* **1991**, *113*, 9417- 9419.

(93) Terada, H.; Hayashi, T.; Kawai, S.; Ohno, T. *J. Chromatogr.* **1977**, *130*, 281-6.

(94) Zhu, X.; Cai, J.; Yang, J.; Su, Q. *Carbohydr. Res.* **2005**, *340*, 1732-8.

(95) Wiseman, T.; Williston, S.; Brandts, J. F.; Lin, L. N. *Anal. Biochem.* **1989**, *179*, 131-137.

(96) Turnbull, W. B.; Daranas, A. H. *J. Amer. Chem. Soc.* **2003**, *125*, 14859-14866.

(97) Brogan, A. P.; Widger, W. R.; Bensadek, D.; Riba-Garcia, I.; Gaskell, S. J.; Kohn, H. *J. Amer. Chem. Soc.* **2005**, *127*, 2741-2751.

(98) Srinivas, V. R.; Reddy, G. B.; Surolia, A. *Febs Lett.* **1999**, *450*, 181-185.

(99) Zidovetzki, R.; Blatt, Y.; Schepers, G.; Pecht, I. *Mol. Immunol.* **1988**, *25*, 379-383.

(100) Ghislain, M.; Frankard, V.; Jacobs, M. *Plant Journal* **1995**, *8*, 733-743.

(101) Sturtevant, J. M. *Proc. Natl. Acad. Sci. U S A* **1977**, *74*, 2236-2240.

(102) Gallagher, K.; Sharp, K. *Biophys. J.* **1998**, *75*, 769-776.

(103) Niedzwiecka, A.; Stepinski, J.; Darzynkiewicz, E.; Sonenberg, N.; Stolarski, R. *Biochemistry* **2002**, *41*, 12140-8.

(104) Robblee, J. P.; Cao, W.; Henn, A.; Hannemann, D. E.; De La Cruz, E. M. *Biochemistry* **2005**, *44*, 10238-49.

(105) Luther, M. A.; Cai, G. Z.; Lee, J. C. *Biochemistry* **1986**, *25*, 7931-7.

(106) Matulis, D.; Rouzina, I.; Bloomfield, V. A. *J. Mol. Biol.* **2000**, *296*, 1053-63.

(107) Gilli, P.; Ferretti, V.; Gilli, G.; Borea, P. A. *J. Phys. Chem.* **1994**, *98*, 1515-1518.

(108) Srinivas, V. R.; Bhanuprakash Reddy, G.; Surolia, A. *FEBS Lett.* **1999**, *450*, 181-5.

(109) A.M., R.; Guedat, P.; Schlewer, G.; Spiess, B.; Potter, B. V. L. *J. Org. Chem.* **1998**, *63*, 295 - 305.

(110) Bone, J. A.; Whiting, M. C. *Chem. Comm.* **1970**, 115-116.

(111) Subramaniam, R.; Fort Jr., R. C. *J. Org. Chem.* **1984**, *49*, 2891-2896.

(112) Sarmah, M. P.; S., M.; Shashidhar, A.; Sureshan, K. M.; Gonnadeb, R. G.; Bhadbhade, M. M. *Tetrahedron* **2005**, *61*, 4437-4446.

(113) Wu, Y.; Zhou, C.; Roberts, M. F. *Biochemistry* **1997**, *36*, 356 - 363.

(114) Riley, A. M.; Guedat, P.; Schweler, G.; Spiess, B.; Potter, B. V. L. *J. Org. Chem.* **1998**, *63*, 295-305.

(115) Daniellou, R.; Palmer, D. R. J. *Carbohydr. Res.* **2006**, *341*, 2145-2150.

(116) Angyal, J.; M.J., T. *J. Chem. Soc.* **1965**, 6949-6953.

(117) David, S.; Hanessian, S. *Tettrahedron* **1985**, *41*, 643-663.

(118) David, S.; Thieffry, A.; Veyieres, A. *J. Chem. Soc. Perkin Trans. I* **1981**.

(119) David, S.; Malleron, A. *Carbohydr. Res.* **2000**, *329*, 215-218.

(120) Simas, A. B. C.; Pais, K. C.; da Silva, A. A. T. *J. Org. Chem.* **2003**, *68*, 5426-5428.

(121) Azev, V. N.; d'Alarcao, M. *J. Org. Chem.* **2004**, *69*, 4839-4842.

(122) Hori, H.; Nishida, Y.; Ohrui, H.; Meguro, H. *J. Org. Chem.* **1988**, *54*, 1346-1353.

(123) Al-Mudhaffer, S. A.; Rassam, M. B. *Biochem. Exp. Biol.* **1979**, *15*, 155-165.

(124) Chang, Y. Y.; Cronan, J. E. J. *Biochem. J.* **2000**, *352*, 717-724.

(125) Park, Y. J.; Yoo, C. B.; Choi, S. Y.; Lee, H. B. *J. Biochem. Mol. Biol.* **2006**, *39*, 46-54.

(126) Allen, C. F. H. *J. Amer. Chem. Soc.* **1930**, *52*, 2955-2959.

(127) Hemming, B. C.; Gubler, C. J. *Anal. Biochem.* **1979**, *92*, 31-40.

(128) Qureshi, A. A.; Elson, C. E.; Lebeck, A. *J. Chromatogr.* **1982**, *249*, 333-345.

(129) Zhang, Z.; Renen, Z.; Liu, G. *J. Chromatogr. A* **1996**, *730*, 107-114.

(130) Hagen, S. R. *J. Chromatogr.* **1993**, *632*, 63-68.

(131) Anumula, K. R.; Taylor, P. B. *J. Chromatogr. A.* **1991**, *730*, 113-120.

(132) Altmann, F. *Anal. Biochem.* **1992**, *204*, 215-219.

(133) Stead, D. A.; Richards, R. M. E. *J. Chromatogr.* **1996**, *675*, 295-302.

(134) Einarsson, S.; Josefsson, B.; Lagerkvist, S. *J. Chromatogr.* **1983**, *282*, 609-617.

(135) Anson Moye, H.; Boning Jr., A. J. *Anal. Lett.* **1979**, *12*, 12.

(136) Lacey, J. E.; Parfitt, R. T.; Rowan, M. G. *Int. J. Pharm.* **1988**, *43*.

(137) Ziqi Zhou, J.; Waszkuc, T.; Mohammed, F. *J. AOAC Int.* **2005**, *88*, 1048-1058.

(138) Zhou, J. Z.; Waszkuc, T.; Mohammed, F. *J. AOAC Int.* **2004**, *87*, 1083-92.

(139) Martin, J. L.; McMillan, F. M. *Curr. Opin. Struct. Biol.* **2002**, *12*, 783-793.

(140) She, Q.; Nagao, I.; Hayakawa, T.; Tsuge, H. *Biochem. Biophys. Res. Commun.* **1994**, *205*, 1748-1754.

(141) Pihlavisto, P.; Reenila, I. *J. Chromatogr. B* **2002**, *781*, 359-372.

(142) Futterer, J.; Hohn, T. *Nucleic Acids Res.* **1992**, *20*, 3851-3857.

(143) Goldberg, R. N.; Kishore, N.; Lennen, R. M. *J. Phys. Chem.* **2002**, *31*.

(144) Cooper, A.; Johnson, C. M.; Lakey, J. H.; Nollman, M. *Biophys. Chem.* **2001**, *93*, 215-230.

(145) Loladze, V. V.; Ermolenko, D.; Makhatadze, G. I. *Protein Sci.* **2001**, *10*, 1343-1352.

(146) Banerjee, M.; Poddar, A.; Mitra, G.; Surolia, A.; Owa, T.; Bhattacharyya, B. *J. Med. Chem.* **2005**, *48*, 547-555.

(147) Spolar, R. S.; Record Jr., T. *Science* **1994**, *263*, 777-784.

(148) Dragan, A. I.; Klass, J.; Read, C.; Churchill, M. E.; Crane-Robinson, C.; Privalov, P. L. *J. Mol. Biol.* **2003**, *331*, 795-813.

(149) Brummell, D. A.; Sharma, V. P.; Naveen, N.; Ginette, D.; Michniewicz, J.; MacKenzie, C. R.; Sadowska, J.; Sigurskjold, B. W.; Sinnott, B.; Young, N. M.; Bundle, D. R.; Narang, S. A. *Biochemistry* **1993**, *32*, 1180-1187.